

University of Würzburg

Institute for Theoretical Physics II

Master Thesis

Calculation of QCD cross sections in a basis of $SU(3)$ coherent states

Florian Amann

September 6, 2016



Supervision: Prof. Dr. Thorsten Ohl

Summary of the Thesis

We studied the coherent state system for $SU(n)$ in this thesis. Therefore we developed the construction of the generalized coherent states based on the well known case of the harmonic oscillator. Our motivation for this approach is to calculate the color factors of Quantum Chromodynamics in this system as well as understanding the color-flow in more depth. Thus we emphasized the construction of the coherent states for a better comprehension. Further we numerically integrated the color factors as well as the cross section for the example process of a quark and an antiquark into two gluons. These results were compared to the analytic solution and we found simplifications for these calculations. In addition the correlation of the coherent states between the distinct particles of our process obtained insights into the color-flow.

Zusammenfassung der Arbeit

In dieser Arbeit wurde das kohärente Zustandssystem für $SU(n)$ untersucht. Dafür wurde die Konstruktion der kohärenten Zustände entwickelt, was auf der Grundlage des bekannten Falles des harmonischen Oszillators durchgeführt wurde. Unsere Motivation für die Verwendung der kohärenten Zustände ist die Berechnung der Farbfaktoren der Quantenchromodynamik in diesem System, sowie ein besseres Verständnis für den zugrunde liegenden Farbfluss. Insbesondere haben wir die Konstruktion der kohärenten Zustände sehr detailliert besprochen, um diese besser zu verstehen. Des Weiteren haben wir sowohl die Farbfaktoren als auch den Wirkungsquerschnitt für den Beispielprozess von Quark und Antiquark in zwei Gluonen numerisch integriert. Diese Ergebnisse haben wir mit der analytischen Lösung verglichen und haben Vereinfachungen für die Berechnungen gefunden. Außerdem haben die Korrelationen zwischen kohärenten Zuständen von den verschiedenen Teilchen dieses Prozesses einen Einblick in den Farbfluss gewährt.

Contents

1	Introduction	1
2	Basic theory of generalized coherent states	4
2.1	Lie groups and Lie algebras	4
2.2	Coherent states of the harmonic oscillator	5
2.2.1	The Heisenberg-Weyl group	5
2.2.2	The coherent states	9
2.3	Generalized coherent states	13
3	Coherent states for SU(n)	21
3.1	SU(2)	21
3.1.1	Representation of SU(2)	21
3.1.2	Coherent states of SU(2)	22
3.1.3	Another way to construct the SU(2) coherent states	29
3.2	SU(3)	39
3.2.1	Representation of SU(3)	39
3.2.2	Coherent states of SU(3)	39
3.3	Finding the isotropy subgroup	47
4	QCD cross sections	52
4.1	Feynman rules	52
4.2	Process example: $q\bar{q} \rightarrow gg$	54
4.3	Calculation of the color terms	61
4.3.1	Color basis	64
4.3.2	Coherent state system	65
4.3.3	Averaging over only a part of the external indices	68
5	Numeric calculations	70
5.1	Numeric tools	70
5.1.1	VAMP basics	70

CONTENTS

5.1.2	Missing features of VAMP	73
5.2	Numeric results	73
5.2.1	Features of our program	74
5.2.2	Results	75
6	Conclusion	98
	Bibliography	101

Acronyms

AdR adjoint representation.

CS coherent state.

CSS coherent state system.

FuR fundamental representation.

HWA Heisenberg-Weyl algebra.

HWG Heisenberg-Weyl group.

MC Monte Carlo.

QCD Quantum Chromodynamics.

QFT Quantum Field Theory.

RoU resolution of unity.

1 Introduction

For most students and even graduate physicists, a coherent state (CS) is closely related to the concept of the quantum mechanical, harmonic oscillator. The CS are introduced in this context as the eigenstates of the annihilation operator. In most quantum mechanics courses one only learns that they are the states closest to the classical ones as they minimize the uncertainty relation as well as they can be described via the classical equations of motion. If you were lucky you could also catch a deeper insight into their properties and their construction via the displacement operator. Thus one does not and maybe cannot grasp the powerful tool they can offer. The CS shared the same fate during their history as they already emerged with the birth of quantum mechanics in the 1920s. As early as one of Schrödinger's first works [Sch26] contained their concept. But it was only in the 1960s when they were studied in more depth [Kla60, Bar61] and Glauber [Gla63] eventually established the term 'coherent states'. He used them in quantum optics to describe coherent laser beams which gave them their name. But nonetheless they are used also in the field of solid-state physics when describing spin waves in ferromagnetism or for the effect of superfluidity. The CS are also applied to Quantum Field Theory (QFT), where the final states of scattering processes can be written in the form of a displacement operator. But the reader may be aware that this is not the track we are pursuing in this work as we are aiming at another approach.

The property that enables the CS to be such a versatile and powerful tool is their over-completeness, i.e. they contain more states as would be necessary to span the whole Hilbert space. Thus they cannot be mutually orthogonal as well as linear independent. This enables them to solve certain problems but on the other hand one is not used to work with these properties. In most other cases one has the freedom of choice of basis and could always take a complete, orthogonal and normalized set. This was the first interesting part of this work as many concepts learned about a change of basis could not be easily applied to the set of CS and one needed to find different approaches. As the CS are linear depend, the expansion of an arbitrary state in their system is not unique but it is this freedom which makes certain tasks easier.

Moving from the original idea of the CS to a generalization of any group, it was Perelomov [Per86] and Gilmore [ZFG90] who worked in this direction and their name is still closely related to this topic. To understand their concepts one needs to have some knowledge in the field of group theory. This is such a universal theory as one can for example already tell so much about a system by just knowing its symmetry groups. Combining such a comprehensive tool as the theory of groups with the unfamiliar properties of the CS was a great challenge over the course of this work. Finally we applied these methods in the scope of QFT, which is currently our most accurate theory of nature. From this, we hoped to get a new insight into the mechanics of the color-flow in Quantum Chromodynamics (QCD). The idea behind this approach is the Lund string model [And+83] for hadronization. This model is one of the most common and successful one to explain the confinement of quarks and is the basic idea implemented in PYTHIA [SMS06]. Quarks in a colorless particle are connected via strings and if you pull them apart you need to afford more and more energy as these strings act like rubber bands. At a certain point you have put enough energy into the strings to create a new pair of quark and antiquark which shortens the strings again. This model does not involve quantum mechanical concepts in any way but however describes the quantum mechanical particles very well. Thus we hope to gain insight into the color-flow when we describe the quarks and gluons of QCD as quantum mechanical particles as close as possible to the classical case. As we know from the harmonic oscillator the CS are a good approach for this kind of problem as in this case they describe the quantum mechanical harmonic oscillator and their trajectory is the classical one.

Our goal is to start at the point mentioned at the beginning where almost nothing about the CS is familiar. Then the first two chapters are following the course of [Per86] and will add certain steps where it is necessary or we will be more concise if some concepts are not important for our work. Thus there are parts which are left to Perelomov to be discussed in more detail especially as they will not be needed but we will focus on concepts that are essential for our purpose and understanding. From the basic theory of CS, we will construct them for SU(2) and then for SU(3) as this is the relevant color group of QCD. But the step from SU(2) to SU(3) is such a huge one that the reader is suggested to completely grasp the idea in the easier case before moving on. This difference is due to the fact that the SU(2) has a very special place among the SU(n): First the definition of higher and lower weights is straightforward as it is only one dimensional. Secondly it does not have a different complex conjugate representation. Thus one can construct all higher dimensional representations only from the single fundamental one and in all other cases we need two or more due to the rank being $n - 1$ of SU(n). Then in Ch. 4 we are considering a concrete example in the

scope of QCD which will be our guideline for the numerical implementation of the CS. Our approach here is more of a heuristic one as we assume we can easily move from the Feynman rules in the color basis to the system of CS. An analysis of the validity of this assumption starting with the QCD Lagrangian can be found in the masterthesis of Katharina Eisenhut [Eis16], also under the supervision of Prof. Dr. Thorsten Ohl. Finally in the last chapter we are presenting the numerical results of our Monte Carlo (MC) integrations.

Before moving on, I personally want to make a remark about the basic idea behind the concepts presented in this work: During the course of this work, we will need some theorems, terms and statements from the theory of Lie groups and algebras. As this is not the main subject of this thesis, we won't have the space to introduce all these concepts in their full beauty as well as my knowledge in this subject is not deep enough to establish them from the basic theory. Thus from a mathematical point of view the arguments might seem a bit heuristic at some parts. But the goal is to motivate them from a physics point of view with his knowledge based more on representation theory and applications. Thus the statements made should be clear, at least in the framework of $SU(n)$ needed for this work. Furthermore we will refer to the mathematical literature where the proofs of these statements can be found in their complete scope and universality.

2 Basic theory of generalized coherent states

2.1 Lie groups and Lie algebras

In this section we want to introduce some basic terms and concepts from the theory of Lie groups and algebras [Geo99, Ram10, Dui00, Her66] which will be needed over and over again in the course of this work. Some deeper concepts which are only needed at a specific point are introduced later on the fly.

A Lie algebra \mathcal{G} is characterized via the structure constants from the commutation relation

$$[T_a, T_b] = if_{abc}T_c. \tag{2.1}$$

Here and during the whole thesis we will use the Einstein sum convention where we sum over repeated indices unless particular noted otherwise. Be aware that this notation only applies to indices occurring twice and thus indices appearing thrice or more are not meant to be summed over unless explicitly written in form of a sum symbol. In general the square bracket is the Lie bracket which is defined via its bilinearity, anticommutativity and the Jacobi identity. In our case it is simply the commutator $[A, B] = AB - BA$ of two operators A and B . The $T_a \in \mathcal{G}$ are the generators of the Lie group \mathcal{G} and this we get via the exponential map as

$$\mathcal{G} \ni g = e^{i\theta_a T_a}. \tag{2.2}$$

The rank r of the group is the maximum number of generators which commute with each other. We call these operators H_k , $1 \leq k \leq r$, the Cartan operators and they can be simultaneously diagonalized. The eigenvalues of the eigenstates of the Cartan operators are the weights of these states. In the complex algebra \mathcal{G}^c we can define raising and lowering operators $E_{\pm\alpha}$ which represent the roots of the algebra and change the weights. Instead of the generators $\{T_a\}$, this system $\{H_k, E_{\pm\alpha}\}$ is equivalent as

the generators can be written as linear combinations of the second system. Further we want to remind the reader of the four group axioms: Closure, associativity, existence of a unique identity element as well as a unique inverse for each group element.

2.2 Coherent states of the harmonic oscillator

The CS are the ones most closely connected to the classical case as they minimize the Heisenberg uncertainty relation

$$\Delta q \Delta p = \frac{1}{2}. \quad (2.3)$$

Here q and p are respectively the coordinate and momentum of a particle in the phase space and we have chosen to work in the framework of natural units, aka $\hbar = 1$. Via the average $\langle \hat{A} \rangle$ of an operator \hat{A} , we can define its uncertainty

$$(\Delta A)^2 = \langle (\hat{A} - \langle \hat{A} \rangle)^2 \rangle. \quad (2.4)$$

Moving onwards, we will not make the distinction between an operator \hat{A} and the variable A as it can be easily figured out from the context. The operators q and p are considered to act on the standard Hilbert space \mathfrak{H} . Furthermore the vectors of the Hilbert space are indicated by $|\psi\rangle$ via Dirac's bra-ket-notation. We represent the scalar product with $\langle \varphi | \psi \rangle$ and the projection operator with $|\psi\rangle \langle \psi|$.

The remaining part of this section is dedicated to review the well known CS of the harmonic oscillator, to focus on some of its properties and then develop a definition to generalize this idea for arbitrary (Lie-)groups. We mainly follow the thread of Perelomov's book [Per86] and highlight deviations from it.

2.2.1 The Heisenberg-Weyl group

This group was first studied by Weyl [Wey28] and is a Lie group which is defined through its algebra.

Definition 2.1. A real three-dimensional Lie algebra with the commutation relations

$$[e_1, e_2] = e_3, \quad [e_1, e_3] = 0 = [e_2, e_3] \quad (2.5)$$

is called the Heisenberg-Weyl algebra (HWA).

The Heisenberg-Weyl group (HWG) is then constructed as usual via exponentiation of the elements of the algebra as in (2.2). We immediately see the relation to quantum mechanics as the coordinate and momentum operators acting in the Hilbert space \mathfrak{H} fulfill this algebra together with the identity operator $\mathbb{1}$:

$$[q, p] = i\mathbb{1}, \quad [q, \mathbb{1}] = 0 = [p, \mathbb{1}]. \quad (2.6)$$

When we study the harmonic oscillator with its Hamiltonian

$$H = \frac{p^2}{2} + \frac{q^2}{2} \quad (2.7)$$

it is convenient to use another set of operators, namely the annihilation and creation operators a and a^\dagger , where the \dagger means Hermitian conjugation. From their definition

$$a = \frac{q + ip}{\sqrt{2}} \quad \text{and} \quad a^\dagger = \frac{q - ip}{\sqrt{2}} \quad (2.8)$$

we can deduce the commutation relations

$$[a, a^\dagger] = \mathbb{1}, \quad [a, \mathbb{1}] = 0 = [a^\dagger, \mathbb{1}] \quad (2.9)$$

and see that they also fulfill the HWA.

In the case of the harmonic oscillator the annihilation and creation operator enable us to write the Hamiltonian (2.7) as a function of the number operator $N = a^\dagger a$. Thus we get the energy eigenstates as the eigenstates of N . The CS are then motivated as the eigenstates of the annihilation operator a . We are going to construct the CS of the HWG, show that these are the eigenstates of the annihilation operator and derive certain properties.

We can classify an element x of the HWA via three real parameters in the form of a real and a complex number, i.e. $s \in \mathbb{R}$ and $\alpha \in \mathbb{C}$:

$$x = is\mathbb{1} + \alpha a^\dagger - \bar{\alpha} a. \quad (2.10)$$

The $\bar{\cdot}$ represents complex conjugation and the signs and the factor i are pure convention from the fact of interpreting the elements e_i of the algebra (2.5) with q , p and $\mathbb{1}$ and then transforming to a and a^\dagger via (2.8). As mentioned before we get the group elements from exponentiation:

$$e^x = e^{is\mathbb{1}} e^{\alpha a^\dagger - \bar{\alpha} a} \equiv (s, \alpha). \quad (2.11)$$

We see from the commutation relation (2.9) of a and a^\dagger that they are annihilation and creation operator. In this basis we can define the representation of a group element with

$$D(\alpha) = e^{\alpha a^\dagger - \bar{\alpha} a} \quad (2.12)$$

which is called the displacement operator. It will be the subject and main point of interest in the following discussion. As we can see already from its definition it is a unitary operator and (2.12) gives us a unitary representation of the HWG.

Properties of the Heisenberg-Weyl group

For the properties of the HWG, it is important to look at the multiplication law of two group elements. For the first term in (2.11) with the identity matrix this is trivial and thus we are only left with the multiplication of two different displacement operators. To calculate this, we use the formula

$$e^X e^Y = e^{\frac{1}{2}[X,Y]} e^{X+Y} \quad (2.13)$$

which is a special case of the Baker-Campbell-Hausdorff formula¹

$$e^X e^Y = e^{Y+[X,Y]+\frac{1}{2!}[X,[X,Y]]+\frac{1}{3!}[X,[X,[X,Y]]]+\dots} e^X \quad (2.14)$$

if $[X, [X, Y]] = 0 = [Y, [X, Y]]$. In our case, viz $X = a$ and $Y = a^\dagger$, this is true per definition of the HWA in (2.5). This gives us the result

$$D(\alpha)D(\beta) = e^{i\text{Im}\alpha\bar{\beta}} D(\alpha + \beta) \quad (2.15)$$

Let us also take a closer look at the commutator between $D(\alpha)$ and the annihilation operator a :

Theorem 2.1. *The commutator $[a, D(\alpha)]$ is given by*

$$[a, D(\alpha)] = \alpha D(\alpha) \quad (2.16)$$

¹It was actually Schur [Sch91, Sch93] who did the first work on this formula. Then Campbell [Cam96, Cam97], Baker [Bak05] and Hausdorff [Hau06] did further remarks on it and their name stick with it. But it was Dynkin who eventually wrote it in this form [Dyn50].

Proof. First we consider the simpler case:

$$[a, \alpha a^\dagger - \bar{\alpha} a] = \alpha [a, a^\dagger] = \alpha \mathbb{1}. \quad (2.17)$$

Then we expand the exponential in $D(\alpha)$ in a Taylor series and thus we need to consider $[a, (\alpha a^\dagger - \bar{\alpha} a)^k]$:

$$[a, (\alpha a^\dagger - \bar{\alpha} a)^k] = k\alpha(\alpha a^\dagger - \bar{\alpha} a)^{k-1}. \quad (2.18)$$

This we will prove via induction; the case $k = 1$ is true as we saw in (2.17) and we only need to show that it is then also true for $k + 1$. Therefore we use the trivial property

$$[A, BC] = B[A, C] + [A, B]C \quad (2.19)$$

of the commutator and we get:

$$\begin{aligned} [a, (\alpha a^\dagger - \bar{\alpha} a)^k] &= (\alpha a^\dagger - \bar{\alpha} a)[a, (\alpha a^\dagger - \bar{\alpha} a)^{k-1}] + [a, (\alpha a^\dagger - \bar{\alpha} a)](\alpha a^\dagger - \bar{\alpha} a)^{k-1} \\ &= ((k-1)\alpha + \alpha)(\alpha a^\dagger - \bar{\alpha} a)^{k-1} = k\alpha(\alpha a^\dagger - \bar{\alpha} a)^{k-1}. \end{aligned}$$

In the second line we used the induction step and we have proved (2.18). Now we can summarize all the results which yields us the proof when we once rename the summing index:

$$\begin{aligned} [a, D(\alpha)] &= \sum_{k=0}^{\infty} \frac{1}{k!} [a, (\alpha a^\dagger - \bar{\alpha} a)^k] = \sum_{k=1}^{\infty} \frac{1}{k!} k\alpha(\alpha a^\dagger - \bar{\alpha} a)^{k-1} \\ &= \sum_{k=0}^{\infty} \frac{1}{k!} \alpha(\alpha a^\dagger - \bar{\alpha} a)^k = \alpha D(\alpha) \end{aligned}$$

□

This result will help us in [Sec. 2.2.2](#) to construct the [CS](#) from the vacuum state but first we take a look at the representations of our group.

Representations of the Heisenberg-Weyl group

(2.15) was Weyl's suggestion instead of the commutator relations (2.5) for defining the group. The questions that arises now is, if the unitary irreducible representation, i.e. (2.12), of the [HWG](#) is unique. It was Stone [[Sto30](#)] and then notably von Neumann

[Neu31] who addressed this problem and was stated in the famous *Stone-von-Neumann Theorem*:

Theorem 2.2. *Let $T_1(g)$ and $T_2(g)$ be two unitary irreducible representations of the HWG with elements $g = (s, \alpha)$. Then these representations are unitarily equivalent if $T_1(s, 0) = T_2(s, 0)$.*

We cannot prove this theorem but let us understand its meaning: The elements $(s, 0)$ (2.11) trivially commute with all elements of the group and thus are form the center. If $T(g)$ is a unitary irreducible representation of the whole group then $T(s, 0)$ forms a unitary representation of the subgroup $\{(s, 0)\}$ which can be parametrized by a real parameter λ . This λ is just the phase factor between $T(s, 0)$ and the representation of $\mathbb{1}$ as the subgroup only contains elements proportional to the identity. The theorem states that for a fixed value of λ , any representation can be brought into another one by a unitary transformation. This actually means that there is a unique representation which we will use to be (2.12).

2.2.2 The coherent states

As already said before, we now want to construct the CS of the harmonic oscillator. Then we will mention shortly some properties of these but will not go into many details as we will prove them anyways in the next section for the general case. The idea of this part is to motivate what is coming next, on the example of a well known case.

Consider a fixed vector $|\psi_0\rangle$ of our Hilbert space and the corresponding state consists of all vectors $e^{i\varphi} |\psi_0\rangle$ with $|e^{i\varphi}| = 1$. Thus all elements $(s, 0)$ of the HWG - and only those - leave the state $|\psi_0\rangle$ invariant; this is called the isotropy group \mathcal{H} of the state.

We now consider our representation

$$T(g) = T(s, \alpha) = e^{is\mathbb{1}} D(\alpha) \tag{2.20}$$

of the HWG from (2.12) and apply it on $|\psi_0\rangle$. This gives us the set of states $\{|\alpha\rangle\}$:

$$|\alpha\rangle = D(\alpha) |\psi_0\rangle . \tag{2.21}$$

The term $e^{is\mathbb{1}}$ in (2.20) gives us just a phase which does not alter the state $|\alpha\rangle$. This freedom of choice from the isotropy group allows us to take the vector $|\alpha\rangle$ defined

through $s = 0$ as the state to represent all states with the same α . From this we also see that different α lead to different states. Hence the complex number α completely determines the CS. Using [Thm. 2.1](#) we see that these states are eigenstates of the annihilation operator if $|\psi_0\rangle = |0\rangle$, the vacuum state, and thus are the familiar CS:

$$a|\alpha\rangle_0 \equiv aD(\alpha)|0\rangle = (D(\alpha)a + \alpha D(\alpha))|0\rangle = \alpha|\alpha\rangle_0.$$

If we take an arbitrary vector $|\psi_0\rangle$ of our Hilbert space then the states $|\alpha\rangle$ are called the generalized CS and in the special case $|\psi_0\rangle = |0\rangle$ we use the term ordinary CS. The later ones are well known from the harmonic oscillator. But we need not consider a special $|\psi_0\rangle$ to derive most of their properties as we will see in the following. In the following the term CS will refer to the generalized CS and we will mention the special case $|\psi_0\rangle = |0\rangle$ of the ordinary CS explicitly.

Two different CS are in general not orthogonal: Using [\(2.15\)](#) this is equivalent to $|\alpha\rangle$ being usually not orthogonal to $|\psi_0\rangle$ which can be seen easily in the case of ordinary CS. From the same equation we also conclude that an operator $T(g)$ takes one CS into another one. Especially the CS $|\alpha\rangle$ gets transformed into the state $|\alpha + \beta\rangle$ by $D(\beta)$. Thus the HWG acts on the complex plane as translation. This also implies that the integration measure over the α plane is given by

$$d\mu_\alpha = C d\alpha d\bar{\alpha} \tag{2.22}$$

where C is a constant to be chosen. Let us take a look at the following commutator:

$$[D(\alpha), \int d\mu_\beta |\beta\rangle \langle\beta|] = \int d\mu_\beta (|\alpha + \beta\rangle \langle\beta| - |\beta\rangle \langle\beta - \alpha|).$$

In the second integral we can change the integration variable to $\beta - \alpha$ because the CS are closed and we are left twice with the same integral and the commutator vanishes:

$$[D(\alpha), \int d\mu_\beta |\beta\rangle \langle\beta|] = 0. \tag{2.23}$$

From Schur's lemma [\[Geo99\]](#) we can conclude that $A = \int d\mu_\alpha |\alpha\rangle \langle\alpha|$ must be proportional to the unity operator as it commutes with all elements of the group. The proportionality constant can be chosen in such a way that we have

$$\int d\mu_\alpha |\alpha\rangle \langle\alpha| = \mathbb{1} \tag{2.24}$$

which also fixes C in [\(2.22\)](#). This result lets us expand an arbitrary state of the Hilbert

space in terms of the CS - thus they are a complete set and they span our Hilbert space. But our system of CS is even overcomplete, viz removing any states from it still leaves us with a complete set. This can be easily seen from a dimensional argument: The Hilbert space of the Harmonic oscillator is completely spanned from the eigenvectors of the number operator N . Thus it must be countably infinite dimensional but we have uncountably infinite many points α in the complex plane and thus as many CS. As already mentioned all these results are obtained without considering the state $|\psi_0\rangle$ from (2.21). The last property, we want to look at, is the fact that the ordinary CS are said to be the closest to the classical states in the sense that they minimize the Heisenberg uncertainty (2.3). This will give the fixed state $|\psi_0\rangle$ more meaning as a consequence. From (2.16) and the unitarity of our representation we get

$$D^\dagger(\alpha)aD(\alpha) = a + \alpha \quad (2.25)$$

and the same for a^\dagger by hermitian conjugation. Then we reverse the definition of a (2.8) and get a similar relation for q and p :

$$D^\dagger(\alpha)qD(\alpha) = q + \sqrt{2}\operatorname{Re}\alpha, \quad D^\dagger(\alpha)pD(\alpha) = p + \sqrt{2}\operatorname{Im}\alpha \quad (2.26)$$

and also for q^2 and p^2 if we just square both sides of these equations. This enables us to calculate the uncertainties of coordinate and momentum operator for the CS with (2.4):

$$\begin{aligned} (\Delta q)_\alpha^2 &= \langle \alpha | q^2 | \alpha \rangle - \langle \alpha | q | \alpha \rangle^2 = \langle \psi_0 | q^2 | \psi_0 \rangle - \langle \psi_0 | q | \psi_0 \rangle^2 = (\Delta q)_0^2 \\ (\Delta p)_\alpha^2 &= (\Delta p)_0^2. \end{aligned} \quad (2.27)$$

As a result we obtained that the uncertainties in the CS are independent of the state $|\alpha\rangle$ and are given only by $|\psi_0\rangle$ which will be later subject of [Thm. 2.6](#). Furthermore looking at (2.25) we recognize that $\langle \alpha | a | \alpha \rangle$ can vanish if we choose $\alpha = -\alpha_0$ with $\alpha_0 = \langle \psi_0 | a | \psi_0 \rangle$. As q and p are just sums of a and a^\dagger this also holds for them and we can assume without a loss of generality that $\langle q \rangle = 0 = \langle p \rangle$. From Heisenberg's uncertainty (2.3) relation follows:

$$0 \leq 2\Delta q \Delta p - 1$$

which we can multiply by a positive parameter $\lambda > 0$ and if we add something positive on the left side the inequality will still be true:

$$\begin{aligned} 0 &\leq 2\lambda\Delta q \Delta p - \lambda + (\lambda\Delta q - \Delta p)^2 \\ 0 &\leq \lambda^2(\Delta q)^2 - \lambda + (\Delta p)^2. \end{aligned}$$

We keep in mind that $\langle q \rangle = 0 = \langle p \rangle$ and can define the operator $A = \frac{\lambda q + ip}{\sqrt{2\lambda}}$ and get an inequality equivalent to Heisenberg's:

$$\langle A^\dagger A \rangle \geq 0, \quad \forall \lambda > 0. \quad (2.28)$$

To minimize this one, we need to have for some λ that $A|\psi_0\rangle = 0$. This is, among others, true for the vacuum state $|0\rangle$, i.e. $\lambda = 1$. We have now come to the result that the ordinary CS are really the ones closest to the classical one as they minimize the Heisenberg uncertainty relation.

Before moving forward to the generalized CS, we want to summarize quickly the main results of this section and the assumptions we put into. So first of all we managed to arrive at the well known CS from the harmonic oscillator. This was done via a construction with the displacement operator $D(\alpha)$ in such a way that we can easily generalize the idea in the following section. The CS are described completely by a complex number α due to the isotropy group. Notable properties of them are their closure under the displacement operator and their completeness. Thus we are able to construct a resolution of unity (RoU) and they span the entire Hilbert space. To get these results, we only needed the multiplication law (2.15) and the group properties of the HWG. When considering the ordinary CS then they are eigenstates of the annihilation operator and are among others the states closest to the classical ones. The CS having least uncertainty is only dependent on our choice of $|\psi_0\rangle$.

This section was more devoted to recollect the concept of CS of the harmonic oscillator which should be already known and to highlight their properties, which we will meet again in the generalized case. In the next section we will express the results in a more mathematical way. For a deeper understanding it might be helpful to go back and review the upcoming concepts on the case of this section.

2.3 Generalized coherent states

We will now generalize the idea from the previous section. Therefore consider a Lie group \mathcal{G} and a unitary irreducible representation $T(g)$, $g \in \mathcal{G}$, acting in the Hilbert space \mathfrak{H} . Then pick a fixed vector $|\psi_0\rangle$ and we can define the isotropy group [Dui00]:

Definition 2.2. All elements $h \in \mathcal{G}$ which leave the state $|\psi_0\rangle$ unchanged, i.e.

$$T(h) |\psi_0\rangle = e^{i\alpha(h)} |\psi_0\rangle, \quad |e^{i\alpha(h)}| = 1 \quad (2.29)$$

form the isotropy subgroup \mathcal{H} of $|\psi_0\rangle$.

Remark 2.1. The isotropy subgroup trivially is a subgroup of the whole group.

This enables us to define the generalized CS of Perelomov [Per86]:

Definition 2.3. The system of states $\{|\psi_g\rangle \mid |\psi_g\rangle = T(g) |\psi_0\rangle\}$ with elements g of a group \mathcal{G} and its representation $T(g)$ in the Hilbert space \mathfrak{H} is called the coherent state system (CSS) $\{T, |\psi_0\rangle\}$.

Let \mathcal{H} be the isotropy subgroup of the state $|\psi_0\rangle$. Then a point $x = x(g)$ in the coset space $\mathcal{X} = \mathcal{G}/\mathcal{H}$ determines the CS $|\psi_g\rangle$ completely with $|\psi_g\rangle = e^{i\alpha} |x\rangle$.

Remark 2.2. Consider two CS $|\psi_{g_1}\rangle$ and $|\psi_{g_2}\rangle$ which describe the same state, i.e.

$$T(g_1) |\psi_0\rangle = e^{i\alpha} T(g_2) |\psi_0\rangle \quad \Leftrightarrow \quad T(g_2^{-1} g_1) |\psi_0\rangle = e^{i\alpha} |\psi_0\rangle. \quad (2.30)$$

Thus per definition $g_2^{-1} g_1$ must be an element of the isotropy subgroup and this means that g_1 and g_2 are from the same coset \mathcal{X} . Consequently if g_1 and g_2 belong to different cosets of \mathcal{X} they also describe different CS. This enables us to pick a representer $x \in \mathcal{X}$ to completely describe a CS.

Remark 2.3. We will use the notations $|\psi_g\rangle$ and $|x\rangle$ exchangeable as they both describe the same state. But be aware that $|x\rangle$ is a representative of the coset \mathcal{X} . Due to the nature of the isotropy subgroup it is sufficient to only work in the framework of this coset, e.g. when later integrating over our space. In some particular situations we do not want to discuss each time in detail how to switch from one representative to another one by omitting phases and we will stick to $|\psi_g\rangle$.

As already mentioned when we refer to the CS in the rest of this work, we mean the generalized CS from this definition.

Properties of the generalized coherent states

We will formulate these properties as theorems to make it later easier to refer back to them. But most of the times we do not give a complete, detailed proof rather we will sketch the idea for one or it is evidently clear from the statements already made in [Sec. 2.2](#). Directly from the group axioms we get the first theorem:

Theorem 2.3. *The CS are a closed set as applying an operator $T(g')$ on a CS gives again a CS:*

$$T(g') |\psi_g\rangle = T(g'g) |\psi_0\rangle = T(g'') |\psi_0\rangle. \quad (2.31)$$

By assuming that our chosen state $|\psi_0\rangle$ is normalized, the unitarity of the representations grants us:

Theorem 2.4. *The CS are normalized to 1:*

$$\langle x|x\rangle = 1. \quad (2.32)$$

Remark 2.4. The same of course also holds for $|\psi_g\rangle$: $\langle \psi_g|\psi_g\rangle = 1$.

Furthermore if there exists a measure $d\mu_g$ for the whole group \mathcal{G} , we can construct the measure $d\mu_x$ in \mathcal{X} . This lets us define the operator

$$A = \int d\mu_x |x\rangle \langle x| \quad (2.33)$$

if we assume any convergence conditions. With a similar argument as before, i.e. [\(2.23\)](#), this operator must be proportional to the unity operator. The proportionality factor will be absorbed in the integration measure and we get with [Thm. 2.4](#) in mind:

Theorem 2.5. *The RoU of the CSS is given by*

$$\int d\mu_x |x\rangle \langle x| = \mathbb{1} \quad (2.34)$$

where the measure is defined to satisfy

$$\int d\mu_x |\langle x|y\rangle|^2 = \langle y|y\rangle = 1, \quad \forall y \in \mathcal{X}. \quad (2.35)$$

This last integral might not be convergent, but if it is we can do this construction in a meaningful way and the CSS is said to be square integrable. Hence we are again in the position to expand an arbitrary state $|\psi\rangle$ in terms of the CS.

When considering CS, we are interested in states closest to the classical ones and thus with minimal uncertainty. Moving from coordinate and momentum operator to two arbitrary operators A and B , then holds the Schrödinger uncertainty relation [Sch30]:

$$(\Delta A)^2(\Delta B)^2 \geq \left| \frac{1}{2} \langle \{A, B\} \rangle - \langle A \rangle \langle B \rangle \right|^2 + \frac{1}{4} | \langle [A, B] \rangle |^2 \quad (2.36)$$

with the definition of the variance in (2.4). The curly brackets in this equation are the anticommutator $\{A, B\} = AB + BA$. The problem however with this inequality (2.36) in contradistinction to (2.3) is that we have not a constant on the right-hand side in general. This means the equality sign can be achieved either via minimizing the left-hand side, maximizing the right-hand side or anything in between. Thus we need to find a universal criteria for uncertainty that we minimize and which is not dependent on our choice. But nevertheless we want to define this measure depending only on expectation values of our generators T_a . Thus one has to evaluate terms of the form $\langle O \rangle$ for $O = \prod_i T_{a_i}$ and in the case of the CS we have

$$\langle O \rangle = \langle \psi_g | O | \psi_g \rangle = \langle \psi_0 | T^\dagger(g) O T(g) | \psi_0 \rangle. \quad (2.37)$$

But this is just a group transformation and the form of O as well as the unitarity of our representation allow us to use a different set of generators

$$\tilde{T}_a = T^\dagger(g) T_a T(g) \quad (2.38)$$

and then also \tilde{O} and $\langle \tilde{O} \rangle$. Consequently we have proved with (2.37) the following theorem

Theorem 2.6. *The CS meet any measure of minimal uncertainty if and only if the fixed vector $|\psi_0\rangle$ meets it.*

Hence only our choice of this fixed state determines if the CS are closest to classical states or not. The question that arises now is, which criteria of uncertainty is a good measure. To move on, we restrict ourself to semisimple and compact Lie algebras like the $SU(n)$ and we can define the positive Cartan metric, viz the Killing form, from the structure constants of the algebra [Her66]:

$$g_{ab} = \frac{1}{2} f_{acd} f_{dbc}. \quad (2.39)$$

This enables us to define the quadratic Casimir operator

$$\mathbf{T}^2 = g_{ab}T_aT_b \quad (2.40)$$

where we only consider the case $g_{ab} = \delta_{ab}$ for $SU(n)$ and which commutes with all generators [Jac62]. The general case of g_{ab} can be treated similarly [Del77]. Then we can formulate the following theorem:

Theorem 2.7. *The invariant dispersion*

$$\langle(\Delta\mathbf{T})^2\rangle = \langle\delta_{ab}(T_a - \langle T_a\rangle)(T_b - \langle T_b\rangle)\rangle = \langle\delta_{ab}(T_aT_b - \langle T_a\rangle\langle T_b\rangle)\rangle. \quad (2.41)$$

is a relevant measure for the uncertainty.

Proof. This directly arises from the definition of the Casimir operator (2.40) and it is an invariant measure for our states. \square

Remark 2.5. If the reader is not yet comfortable with (2.41) being a good measure, we will motivate it from another point of view and additional examples in different groups can be found in [Del77]. (2.41) can be written in the form of:

$$(\Delta\mathbf{T})^2 = \sum_a (\Delta T_a)^2. \quad (2.42)$$

Then we can look at other terms of the form

$$(\Delta^j\mathbf{T})^2 = \sum_{\text{perm}} \left(\prod_{i=1}^j \Delta T_{a_i}\right)^2 \quad (2.43)$$

where our case (2.42) is $j = 1$. The sum is a sum over all permutations of all a_i with each other which lead to different products. Take for example the case when j is the number of generators, viz the dimension of the group, then we already have a product of the variances of all generators and there is no sum.

These terms in (2.43) are all possible terms that could be in general a measure for the uncertainty. Now we will see that only our choice $j = 1$ is a good and relevant measure in the following sense: For each other j there is always a group transformation which will minimize (2.43). But our uncertainty measure should be invariant under group transformations which we already implied in Thm. 2.6.

Consider the maximum case of j being the number of generators and we can always perform a group transformation into an eigenstate of one T_{a_i} and then $(\Delta T_{a_i})^2$ is

zero. As already mentioned, (2.43) is only a product in this case and thus the whole expression also vanishes. This cannot be a relevant measure for the uncertainty. Going to lower orders of j we are facing a similar problem [Del77]: The states minimizing (2.43) again are those which minimize an arbitrary $(\Delta T_{a_i})^2$. Finally only the case $j = 1$ from (2.41) is invariant under group transformation. Now it should be clear why we want to minimize (2.41) in order to have states closest to the classical ones which have minimal uncertainty.

Next we need to know which properties must the vector $|\psi_0\rangle$ have to meet our criteria of minimal uncertainty. To understand Perelomov's work [Per79a] on this subject we need first:

Definition 2.4. A subalgebra $\mathcal{B} \subset \mathcal{G}^c$ is called maximal if $\mathcal{B} \oplus \overline{\mathcal{B}} = \mathcal{G}^c$ where $\overline{\mathcal{B}}$ is the subalgebra conjugate to \mathcal{B} , i.e. all elements b^\dagger where $b \in \mathcal{B}$.

Remark 2.6. Here \mathcal{G}^c is the set of all linear combinations of elements of \mathcal{G} with complex coefficients, viz the complex hull of \mathcal{G} .

Definition 2.5. The set of elements $h \in \mathcal{G}^c$ with $T(h)|\psi_0\rangle = \alpha(h)|\psi_0\rangle$ form the isotropy subalgebra $\mathcal{H} = \{h\}$.

Remark 2.7. The isotropy subalgebra is trivially a subalgebra of the whole algebra and the set $\{g|g = e^{ih}\}$ is the isotropy subgroup defined in Def. 2.2.

Then we can formulate the following theorem [Per79a]

Theorem 2.8. *The states with maximal isotropy subalgebra are the states which minimize the uncertainty (2.41).*

The proof given by Perelomov can not be understood from our current point of view but we want to prove the following two theorems which will give us a prove of Thm. 2.8.

Theorem 2.8.1. *The maximal weight states are the states which minimize the uncertainty.*

Theorem 2.8.2. *If and only if a state $|\psi\rangle$ is a maximal weight state then it has a maximal isotropy subalgebra.*

Remark 2.8. First we need to clarify the term 'maximal weight states': We choose the canonical basis of eigenstates $|\mathbf{h}\rangle$ of the Cartan operators H_k as mentioned in Sec. 2.1. The weights of theses states are the eigenvalues h_k : $H_k|\mathbf{h}\rangle = h_k|\mathbf{h}\rangle$. The states which

maximize $|\mathbf{h}|^2 = h_k h_k$ are the maximal weight states. In contradistinction the highest weight state is the state which gets annihilated by all raising operators. Equivalently we can define a lowest weight state [Ram10] and both are maximum weight states. Take for example the SU(2) spin one representation. Then the spin-z $|1\rangle$ state is the highest weight state, the spin-z $|-1\rangle$ state is the lowest weight state and both are states of maximum weight. The spin-z $|0\rangle$ state is neither and does not minimize the uncertainty in contrast to the other two, according to Thm. 2.8.1. This can be done in an easy exercise and we will do it explicitly on page 28. We will see later that we have a freedom of choosing the highest weight state among the maximum weight states which enables us to prove Thm. 2.8.2.

Proof of Thm. 2.8.1. Following the arguments of [DF77] we see that $(\Delta T)^2$ is a positive definite operator which has a lowest eigenvalue. In the corresponding state we get the lowest expectation value. Therefore we first search for the eigenstates and then choosing the ones with minimal uncertainty. From (2.41) we see that the eigenstates of $(\Delta T)^2$ must fulfill:

$$(T_a T_a - 2T_a \langle T_a \rangle_\psi + \langle T_a \rangle_\psi \langle T_a \rangle_\psi) |\psi\rangle = \lambda |\psi\rangle. \quad (2.44)$$

As any vector of our Hilbert space is an eigenstate of the quadratic Casimir operator, which must be proportional to $\mathbb{1}$, $|\psi\rangle$ is an eigenstate of the first term. Further it is trivially an eigenstate of the last term and we only need to find eigenstates of the second term. Next we take the already mentioned eigenstates $|\mathbf{h}\rangle$ of the Cartan operators H_k . We will show that they are a valid choice for $|\psi\rangle$ and afterwards we find the most general $|\psi\rangle$. Besides the Cartan operators H_k , the other generators are linear combinations of the raising and lowering operators $E_{\pm\alpha}$ and thus their expectation value of a state $|\mathbf{h}\rangle$ vanishes which results in:

$$T_a \langle T_a \rangle_{\mathbf{h}} |\mathbf{h}\rangle = H_k \langle H_k \rangle_{\mathbf{h}} |\mathbf{h}\rangle = h_k h_k |\mathbf{h}\rangle. \quad (2.45)$$

This way, we already showed the first statement that the $|\mathbf{h}\rangle$ are a valid choice for $|\psi\rangle$. Then the line of arguments in [DF77] lead us back to the basic idea of Thm. 2.6: Note that it is always possible to find a group transformation which transforms $T_a v_a$ into the Cartan subalgebra $H_k a_k$ with \mathbf{v} and \mathbf{a} being unit vectors in the whole space of the algebra and a r -dimensional space, respectively. Thus we can write

$$T^{-1}(g) T_a v_a T(g) = H_k a_k \quad (2.46)$$

and as this is possible for any \mathbf{v} we can make the choice $v_a = \frac{\langle T_a \rangle_\psi}{\sqrt{\langle T_b \rangle_\psi \langle T_b \rangle_\psi}}$ and apply (2.46) on $|\mathbf{h}\rangle$. Then applying from left $T(g)$ and with $|\psi\rangle = T(g)|\mathbf{h}\rangle$ we get:

$$\frac{T_a \langle T_a \rangle_\psi}{\sqrt{\langle T_b \rangle_\psi \langle T_b \rangle_\psi}} |\psi\rangle = h_k a_k |\psi\rangle. \quad (2.47)$$

This is essentially the eigenstate equation we are trying to solve. Now as we already saw $|\psi\rangle = |\mathbf{h}\rangle$ solves this equation with $a_k = \frac{h_k}{|\mathbf{h}|}$ leading to (2.45). As the inner product of (2.47) with $\langle\psi|$ is invariant under group transformation, for $|\psi\rangle = T(g)|\mathbf{h}\rangle$ we have:

$$T_a \langle T_a \rangle_\psi |\psi\rangle = h_k h_k |\psi\rangle. \quad (2.48)$$

This is the most general solution because from our construction we found all eigenstates $|\psi\rangle$ with eigenvalue $h_k h_k$. Furthermore if there would be eigenstates with another eigenvalue, then this is in contradiction to (2.45) as we can always do a group transformation of the kind of (2.46). The nice conclusion of these arguments is that this is a motivation for Perelomov's definition of generalized CS in Def. 2.3 especially as $T(g)$ is an element of the coset space \mathcal{G}/\mathcal{H} when looking at (2.46). Thus as stated already we only need to consider $|\mathbf{h}\rangle$, which are our $|\psi_0\rangle$ in this case, in order to get states of least uncertainty and then the CS are the states with the same property.

Hence going back to find the states $|\mathbf{h}\rangle$ which minimize (2.41), we see that this is equivalent to maximizing $\langle T_a \rangle \langle T_a \rangle$ because all terms are positive as they are quadratic. Thus for $|\mathbf{h}\rangle$ we need to maximize $h_k h_k$ which are the maximum weight states. \square

Proof of Thm. 2.8.2. The basic idea for this proof emerges from the fact that we are completely free in defining positive weights and so also positive roots by choosing the order of the Cartan operators [Geo99]. In addition inherently there is no difference between positive and negative [Ram10], i.e. the pair E_\pm of raising and lowering operators, and any maximum weight state can be defined as a highest weight state. This is nothing else than the so called Weyl group [Geo99]. Further the systems $\{H_k, E_{\pm\alpha}\}$ spans \mathcal{G}^c as already noted in Sec. 2.1.

\Rightarrow : Assuming $|\psi\rangle$ is a maximal weight state, then $|\psi\rangle$ can be defined to be an eigenstate with eigenvalue zero of all raising operators E_α , i.e. α being positive. Then the isotropy subalgebra $\mathcal{B} = \{H_k, E_\alpha\}$ is a maximal subalgebra.

\Leftarrow : For the algebra \mathcal{B} being maximal it must contain at least one operator of each pair of $E_{\pm\alpha}$. This member can always be taken to correspond to a positive root α and

then $|\psi\rangle$ must be a highest weight state [Dui00] which is unique [Her66]². Thus it is a maximal weight state. \square

This now proves Thm. 2.8 and the states with maximal subalgebra, i.e. the maximal weight states, chosen as $|\psi_0\rangle$ give us CS closest to the classical one.

Before moving on to the special case of SU(2) and SU(3) CS, we want to quickly review this section. We constructed the CS of the harmonic oscillator and then it was possible to generalize this for any group. There we found the same properties and relations. These are notably the closure, the normalization and the construction of a RoU of the CS. The proofs of the respective theorems are possible as they are only based upon the group axioms, using an unitary irreducible representation of it and the existence of a square integrable measure on the group. Finally we found a universal criteria for the CS being closest to the classical case as they minimize our uncertainty measure (2.41). In doing so we saw that the uncertainty inequality is not a good measure and motivated our new criteria. There are certain cases when the Schrödinger uncertainty relation (2.36) is equivalent to our criteria of uncertainty if we work in a certain basis. This is used by Perelomov in his book [Per86] in the case of SU(2) but we will stick to our universal measure as we can apply it independently. Now we move on to construct the CS for the special case of SU(n).

²Or rather look at [Jac62] for a proof.

3 Coherent states for SU(n)

With the work of the previous chapter the main focus of this part is mainly on how to construct the CS of SU(n). We will see the statements from the general case on these examples of SU(n) explicitly SU(2) and SU(3). We will focus on these two case as the first one is still relatively simple and the second is relevant for the color of QCD.

3.1 SU(2)

First we are constructing the CS of SU(2) on the basis of [Per86] in a way that is easy to understand. But this method is not generalizable to the case of SU(n) with $n > 2$ and thus we introduce another construction method for the CS of SU(2). This one we apply on the SU(3) case and show how it can be applied for any SU(n). To get started we know from Def. 2.3 that we need a representation of our group.

3.1.1 Representation of SU(2)

Sticking to our notation in Sec. 2.1, we will use the indices a, b, \dots for the adjoint representation (AdR) which then run from 1 to $(n^2 - 1)$, the number of Cartan generators. The indices i, j, \dots are used for the fundamental representation (FuR) and run from 1 to n for a general SU(n). This might be a bit unfamiliar in the case of SU(2) where the Lie-Algebra is given by [Geo99]

$$[J_a, J_b] = i\varepsilon_{abc}J_c. \tag{3.1}$$

Here we inserted the structure constant of SU(2) which is just the Levi-Civita symbol and use the common notation of J_a for the generators. In the case of the FuR the

generators are given via the Pauli-Spin-matrices:

$$[J_a^{j=\frac{1}{2}}]_{ij} = \frac{1}{2}[\sigma_a]_{ij} \quad (3.2)$$

$$\sigma_1 = \begin{pmatrix} 0 & 1 \\ 1 & 0 \end{pmatrix}, \quad \sigma_2 = \begin{pmatrix} 0 & -i \\ i & 0 \end{pmatrix}, \quad \sigma_3 = \begin{pmatrix} 1 & 0 \\ 0 & -1 \end{pmatrix}.$$

With the generators we can construct the raising and lowering operators of our algebra, i.e. $J_{\pm} = J_1 \pm iJ_2$, which fulfill with (3.1):

$$[J_3, J_{\pm}] = \pm J_{\pm}, \quad [J_+, J_-] = 2J_3. \quad (3.3)$$

We take the canonical basis of the vectors $|j, \mu\rangle$ which are eigenvectors of J_3 and \mathbf{J}^2 with the eigenvalues μ and $j(j+1)$, respectively. Where j is a half-integer defining the dimension of our representation, viz

$$\dim_{\text{rep}} = 2j + 1, \quad (3.4)$$

and μ ranges from $-j$ to j in steps of 1. These definitions give us the following action of the raising and lowering operators on the basis states [Geo99]:

$$\begin{aligned} J_+ |j, \mu\rangle &= N_{\mu+1} |j, \mu + 1\rangle \\ J_- |j, \mu\rangle &= N_{\mu} |j, \mu - 1\rangle \\ N_{\mu} &= \sqrt{(j + \mu)(j - \mu + 1)}. \end{aligned} \quad (3.5)$$

3.1.2 Coherent states of $SU(2)$

Now let g be the elements of $\mathcal{G} = SU(2)$ and we take as fixed state $|\psi_0\rangle = |j, -j\rangle$ to construct the CSS. This way according to Thm. 2.8 we are constructing CS which minimize our uncertainty criteria (2.41). Each element of $SU(2)$ can be represented by the Euler angles with [Per77]

$$T(g) = e^{i\varphi J_3} e^{i\theta J_2} e^{i\psi J_3}, \quad \varphi, \psi \in [0, 2\pi] \wedge \theta \in [0, \pi]. \quad (3.6)$$

The Euler angles are known to be an equivalent description of a general rotation in a three dimensional space which leads to this equation. This is a very heuristic point of view based on well known facts. The equivalence can be either shown directly via a concrete calculation in the case of $j = \frac{1}{2}$ where the J_a are given as the Pauli-Spin-

matrices (3.2). This grants the general validity of (3.6) as this is independent of j and thus it is valid for all j if it is valid for one. To show this, one needs to show the equivalence of this equation to $e^{\alpha_a J_a}$. This is also equivalent to $\prod_{a=1}^3 e^{\alpha'_a J_a}$ which can also be shown easily for the FuR. But a more mathematical proof and also motivation of this Euler representation (3.6) will be discussed later in Sec. 3.3 when we have introduced the necessary concepts for a different purpose.

We can use the Baker-Campbell-Hausdorff formula (2.14) to exchange the order of the first two exponential functions in (3.6). The nested commutators give the following results with $X = i\varphi J_3, Y = i\theta J_2$:

$$\begin{aligned} Y &= i\theta J_2 \\ [X, Y] &= i\theta \cdot (i\varphi) \cdot i \cdot (-J_1) \\ [X, [X, Y]] &= i\theta \cdot (i\varphi)^2 \cdot i^2 \cdot (-J_2) \\ &\dots \end{aligned} \tag{3.7}$$

These three lines should be enough to recognize the pattern and we are at a point proportional to Y and can use the first step again. Sorting the terms with J_2 and J_3 , this results in:

$$\begin{aligned} T(g) &= \exp\left(i\theta \left[J_2 \sum_{n=0}^{\infty} (-1)^n \frac{\varphi^{2n}}{(2n)!} + J_1 \sum_{n=1}^{\infty} (-1)^{n-1} \frac{\varphi^{2n-1}}{(2n-1)!} \right]\right) e^{i(\varphi+\psi)J_3} \\ &= e^{i\theta(J_2 \cos \varphi + J_1 \sin \varphi)} e^{i\chi J_3} . \end{aligned} \tag{3.8}$$

As we are in a basis of eigenvectors of J_3 the isotropy subgroup is just given by all elements of the form $h = e^{i\chi J_3}$ and thus the CS can be characterized by a unit vector

$$\mathbf{n} = \begin{pmatrix} \sin \theta \cos \varphi \\ \sin \theta \sin \varphi \\ \cos \theta \end{pmatrix}. \tag{3.9}$$

This means setting the phase χ from the last term in (3.8) to zero and the vector \mathbf{n} is the representative describing the CS completely:

$$|\psi_g\rangle = |\mathbf{n}\rangle = e^{i\theta \mathbf{m} \cdot \mathbf{J}} |j, -j\rangle \equiv D(\mathbf{n}) |j, -j\rangle. \tag{3.10}$$

Where we have defined $\mathbf{m} = (\sin \varphi, \cos \varphi, 0)^T$. Furthermore we can replace J_1 and J_2 by a combination of J_{\pm} from [Sec. 3.1.1](#) to get the following representation:

$$D(\xi) = e^{\xi J_+ - \bar{\xi} J_-}, \quad \xi = \frac{\theta}{2} e^{i\varphi} \quad (3.11)$$

which resembles the displacement operator [\(2.12\)](#) for the harmonic oscillator [CSS](#). The so called normal form [\[Per86\]](#) of this operator [\(3.11\)](#) is given by

$$D(z) = e^{z J_+} e^{\eta J_0} e^{-\bar{z} J_-}, \quad z = \tan \frac{\theta}{2} e^{i\varphi} \quad \text{and} \quad \eta = \ln(1 + |z|^2). \quad (3.12)$$

The equivalence of [\(3.11\)](#) and [\(3.12\)](#) is independent of j and thus it is sufficient to show that it is valid for $j = \frac{1}{2}$ as already mentioned above. This calculation is straightforward and does not give any interesting insight. Recalling the domain of θ from [\(3.6\)](#), we see that z is well defined as $\tan \theta \in [0, \infty[$ and z is just a number in the complex plane. Thus again a complex number is enough to completely describe our [CS](#). The vector \mathbf{n} represents a point on a unit sphere in three dimensional space. The transition from \mathbf{n} to z is only a stereographic projection from the sphere to the plane.

Our task now is to act with the operator D on the fixed state $|\psi_0\rangle = |j, -j\rangle$ to get a representation of the [CSS](#) in the $SU(2)$ basis. This will be done with [\(3.12\)](#), as the action of J_- and J_0 on $|j, -j\rangle$ is known:

$$|\psi_g\rangle = |z\rangle = e^{-j\eta} e^{z J_+} |j, -j\rangle = (1 + |z|^2)^{-j} e^{z J_+} |j, -j\rangle. \quad (3.13)$$

Thus we only need to compute the action of the first exponential from [\(3.12\)](#) with J_+ on the fixed state. We expand this exponential in its Taylor series and from [\(3.5\)](#) we get (for $k \leq 2j$)

$$(J_+)^k |j, -j\rangle = \prod_{i=1}^k \sqrt{(j-j+i)(j+j-i+1)} |j, -j+n\rangle \quad (3.14)$$

and all higher powers vanish. We write the products as quotients of factorials, plug it into the Taylor series $e^{z J_+} = \sum_{k=0}^{\infty} \frac{(z J_+)^k}{k!}$, do the transformation $k \rightarrow j + \mu$ and get:

$$|z\rangle = (1 + |z|^2)^{-j} \sum_{\mu=-j}^j z^{j+\mu} \sqrt{\frac{(2j)!}{(j+\mu)!(j-\mu)!}} |j, \mu\rangle. \quad (3.15)$$

This is in accordance with the results in the book of Perelomov [\[Per86\]](#) but we write them now in a nicer way which will simplify some of the following steps. We plug in

the definition of z from (3.12), write the tangent in the first term as a quotient of sine and cosine and make the replacement $\omega = \frac{\theta}{2}$:

$$|z\rangle = (\cos \omega)^{2j} \sum_{\mu=-j}^j e^{i\varphi(j+\mu)} (\tan \omega)^{j+\mu} \sqrt{\frac{(2j)!}{(j+\mu)!(j-\mu)!}} |j, \mu\rangle, \quad \omega \in [0, \frac{\pi}{2}]. \quad (3.16)$$

Closure

As we saw in the previous Ch. 2, applying an operator D , e.g. (3.12), onto a CS must result in another CS. But we just saw that multiplying group elements of $SU(2)$ is not an easy task as the sum in the Baker-Campbell-Hausdorff formula (2.14) does not terminate, viz (3.7). Thus here we only state the multiplication law of two operators D from [Per86]:

$$D(\mathbf{n}_1)D(\mathbf{n}_2) = D(\mathbf{n}_3) e^{i\Phi(\mathbf{n}_1, \mathbf{n}_2)J_3} \quad (3.17)$$

where Φ is given by the area of the spherical triangle given by \mathbf{n}_1 , \mathbf{n}_2 and the north pole of our sphere, aka $(0, 0, 1)^T$. This can be shown through a direct calculation in the $j = \frac{1}{2}$ representation of $SU(2)$ as the equality is independent of j .

Acting with (3.17) on our fixed state the exponential just gives a phase and thus an equivalent CS to the one represented via \mathbf{n}_3 . This is true if our vector $|\psi_0\rangle$ is an eigenstate of J_3 , otherwise we can always perform a group transformation into a system where $|\psi_0\rangle$ is eigenstate to the new \tilde{J}_3 and the arguments hold in this new system.

Scalar product of two coherent states

Per Definition, the CS are normalized as the operator D is unitary and the fixed state is also normalized, but two different CS are not orthogonal to each other. We use (3.15) and the orthonormality between two basis states of $SU(2)$ to obtain:

$$\langle z|y\rangle = \left((1 + |z|^2)(1 + |y|^2) \right)^{-j} \sum_{\mu=-j}^j \frac{(2j)!}{(j+\mu)!(j-\mu)!} \bar{z}^{j+\mu} y^{j+\mu}. \quad (3.18)$$

We change μ that we sum from 0 to $2j$ and get a representation of the binomial $(1 + \bar{z}y)^{2j}$ [GR94, 1.111]:

$$\langle z|y\rangle = \left((1 + |z|^2)(1 + |y|^2) \right)^{-j} (1 + \bar{z}y)^{2j} \quad (3.19)$$

Here we consider the scalar product of two CS in the representation of a point on the plane. We can also take the inner product in the representation on the sphere. For further applications we are just interested in the absolute value of this quantity which is given by

$$|\langle \mathbf{n}_1 | \mathbf{n}_2 \rangle|^2 = \left(\frac{1 + \mathbf{n}_1 \cdot \mathbf{n}_2}{2} \right)^{2j} \quad (3.20)$$

The equivalence of (3.20) and the square of the absolute value of (3.19) can be shown by putting in the stereographic projection from (3.12) and the relations [GR94, 1.313]

$$\begin{aligned} \cos \theta &= \cos^2 \frac{\theta}{2} - \sin^2 \frac{\theta}{2} \\ \sin \theta &= 2 \sin \frac{\theta}{2} \cos \frac{\theta}{2}. \end{aligned} \quad (3.21)$$

Resolution of unity

According to Thm. 2.5 the operator

$$\int d\mu_z |z\rangle \langle z| \quad (3.22)$$

is proportional to $\mathbb{1}$. We will chose the integration measure [Per86]

$$d\mu_z = d\theta d\varphi \sin \theta \frac{2j+1}{4\pi} \equiv d\mathbf{n} \frac{2j+1}{4\pi} \quad (3.23)$$

and will show below that this results in the right normalization. Further this measure is very easy to motivate: First we have the known measure on the surface of the unit sphere and divide with the volume of our integration domain, i.e. 4π . The factor $2j+1$ is just the dimension of our representation as stated in (3.4). We will see the same structure of the integration measure later again in the $SU(3)$ case in (3.69). Using our convention from (3.16), we make the substitution $\theta = 2\omega$, use (3.21) and we get:

$$d\mu_z = d\omega d\varphi \sin \omega \cos \omega \frac{2j+1}{\pi}. \quad (3.24)$$

For our purpose this will be the measure of choice as we need a compact manifold as integration domain when performing numerical integration. Then we cannot integrate over the whole plane. For completeness we will also state the measure for the representation of the CS in (3.15). Recalling that z is just a complex number in polar coordinates with radius $\tan \omega$ we can calculate the Jacobian and eventually get the

result:

$$d\mu_z = \frac{2j+1}{\pi(1+|z|^2)^2} dz d\bar{z}. \quad (3.25)$$

Now we go back to prove that (3.22) is indeed the RoU with the correct measure (3.24) and plug in (3.16):

$$\int d\omega d\varphi \sin \omega \cos \omega \frac{2j+1}{\pi} (\cos \omega)^{4j} \sum_{\mu=-j}^j \sum_{\mu'=-j}^j e^{-i\varphi(\mu-\mu')} (\tan \omega)^{2j+\mu+\mu'} \mathcal{F}(\mu) \mathcal{F}(\mu') |j, \mu\rangle \langle j, \mu'|.$$

Where we defined $\mathcal{F}(\mu) = \sqrt{\frac{(2j)!}{(j+\mu)!(j-\mu)!}}$ and we can easily perform the integration over φ which results in a Kronecker Delta $\delta_{\mu\mu'} 2\pi$. Thus we can evaluate one sum, plug in sine and cosine into the tangent, use the well known identity [GR94, 1.312]

$$\sin^2 \omega = 1 - \cos^2 \omega \quad (3.26)$$

and finally we make the substitution $u = \cos \omega$ which results in:

$$\sum_{\mu=-j}^j 2(2j+1) \mathcal{F}(\mu)^2 |j, \mu\rangle \langle j, \mu| \int_0^1 du \frac{(1-u^2)^{j+\mu}}{u^{2(\mu-j)-1}}.$$

To solve this integral we take a look into the tables of Gradshteyn [GR94, 8.380]: We see that the integral is nothing else as the definition of the beta function:

$$B(x, y) = 2 \int_0^1 du u^{2x-1} (1-u^2)^{y-1} \quad (3.27)$$

and we can identify our values: $x = j - \mu + 1$ and $y = j + \mu + 1$. Then using [GR94, 8.384.1], we can express the beta function in terms of gamma functions [GR94, 8.310] and thus factorials:

$$\int_0^1 du \frac{(1-u^2)^{j+\mu}}{u^{2(\mu-j)-1}} = \frac{(j-\mu)!(j+\mu)!}{2(2j+1)!} \quad (3.28)$$

In our case of integer exponents, this result can also be obtained via integration by parts of (3.27) as the boundary terms always vanish. Our result (3.28) is nothing else then $(2(2j+1)\mathcal{F}(\mu)^2)^{-1}$ and putting everything together, we have proved the RoU:

$$\int d\mu_z |z\rangle \langle z| = \sum_{\mu=-j}^j |j, \mu\rangle \langle j, \mu| = \mathbb{1}. \quad (3.29)$$

Minimizing the uncertainty

As already mentioned above our choice of the fixed state $|\psi_0\rangle = |j, -j\rangle$ as a maximal weight state guarantees us that the CS are states minimizing our uncertainty measure (2.41). Our goal is to get new insights into the color-flow of QCD and therefore we need to be as close to the classical case as possible. This is why we constructed the CS this way.

We can verify this fact by evaluating (2.41) for the CS explicitly in the FuR and AdR:

$$\frac{(\Delta T)^2}{\left| \begin{array}{c|cc|cc|c} & \left| \frac{1}{2}, \frac{1}{2} \right\rangle & |z\rangle_{\text{FuR}} & |1, 1\rangle & |z\rangle_{\text{AdR}} & |1, 0\rangle \\ \hline (\Delta T)^2 & \frac{1}{2} & \frac{1}{2} & 1 & 1 & 2 \end{array} \right.}.$$

We see that the uncertainty for the highest weight state as well as the CS is always the same. Furthermore the state $|1, 0\rangle$ of the AdR is not a maximal weight state and thus the uncertainty is not minimal.

Simplified representation of the $SU(2)$ coherent states

When reviewing the calculation of the RoU, we recognize that only the integration over φ was important to obtain the RoU as this already gives us the Kronecker Delta. The left over integration over ω is just responsible for the right normalization and we can formulate the following theorem.

Theorem 3.1. *The RoU of the $SU(2)$ CS can be written as*

$$\frac{2j+1}{2\pi} \int d\varphi |\varphi\rangle \langle \varphi| = \mathbb{1}, \quad \text{with } |\varphi\rangle = \frac{1}{\sqrt{2j+1}} \sum_{\mu=-j}^j e^{i\varphi(j+\mu)} |j, \mu\rangle. \quad (3.30)$$

This just means that we can simplify the calculation of the integral in the RoU especially when we are doing numerics. This also applies to integrations of squared absolute values

$$\int d\mu_z d\mu_{z'} |\langle z|O|z'\rangle|^2 = \int d\varphi d\varphi' |\langle \varphi|O|\varphi'\rangle|^2 \quad (3.31)$$

with an arbitrary operator O . We have chosen the states $|\varphi\rangle$ of Thm. 3.1 to be normalized and for the FuR they are obtained via setting $\omega = \frac{\pi}{4}$ of the CS in (3.16).

But for the AdR upwards this is not possible as we cannot account for the factorial terms in (3.16). This seems at first like a contradiction as we have two different RoU but this is possible due to the fact of the overcompleteness of our CSS. One can imagine that one shifts portions of certain CS to other CS as they are linear dependent. This ambiguity of composing not only the $\mathbb{1}$ but also any state or other operator in terms of CS will be again touched in Sec. 4.3.2. But as the states $|\varphi\rangle$ are no subset of our CS in general, they are also not supposed to minimize the uncertainty (2.41). This gives the following values:

$$\frac{(\Delta T)^2}{|\varphi\rangle_{\text{FuR}} \quad |\varphi\rangle_{\text{AdR}}} \left| \begin{array}{cc} \frac{1}{2} & \frac{10}{9} \end{array} \right.$$

and comparing with the previous section we see that for the FuR the states $|\varphi\rangle$ are minimizing the uncertainty as expected as they can be derived from our CS of before. But in the case of the AdR this is different and the states $|\varphi\rangle$ are no longer closest to the classical ones. Recalling our motivation that we want to use states with minimal uncertainty due to the Lund string model [And⁺83], we see that the states $|\varphi\rangle$ are not our desired states. But nevertheless the simplification from Thm. 3.1 are a mathematical trick to save us some calculation as we need to perform less integrals. This will be helpful when we are doing numerics. As we saw for the FuR the states $|\varphi\rangle$ are a subset of our actual CS of $SU(2)$ but for the AdR and higher representation this is not the case anymore. Thus when we are averaging over all initial and final states anyways, we can use the states $|\varphi\rangle$ to completely calculate the color factors of a process. But if there are particles we do not want to average, then these states give different results than the CS $|z\rangle$ (3.16). This is for example the case if we look at our process with particular initial states and do not want to average over all possible initial states. On the other hand we almost always average over final states and thus for processes with colorless initial states, we can use the states $|\varphi\rangle$ anyways. However if we want to study the color-flow, then be aware that the parameters of the states $|\varphi\rangle$ for the AdR are slightly different from the ones of the CS $|z\rangle$.

3.1.3 Another way to construct the $SU(2)$ coherent states

When we were constructing the CS in the previous section we used the representation of the Lie group, the isotropy group of $|\psi_0\rangle$ and the corresponding coset space. The problem when doing this is that the commutator $[J_3, [J_3, J_2]]$ does not vanish as in

the case of the HWG (2.9). This means we can not just simply use the formula (2.13) as before but need the general case of the Baker-Campbell-Hausdorff formula (2.14) when manipulating (3.6) to calculate (3.8). When we are constructing the $SU(3)$ CS these calculations will be even more difficult and thus we will present another way of constructing the $SU(2)$ CS via annihilation and creation operator, therefore similar to the HWG. For this task we mainly follow the ideas from Mathur and Sen [MS01] but we deviate their construction a bit to resemble more the $SU(3)$ case later on.

This means we construct all representations from the FuR 2 and its conjugate $\bar{2}$. This procedure is actually too much when only considering the $SU(2)$ case as we have a redundancy in it. This is due to the fact that the rank of $SU(2)$ is only one and it would suffice to use only one representation of the two, as the other one is equivalent to it. But as $SU(3)$ has rank two we will have to use the representations 3 and $\bar{3}$ in this case. This idea can then be generalized to any $SU(n)$ [MM02] by just taking a number of basic representations equal to the rank of the group, viz $n - 1$, and repeat this scheme.

Schwinger representation of $SU(2)$

First we need annihilation and creation operators satisfying the HWA (2.5) and which allow us to implement the $SU(2)$ algebra (3.1). To achieve this we use the Schwinger representation of the $SU(n)$ group [Sch52, Mat81]: As discussed above we want to construct all representations of $SU(2)$ from its FuR which is two dimensional and thus we use a pair of operators $(a_1, a_2)^T \equiv \mathbf{a}$ and its hermitian conjugate satisfying $[a_i, a_j^\dagger] = \delta_{ij} \mathbb{1}$ and all other commutators vanish. Then consider the operators

$$J_a = \frac{1}{2} a_i^\dagger [\sigma_a]_{ij} a_j. \quad (3.32)$$

and it is an easy task to check that these operators fulfill the $SU(2)$ algebra (3.1) and that the well known Casimir operator is

$$\mathbf{J}^2 = \mathbf{J} \cdot \mathbf{J} = J_a J_a = \frac{1}{4} \mathbf{a}^\dagger \cdot \mathbf{a} (\mathbf{a}^\dagger \cdot \mathbf{a} + 2). \quad (3.33)$$

Knowing that the eigenvalues of \mathbf{J}^2 are $j(j + 1)$, we can define the operator \hat{j} which has the eigenvalues j :

$$\hat{j} = \frac{1}{2} \mathbf{a}^\dagger \cdot \mathbf{a} = \frac{1}{2} (\hat{N}_1 + \hat{N}_2) \quad (3.34)$$

Here we introduced the number operators $\hat{N}_i = a_i^\dagger a_i$ which have eigenvalue N_i . Then we can use the eigenstates $|N_1, N_2\rangle$ of these operators from the Fock space [Foc32]. Further we see from (3.32) and (3.33) that \mathbf{J}^2 and J_3 can be expressed in terms of $\hat{\mathbf{N}} = (\hat{N}_1, \hat{N}_2)$ and thus the states $|N_1, N_2\rangle$ are also eigenstates of these. This enables us to calculate j from the sum and μ from the difference of N_1 and N_2 . Hence we have a one-to-one correspondence between the states $|j, \mu\rangle$ of SU(2) and $|N_1, N_2\rangle$ of the Fock space and we can just continue in the number basis. This is also possible because when constructing all representations of SU(2) from tensor products of the FuR, we are always looking at the highest dimensional, irreducible representation contained in the product space. This representation is always the totally symmetric one and the Fock states are a complete system of totally symmetric states of our Hilbert space [Sch08].

With the given definitions, the index $i = 1$ is referring to the number of states N_1 with $\mu = \frac{1}{2}$ and the other index to N_2 with $\mu = -\frac{1}{2}$ in the 2 representation. It is a nice exercise left to the reader to show that a_i^\dagger is really transforming as this FuR of SU(2) and consequently also the state $a_i^\dagger |0, 0\rangle$, i.e. to show

$$[J_a, a_i^\dagger] = \frac{1}{2} a_j^\dagger [\sigma_a]_{ji}. \quad (3.35)$$

To move on, we introduce an equivalent pair of operators $\mathbf{b} = (b_1, b_2)$ which commutes with all a_i and a_i^\dagger and we define

$$\tilde{J}_a = -\frac{1}{2} b_i^\dagger [\bar{\sigma}_a]_{ij} b_j. \quad (3.36)$$

Thus \mathbf{b} transforms as the $\bar{2}$ representation of SU(2):

$$[\tilde{J}_a, b_i^\dagger] = -\frac{1}{2} b_j^\dagger [\bar{\sigma}_a]_{ji} \quad (3.37)$$

and consequently \tilde{J}_a as well as

$$Q_a = \frac{1}{2} a_i^\dagger [\sigma_a]_{ij} a_j - \frac{1}{2} b_i^\dagger [\bar{\sigma}_a]_{ij} b_j \quad (3.38)$$

fulfill the SU(2) algebra. In addition Q_a fulfills the commutator relation (3.35) with a_i^\dagger and (3.37) with b_i^\dagger instead of J_a or \tilde{J}_a respectively and all the other commutators vanish:

$$[Q_a, \mathbf{a}^\dagger \cdot \mathbf{a}] = [Q_a, \mathbf{b}^\dagger \cdot \mathbf{b}] = [Q_a, \mathbf{a}^\dagger \cdot \mathbf{b}^\dagger] = [Q_a, \mathbf{a} \cdot \mathbf{b}] = 0. \quad (3.39)$$

But the Casimir $Q_a Q_a$ cannot be written similar to (3.33) only depending on the

number operators. Thus the eigenstates of our number operators are not eigenstates of the Casimir and are consequently not in our representation as we will see below. Via the Schwinger representation we accomplished a $SU(2)$ algebra constructed by annihilation and creation operators in the Fock space. These steps are easily generalized for any $SU(n)$. Before proceeding to the next step it is handy to introduce the Tensor notation of representations.

Tensor notation and irreducible representation

After all these definitions the indices can get overwhelming quickly especially when it comes to distinguish the two representations 2 and $\bar{2}$. For this task tensors are suited very well and we will switch to the notation from Georgi [Geo99]. We label the states 'spin up' and 'spin down' of the 2 respectively as $|^1\rangle$ and $|^2\rangle$ with upper indices and correspondingly the states of $\bar{2}$ as $|_1\rangle$ and $|_2\rangle$ with lower indices. With the definition

$$[J_a]_i^j = \frac{1}{2}[\sigma]_{ij} \quad (3.40)$$

we can rewrite the transformation of these states as

$$J_a |^i\rangle = |^j\rangle [J_a]_j^i \quad \text{and} \quad J_a |_i\rangle = -|_j\rangle [J_a]_i^j. \quad (3.41)$$

Thus we are always summing over an upper and a lower index. We can extend this to the tensor product space of arbitrary numbers of 2 and $\bar{2}$

$$|_{j_1 \dots}^{i_1 \dots}\rangle = |^{i_1}\rangle \dots |_{j_1}\rangle \dots \quad (3.42)$$

and introduce for each a corresponding index. Then the transformation of such a state is just given by

$$J_a |_{j_1 \dots}^{i_1 \dots}\rangle = \sum_{l=1} |_{j_1 \dots}^{i_1 \dots i_{l-1} k i_{l+1} \dots}\rangle [J_a]_k^i - \sum_{l=1} |_{j_1 \dots j_{l-1} k j_{l+1} \dots}\rangle [J_a]_{j_l}^k. \quad (3.43)$$

When we want to have an irreducible representation for this tensor product space, we can just start with the highest weight state and then construct the whole representation via lowering operators as known from spin and angular momentum addition. In the $SU(2)$ case the highest spin state is the one corresponding to all states of the 2 -representation being in the state with label 1 and of the $\bar{2}$ -representation in the state with label 2 as can be seen from (3.38) for $a = 3$: $|\frac{11}{22} \dots\rangle$. This state has two properties

which are preserved by a $SU(n)$ transformation: It is symmetric in the upper and in the lower indices and it satisfies the traceless condition:

$$\sum_{i,j,k=1}^n \delta_{jk}^{i_l} \left| \begin{matrix} i_1 \dots \\ j_1 \dots \end{matrix} \right\rangle = 0. \quad (3.44)$$

The symmetry in the indices is preserved as the generators transform all upper indices the same way and also all lower indices. The minus sign in (3.43) and the tracelessness of the generators T_a guarantee the second property. Thus all states in the irreducible representation have these two properties and also vice versa: Each state fulfilling these is a state of the highest dimensional irreducible representation contained in our tensor product space [Geo99].

Constructing a $SU(2)$ matrix

The last piece we need to construct the CS, is a $SU(2)$ invariant unit vector

$$\mathbf{z} = \begin{pmatrix} \cos \omega e^{i\alpha} \\ \sin \omega e^{i\beta} \end{pmatrix} = \begin{pmatrix} z_1 \\ z_2 \end{pmatrix}, \quad |\mathbf{z}|^2 = \bar{\mathbf{z}} \cdot \mathbf{z} = 1 \quad (3.45)$$

which is described by three real parameters $\omega \in [0, \frac{\pi}{2}]$, $\alpha \in [0, 2\pi]$ and $\beta \in [0, 2\pi]$. We want this one to transform as the 2 representation. Furthermore we define another $SU(2)$ invariant unit vector \mathbf{w} with the property

$$\mathbf{z} \cdot \mathbf{w} = 0 \quad (3.46)$$

which then transforms as the $\bar{2}$. Then the most general form of \mathbf{w} is given as

$$\mathbf{w} = \begin{pmatrix} -\sin \omega e^{i\beta} \\ \cos \omega e^{i\alpha} \end{pmatrix} \quad (3.47)$$

and then the matrix

$$\begin{pmatrix} \mathbf{z} & \bar{\mathbf{w}} \end{pmatrix} = \begin{pmatrix} \cos \omega e^{i\alpha} & -\sin \omega e^{-i\beta} \\ \sin \omega e^{i\beta} & \cos \omega e^{-i\alpha} \end{pmatrix} \quad (3.48)$$

is a $SU(2)$ matrix. The measure in this space is given via

$$d\Omega = d\omega d\alpha d\beta \frac{1}{2\pi^2} \cos \omega \sin \omega. \quad (3.49)$$

The coherent states

Now we can put all the parts together and construct the CS. First we fix the eigenvalues of $N = \mathbf{a}^\dagger \cdot \mathbf{a}$ and $M = \mathbf{b}^\dagger \cdot \mathbf{b}$ and thus the dimension of our representation as we will see. Such states are obtained via

$$a_{i_1}^\dagger a_{i_2}^\dagger \dots a_{i_N}^\dagger b_{j_1}^\dagger b_{j_2}^\dagger \dots b_{j_M}^\dagger |0\rangle \quad (3.50)$$

where the indices i_k and j_l , as already mentioned, can have the values 1 and 2 in the $SU(2)$ case corresponding to the 'up' and 'down' states of the 2 and the $\bar{2}$ respectively. We can characterize such a state via the eigenvalues of $N_i = a_i^\dagger a_i$ and $M_j = b_j^\dagger b_j$ and will label it as

$$|{}_{M_1 M_2}^{N_1 N_2}\rangle = \frac{(a_1^\dagger)^{N_1} (a_2^\dagger)^{N_2} (b_1^\dagger)^{M_1} (b_2^\dagger)^{M_2}}{\sqrt{N_1! N_2! M_1! M_2!}} |0\rangle, \quad \sum_i N_i = N, \quad \sum_i M_i = M. \quad (3.51)$$

We know from our tensor product of 2s and $\bar{2}$ s, which irreducible representation of $SU(2)$ is the highest dimensional contained in the tensor product. We label this representation as usual with j connected to the eigenvalue of the Casimir Q^2 from our notation of (3.38) and j is fixed from N and M :

$$j = \frac{1}{2}(N + M) \quad (3.52)$$

as we can see from the maximum eigenvalue of Q_3 . In our case of $SU(2)$ there is a redundancy in this equation as j does not fix N and M which is due to the equivalence of 2 and $\bar{2}$. In the case of $SU(3)$ the representation will completely fix N and M and vice versa.

However as we noted before these states (3.51) are not necessary in the irreducible representation. This is different than before in (3.34) as the Fock states $|N_1, N_2\rangle$ are automatically a basis of our irreducible representation as they are the totally symmetric states. But now when we consider the tensor product of 2 and $\bar{2}$ we also need to account for the traceless condition (3.44) which is not intrinsic to the Fock states $|{}_{M_1 M_2}^{N_1 N_2}\rangle$. The symmetrization in upper and lower indices is already guaranteed as before but we still need to subtract the traces to fulfill (3.44). Thus the states $|{}_{M_1 M_2}^{N_1 N_2}\rangle$ span in general a larger space than the highest dimensional irreducible representation contained in our tensor product. However if either $N = 0$ or $M = 0$ we are again in the case where no traceless condition needs to be fulfilled or rather is satisfied trivially and for example the states $|N_1 N_2\rangle$ span our irreducible representation.

In the case where there is a tensor product of at least one **FuR** and its conjugate we need a different basis for our highest dimensional irreducible representation which we will label with $|V_i\rangle$. The index i ranges from 1 to the dimension $D(N, M)$ of the representation which we obtain via the following thoughts: In the case $M = 0$ we have no traceless condition and have $N + 1$ choices for N_1 and then N_2 is fixed from $\sum_i N_i = N$. Similarly for the case $N = 0$ and we have $D(N, 0) = N + 1$ as well as $D(0, M) = M + 1$. Then $D(N, 0)D(0, M)$ is the number of states satisfying $\sum_i N_i = N$ and $\sum_i M_i = M$. Due to the traceless condition (3.44), we need to subtract from these the number of states fulfilling $\sum_i N_i = N - 1$ and $\sum_i M_i = M - 1$ and get eventually in the case of $SU(2)$:

$$D(N, M) = N + M + 1. \quad (3.53)$$

This agrees with the statements from (3.52) and (3.4). Furthermore we have the **RoU**

$$\sum_{i=1}^{D(N, M)} |V_i\rangle \langle V_i| = \mathbb{1}. \quad (3.54)$$

Now consider states constructed via the generating function

$$\sqrt{N!M!} e^{z \cdot \mathbf{a}^\dagger + \mathbf{w} \cdot \mathbf{b}^\dagger} |0\rangle \quad (3.55)$$

and we project onto the subspace with fixed N and M . Then the states

$$|\mathbf{z}, \mathbf{w}\rangle = \frac{(z \cdot \mathbf{a}^\dagger)^N (\mathbf{w} \cdot \mathbf{b}^\dagger)^M}{\sqrt{N!M!}} |0\rangle \quad (3.56)$$

will be in the irreducible representation: As \mathbf{z} and \mathbf{w} transform as the 2 and the $\bar{2}$ respectively, these states will be symmetric in upper and lower indices and fulfill the traceless condition (3.44) per construction. We can rewrite the binomials [GR94, 1.111] in (3.56):

$$|\mathbf{z}, \mathbf{w}\rangle = \sum_{\substack{N_1, N_2 \\ N_1 + N_2 = N}} \sum_{\substack{M_1, M_2 \\ M_1 + M_2 = M}} \sqrt{\frac{N!M!}{N_1!N_2!M_1!M_2!}} z_1^{N_1} z_2^{N_2} w_1^{M_1} w_2^{M_2} |_{M_1 M_2}^{N_1 N_2}\rangle \quad (3.57)$$

and these are the **CS** of $SU(2)$ because from the construction in (3.55) we can argue according to the construction via the operator D in (2.21). Here we are considering ordinary **CS** constructed from the vacuum state, i.e. $|\psi_0\rangle = |0\rangle$, and thus the part with the annihilation operator a in D (2.12) vanishes and we have the form of (3.55) as \mathbf{z} and \mathbf{w} are unit vectors. Accordingly we can conclude that the **CS** $|\mathbf{z}, \mathbf{w}\rangle$ are states

closest to the classical states. In contradistinction to the case of the harmonic oscillator in Sec. 2.2.2, we are not looking at the whole space but only at a $D(N, M) = 2j + 1$ dimensional subspace. In the case of the harmonic oscillator this is not very fruitful as all these subspaces with fixed N are one dimensional. But in the case of $SU(n)$ we are always working in a certain representation instead of looking at the whole group. Now we are only left with one conceptual difference between the CS of Perelomov from Sec. 3.1.2 and this construction here: In Def. 2.3 we saw that a point in the coset space \mathcal{X} completely determines our CS which lead to two parameters in (3.16). But looking at the definition of \mathbf{z} in (3.45) and \mathbf{w} in (3.47), we see that we still have three parameters. But in (3.57) and already in (3.56) we see that we can pull a total phase factor $e^{i(N+M)\alpha}$ out. This phase does not change our state and thus can be omitted and we are only left with two parameters $\varphi = \beta - \alpha$ and ω . This can only be done in a certain representation as it is not possible in (3.55) and thus the value of this phase determines our representation. This can also be seen when acting with (3.8) on a maximum weight state which results in the same phase factor. This can be easily seen via comparison of the parameters of (3.48) and (3.6).

Next we will show the RoU through the operator

$$A = D(N, M) \int d\Omega |\mathbf{z}, \mathbf{w}\rangle \langle \mathbf{z}, \mathbf{w}|. \quad (3.58)$$

This operator A commutes with all generators Q_a of our $SU(2)$ as \mathbf{a} and \mathbf{b} transform as the 2 and the $\bar{2}$ respectively and it must be proportional to the $\mathbb{1}$. Here in the case of the $SU(2)$ the normalization can easily be proved by directly calculating the integral in (3.58) as before. But it is also sufficient to consider one element $\langle V_1 | A | V_1 \rangle$ and show that it is equal to one as we already know that A is proportional to $\mathbb{1}$. The mapping from the states $|\begin{smallmatrix} N_1 & N_2 \\ M_1 & M_2 \end{smallmatrix}\rangle$ to basis states $|V_i\rangle$ is not an easy task in general but here it is sufficient that we know one, which we take to be $|V_1\rangle$. From Q_3 in (3.38) we see that $|\begin{smallmatrix} N_0 \\ 0 & M \end{smallmatrix}\rangle$ is a state in our representation as we can identify it with the highest weight state $|j, j\rangle$. Another way to see this is that this vector already fulfills (3.44). Thus we take $|V_1\rangle = |\begin{smallmatrix} N_0 \\ 0 & M \end{smallmatrix}\rangle$ and the resulting integral

$$\langle \begin{smallmatrix} N_0 \\ 0 & M \end{smallmatrix} | A | \begin{smallmatrix} N_0 \\ 0 & M \end{smallmatrix} \rangle = D(N, M) \int d\Omega |z_1|^{2N_1} |w_2|^{2M_2} = D(N, M) \int d\Omega (\cos \omega)^{2(N+M)} = 1$$

can be solved easily and we have proved the RoU. Further from (3.58) and (3.49) we get the same integration measure as in (3.24) when executing the integration over the phase α of our isotropy group.

Lastly we want to show that the CS (3.57) are equal to the ones from Perelomov (3.16). As already mentioned the problem that occurs here is that it is not easy to perform the transformation from our $|_{M_1 M_2}^{N_1 N_2}\rangle$ vectors in (3.57) to the $|V_i\rangle$, viz $|j, \mu\rangle$, basis in general. Thus our approach is the following: We know that we can construct all representations of $SU(2)$ just from the 2 representation. The construction in this section was just done together with the $\bar{2}$ representation to facilitate the step to $SU(3)$ later on. Thus we will show the correspondence of (3.57) to (3.16) in the case of $M = 0$ when we only have tensor products of 2s. Then we will look explicitly into the AdR and show how the mapping from $|_{M_1 M_2}^{N_1 N_2}\rangle$ to $|V_i\rangle$ can be done in a special case. In the case $M = 0$ all the states $|_0^{N_1 N_2}\rangle$ evidently fulfill the traceless condition (3.44) and we have the same one-to-one correspondence to $|j, \mu\rangle$ as before in the context of (3.32) and (3.34). We can reduce the double sum with the constraint $N_1 + N_2 = N$ to one sum over N_2 from 0 to N . From (3.52) we know that $2j = N$ and we shift the summation to run from $-j$ to j :

$$|z\rangle = e^{i2j\alpha} \sum_{\mu=-j}^j \sqrt{\frac{(2j)!}{(j+\mu)!(j-\mu)!}} e^{i((j-\mu)\alpha+(j+\mu)\beta-2j\alpha)} (\cos\omega)^{j-\mu} (\sin\omega)^{j+\mu} |j, \mu\rangle. \quad (3.59)$$

Here we already put the phase factor $e^{iN\alpha}$ before the sum as discussed above and we get in the exponential in the sum $(j+\mu)(\beta-\alpha)$. This leaves us with one phase $\varphi = \beta - \alpha$ as in the Perelomov case and corresponds to taking complex numbers from the coset space \mathcal{X} in Def. 2.3. Finally we take a $(\cos\omega)^{2j}$ out of the sum and get a tangent and thus the same as in (3.16).

Now we want to look at the CS of the AdR obtained via a tensor product of a 2 and a $\bar{2}$ and show the equivalence to the CS of Perelomov. Using (3.57) with $N = 1 = M$ we get

$$|z, \mathbf{w}\rangle_{\text{AdR}} = z_1 w_1 |_{10}^{10}\rangle + z_1 w_2 |_{01}^{10}\rangle + z_2 w_1 |_{10}^{01}\rangle + z_2 w_2 |_{01}^{01}\rangle. \quad (3.60)$$

We know that the dimension of the AdR, viz $j = 1$, is three but currently we still have four vectors. But from (3.46) we see that the sum of the coefficients of the vectors $|_{10}^{10}\rangle$ and $|_{01}^{01}\rangle$ vanishes which means that we have only four linear independent vectors in (3.60). These are $|_{01}^{10}\rangle$, $|_{10}^{01}\rangle$ and $(|_{10}^{10}\rangle - |_{01}^{01}\rangle)$ and we see that this procedure is not easily generalizable to the arbitrary case N and M . These three states would be enough to write down the CS in terms of our basis $|V_i\rangle$ but as we want to compare it to (3.16) we need to find the correspondence to the states $|1, \mu\rangle$. This correspondence will later for $SU(3)$ no longer be performed as we are only interested in a RoU. This correspondence is done via the raising and lowering operators $Q_{\pm} = Q_1 \pm iQ_2$. As already mentioned

above, $|\begin{smallmatrix} 10 \\ 01 \end{smallmatrix}\rangle$ must be the highest weight state $|1, 1\rangle = |1\rangle$ and then we are just left with calculating the Clebsch-Gordan coefficients¹ resulting in:

$$|1\rangle = |\begin{smallmatrix} 10 \\ 01 \end{smallmatrix}\rangle, \quad |0\rangle = \frac{1}{\sqrt{2}}(|\begin{smallmatrix} 01 \\ 01 \end{smallmatrix}\rangle - |\begin{smallmatrix} 10 \\ 10 \end{smallmatrix}\rangle), \quad |-1\rangle = -|\begin{smallmatrix} 01 \\ 10 \end{smallmatrix}\rangle. \quad (3.61)$$

Now all we need to do, is inserting \mathbf{z} and \mathbf{w} in (3.60), using (3.61), factorizing the phase as in the general case and we get (3.16) for $j = 1$.

In this section we showed how to construct the CS in general for any $SU(n)$ on the example of the $SU(2)$ with all the subtleties that are not part of $SU(2)$ but for $n > 2$. We kept this part such general to facilitate the step in the next section to $SU(3)$ or to any $SU(n)$ if needed. In the end we saw that the tracelessness condition is not necessary in the case of $SU(2)$ but it will be for $SU(3)$. But we included this subtlety in the last paragraph on the example of the AdR and thus the step to $SU(3)$ should be straight forward.

Lastly we want to recall the main ideas and steps of this section: When we do the tensor product of two FuR of $SU(n)$ we get a n^2 dimensional space. But in the Fock space the states in the number basis are only the totally symmetric states and we are only left with one irreducible representation. Thus in the last part, where we showed the equivalence to the Perelomov CS, we got a one to one correspondence between the $|N_1 N_2\rangle$ and the $|j, \mu\rangle$ states. If we consider e.g. $2 \otimes 2$ which is $3 \oplus 1$ the Fock states are automatically in the AdR 3. In the general case where we have a tensor product of 2 and $\bar{2}$, it is not so trivial. But as mentioned before the CS in (3.57) are constructed in a way that they fulfill the tracelessness. Consequently, the CS are automatically from the AdR 3 if we consider $2 \otimes \bar{2}$. But now the one-to-one correspondence between the $|\begin{smallmatrix} N_1 N_2 \\ M_1 M_2 \end{smallmatrix}\rangle$ and the $|j, \mu\rangle$ states is not easily given as we also saw in the last example. Furthermore the definition of Def. 2.3 from Perelomov is based on the isotropy subgroup of the fixed vector $|\psi_0\rangle$. This leaves us with only two parameters ω and φ when we first considered the CS. But with the construction in this section we always have the three parameters of \mathbf{z} , viz ω , α and β . But the representation of the CS in (3.57) shows that we can get rid of one overall phase as we then did in (3.59) and are left with only two parameters. When we do the construction via the Schwinger representation of $SU(n)$ we need to think about the isotropy subgroup later and not at the beginning.

¹The Clebsch-Gordan coefficients of $SU(2)$ and $SU(3)$ for the representations needed in this thesis can easily be derived by a quick calculation. Further they can be found in [Che⁺87] and there is a nice on-line tool [Ale⁺] available for calculating them.

3.2 $SU(3)$

3.2.1 Representation of $SU(3)$

In the $SU(3)$ case there is no closed expression for the structure constants f_{abc} from (2.1). However the most common representation of the FuR is given via the Gell-Mann matrices [Geo99]:

$$\begin{aligned}
 \lambda_1 &= \begin{pmatrix} 0 & 1 & 0 \\ 1 & 0 & 0 \\ 0 & 0 & 0 \end{pmatrix}, & \lambda_2 &= \begin{pmatrix} 0 & -i & 0 \\ i & 0 & 0 \\ 0 & 0 & 0 \end{pmatrix}, & \lambda_3 &= \begin{pmatrix} 1 & 0 & 0 \\ 0 & -1 & 0 \\ 0 & 0 & 0 \end{pmatrix}, \\
 \lambda_4 &= \begin{pmatrix} 0 & 0 & 1 \\ 0 & 0 & 0 \\ 1 & 0 & 0 \end{pmatrix}, & \lambda_5 &= \begin{pmatrix} 0 & 0 & -i \\ 0 & 0 & 0 \\ i & 0 & 0 \end{pmatrix}, & \lambda_6 &= \begin{pmatrix} 0 & 0 & 0 \\ 0 & 0 & 1 \\ 0 & 1 & 0 \end{pmatrix}, & (3.62) \\
 \lambda_7 &= \begin{pmatrix} 0 & 0 & 0 \\ 0 & 0 & -i \\ i & 0 & 0 \end{pmatrix}, & \lambda_8 &= \frac{1}{\sqrt{3}} \begin{pmatrix} 1 & 0 & 0 \\ 0 & 1 & 0 \\ 0 & 0 & -2 \end{pmatrix}
 \end{aligned}$$

and from these one can calculate f_{abc} with the generators

$$T_a = \frac{1}{2} \lambda_a. \quad (3.63)$$

Looking at the Gell-Mann matrices we see that λ_3 and λ_8 are already diagonal and they are chosen to be the two Cartan operators. Their eigenvalues give the weights of the eigenstates of the FuR which can be visualized via a triangle in a plane, which can be seen in Fig. 3.1b. The raising and lowering operators are just obtained like in Sec. 3.1.1 from the three $SU(2)$ subalgebras: 1-2, 4-5 and 6-7 together with the respectively according Cartan operator which is a linear combination of λ_3 and λ_8 .

3.2.2 Coherent states of $SU(3)$

After all the groundwork in the $SU(2)$ section, we can construct the $SU(3)$ CS straightforward. First we replace the Pauli-Spin-matrices in (3.38) with the Gell-Mann-matrices λ_a and get the Schwinger representation:

$$Q_a = \frac{1}{2} \left(a_i^\dagger [\lambda_a]_{ij} a_j - b_i^\dagger [\lambda_a]_{ij} b_j \right). \quad (3.64)$$

To move on, we need two complex vectors of unit norm, namely

$$\mathbf{z} = \begin{pmatrix} \sin \theta \cos \varphi e^{i\alpha_1} \\ \sin \theta \sin \varphi e^{i\alpha_2} \\ \cos \theta e^{i\alpha_3} \end{pmatrix} \text{ and } \mathbf{w} = \begin{pmatrix} e^{i(\beta_1-\alpha_1)} \cos \chi \cos \theta \cos \varphi + e^{i(\beta_2-\alpha_1)} \sin \chi \sin \varphi \\ e^{i(\beta_1-\alpha_2)} \cos \chi \cos \theta \sin \varphi - e^{i(\beta_2-\alpha_2)} \sin \chi \cos \varphi \\ - e^{i(\beta_1-\alpha_3)} \cos \chi \sin \theta \end{pmatrix} \quad (3.65)$$

which satisfy $\mathbf{z} \cdot \mathbf{w} = 0$. Then the matrix

$$\begin{pmatrix} \mathbf{z} & \bar{\mathbf{w}} & \bar{\mathbf{z}} \times \mathbf{w} \end{pmatrix} \quad (3.66)$$

is a $SU(3)$ matrix. This is a eight dimensional space with the following integration measure as well as the integration borders [MS01]:

$$d\Omega = \frac{1}{2\pi^5} \sin^3 \theta \cos \theta \cos \varphi \sin \varphi \cos \chi \sin \chi d\theta d\varphi d\chi d\alpha_1 d\alpha_2 d\alpha_3 d\beta_1 d\beta_2 \quad (3.67)$$

$$\theta, \varphi, \chi \in [0, \frac{\pi}{2}], \quad \alpha_i, \beta_i \in [0, 2\pi].$$

Now we consider \mathbf{z} to transform as the $\mathbf{3}$ and \mathbf{w} as the $\bar{\mathbf{3}}$ and we can construct all representations via tensor products and the CS as before. Another way is to construct all representations out of $\mathbf{3}$ and $\mathbf{3} \wedge \mathbf{3}$ where this means an antilinear combination of two $\mathbf{3}$ s. Then we need to use the vectors \mathbf{z} and $\mathbf{z} \times \bar{\mathbf{w}}$ when constructing the CS. This is done in [MM02] where it is also generalized to $SU(n)$ and gives the same results in the end. We stick to the first way and use \mathbf{z} and \mathbf{w} and we get the CS with (3.56) as

$$|\mathbf{z}, \mathbf{w}\rangle = \sum_{\substack{N_1, N_2, N_3 \\ N_1 + N_2 + N_3 = N}} \sum_{\substack{M_1, M_2, M_3 \\ M_1 + M_2 + M_3 = M}} \sqrt{\frac{N!M!}{N_1!N_2!N_3!M_1!M_2!M_3!}} z_1^{N_1} z_2^{N_2} z_3^{N_3} w_1^{M_1} w_2^{M_2} w_3^{M_3} | \begin{smallmatrix} N_1 & N_2 & N_3 \\ M_1 & M_2 & M_3 \end{smallmatrix} \rangle. \quad (3.68)$$

As before this construction does not account for any global phases that can be extracted which are equivalent to the isotropy subgroup considered by Perelomov. This can be easily done at this step just as in the $SU(2)$ case and we can extract a factor $e^{i\alpha_1}$ from \mathbf{z} and a factor $e^{i(\beta_1-\alpha_1)}$ from \mathbf{w} . Then the construction via (3.56) gives us an overall factor $e^{i(\alpha_1(N-M)+\beta_1M)}$ which can be represented by two phases. The remaining six parameters are enough to describe the remaining vectors $\tilde{\mathbf{z}}$ and $\tilde{\mathbf{w}}$ instead of eight. Thus the CS can also be described by only six parameters as the overall phases do not change the states. In the following we will omit the tilde and the term CS of $SU(3)$ will refer to the ones with the tilde. Also α_2 will mean $\tilde{\alpha}_2$, i.e. $\alpha_2 - \alpha_1$ and accordingly for α_3 as well as β_2 . In addition we omit the phases with the index one, viz α_1 and

β_1 . As already mentioned these phases are the phases omitted by Perelomov from the isotropy subgroup. In the considered representation of \mathbf{z} and \mathbf{w} we see that we cannot extract another global phase. We will show later that we cannot get rid of more than two parameters in the general case and discuss in which cases this is possible.

Resolution of unity

The operator

$$A = D(N, M) \int d\Omega |\mathbf{z}, \mathbf{w}\rangle \langle \mathbf{z}, \mathbf{w}| \quad (3.69)$$

must be proportional to the $\mathbb{1}$ as it commutes with all generators Q_a . In the case of $SU(3)$, calculating the integral in this operator is not straightforward and we consider again one element $\langle V_1|A|V_1\rangle$ and show that it is one and it follows $A = \mathbb{1}$. We take again the highest weight state $|V_1\rangle = \begin{smallmatrix} N & 0 & 0 \\ 0 & 0 & M \end{smallmatrix}$.

First we need to calculate the dimension of the representation of the CS. Therefore we consider again the case $M = 0$: We rewrite the sum with constraint in (3.68) over N_i as two sums over N_1 and N_2 as N_3 is then already fixed. For each N_1 we have $N_1 + 1$ choices for N_2 which results in total in $\sum_{N_1=0}^N (N_1 + 1)$ choices. This is a sum over the natural numbers from 1 to $N + 1$ and resolves to $D(N, 0) = \frac{(N+1)(N+2)}{2}$. Similarly $D(M, 0) = \frac{(M+1)(M+2)}{2}$ and $D(N, 0)D(M, 0)$ states fulfill $\sum_i N_i = N$ as well as $\sum_i M_i = M$. From this we need to subtract the number of states satisfying $\sum_i N_i = N - 1$ and $\sum_i M_i = M - 1$ because of the traceless condition. This results in

$$D(N, M) = \frac{1}{2}(N + 1)(M + 1)(N + M + 2). \quad (3.70)$$

Now we are only left to calculate the following integral and show that it is equal to one:

$$\begin{aligned} \langle V_1|A|V_1\rangle &= D(N, M) \int d\Omega |\langle V_1|\mathbf{z}, \mathbf{w}\rangle|^2 \\ &= D(N, M) \int d\Omega \frac{N!M!}{N!M!} |z_1|^N |w_3|^M \langle \begin{smallmatrix} N & 0 & 0 \\ 0 & 0 & M \end{smallmatrix} | \begin{smallmatrix} N & 0 & 0 \\ 0 & 0 & M \end{smallmatrix} \rangle. \end{aligned} \quad (3.71)$$

We consider only the integral and insert z_1 (3.65), w_3 (3.65) and the volume element (3.67) where we have already executed the trivial integration over the parameters of

the isotropy group:

$$\int d\theta d\varphi d\chi d\alpha_2 d\alpha_3 d\beta_2 \frac{2}{\pi^3} \sin^3 \theta \cos \theta \cos \varphi \sin \varphi \cos \chi \sin \chi (\sin \theta \cos \varphi)^{2N} (\cos \chi \sin \theta)^{2M}.$$

After performing the trivial integration over the phases we are only left with integrals consisting of a product of odd powers of a sine and a cosine of the same argument:

$$\int_0^{\frac{\pi}{2}} dx (\sin x)^{2i+1} (\cos x)^{2j+1} = \frac{i!j!}{2(i+j+1)!}.$$

This can be solved as in the $SU(2)$ case via the substitution $u = \cos x$ and we are left with the form of (3.28). Inserting our values for i and j , we get:

$$16 \frac{(N+M+1)!}{2(N+M+2)!} \frac{N!}{2(N+1)!} \frac{M!}{2(M+1)!} = \frac{2}{(N+M+2)(N+1)(M+1)} = \frac{1}{D(N, M)}.$$

And thus the RoU is given by A in (3.69) as we showed that (3.71) is equal to one.

Now we have the CS of $SU(3)$ and a RoU which allows us to write any state of our Hilbert space in terms of the CS. The only missing part is a representation of the CS in terms of the eigenstates of the Cartan operators which is our natural basis in any representation of $SU(3)$. We mentioned already above that it is sufficient for our purpose to have a representation in terms of the $|V_i\rangle$ as we only want a RoU. As we saw on the case of the AdR of $SU(2)$ this is best done for each representation individually. For us it is enough to have the CS of the FuR and AdR as Quarks transform according to the first one and gluons according to the second one regarding color. In contrast to the $SU(2)$ case there are different simplifications possible especially concerning the isotropy group. Next we look at these two cases consecutively and we will also refer to the generalization of both representations. In the subsequent section we will give a general proof for the statements made on these two cases.

Coherent states of the fundamental representation

Considering the FuR of $SU(3)$ and any representation that can be constructed via a tensor product only of this one, viz $3^{\otimes k}$, we see that $M = 0$. Thus the parameters of \mathbf{w} are not relevant to describe the CS and can be omitted, i.e. only the four parameters α_2 , α_3 , θ and φ are needed. Furthermore already the states $\begin{bmatrix} N_1 & N_2 & N_3 \\ 0 & 0 & 0 \end{bmatrix}$ are a basis as

we have no traceless condition in this case and they span our desired representation. We can write the RoU (3.69) of this space as

$$\begin{aligned} \mathbb{1} = D(N, 0) \int d\Omega & \sum_{\substack{N_1, N_2, N_3 \\ N_1 + N_2 + N_3 = N}} \sum_{\substack{N'_1, N'_2, N'_3 \\ N'_1 + N'_2 + N'_3 = N}} \sqrt{\frac{N!M!N!M!}{N_1!N_2!N_3!N'_1!N'_2!N'_3!}} \\ & (\sin \theta \cos \varphi)^{N_1 + N'_1} (\sin \theta \sin \varphi)^{N_2 + N'_2} (\cos \theta)^{N_3 + N'_3} \\ & e^{i\alpha_2(N_2 - N'_2)} e^{i\alpha_3(N_3 - N'_3)} |N_1 N_2 N_3\rangle \langle N'_1 N'_2 N'_3| \quad (3.72) \end{aligned}$$

and the integrations over the two phases α_2 and α_3 give us $\delta_{N_2 N'_2}$ and $\delta_{N_3 N'_3}$. This also fixes N'_1 with $\delta_{N_1 N'_1}$ from the constraint that the sum of N_i and also of N'_i must be equal to N . Similar to the case of $SU(2)$ we see that the integration over the other two parameters are only relevant for the normalization and we can conclude similar to [Thm. 3.1](#):

Theorem 3.2. *The RoU of the FuR of $SU(3)$ CS and representations only constructed from it, can be written as*

$$\begin{aligned} \int d\alpha_2 d\alpha_3 \frac{D(N, 0)}{4\pi^2} |\alpha_2, \alpha_3\rangle \langle \alpha_2, \alpha_3| &= \mathbb{1}, \\ \text{with } |\alpha_2, \alpha_3\rangle &= \frac{1}{\sqrt{D(N, 0)}} \sum_{\substack{N_1, N_2, N_3 \\ N_1 + N_2 + N_3 = N}} e^{i(N_2 \alpha_2 + N_3 \alpha_3)} |N_1 N_2 N_3\rangle. \quad (3.73) \end{aligned}$$

At this point we can take a quick look at the uncertainty (2.41) of our CS as at [page 28](#). Therefore we need to calculate first the uncertainty for the highest weight state $|T_3, T_8\rangle = \left|\frac{1}{2}, \frac{1}{\sqrt{3}}\right\rangle$ as a reference:

$$\frac{(\Delta \mathbf{T})^2}{\left| \begin{array}{c|ccc} \left|\frac{1}{2}, \frac{1}{\sqrt{3}}\right\rangle & |z\rangle_{\text{FuR}} & |\alpha_2, \alpha_3\rangle \\ \hline 1 & 1 & 1 \end{array} \right.}.$$

We see again that our CS are indeed states with minimal uncertainty as we expect from our construction with the vacuum state $|0\rangle$ similar to the harmonic oscillator. Further also the states $|\alpha_2, \alpha_3\rangle$ for the simpler RoU of the FuR from [Thm. 3.2](#) are states of minimal uncertainty as they are a subset of the CS equivalent to the $SU(2)$ case.

In the $SU(2)$ case there were two parameters enough to describe the CS completely and now we only needed four parameters. From these only respectively one for $SU(2)$

and two phases for $SU(3)$ are enough for the simpler **RoU**.

This is generalized to any $SU(n)$ and tensor products of the **FuR** in [Nem00]. There the symmetric decomposition

$$\begin{pmatrix} 1 & 0 & & \dots & 0 \\ 0 & & & & \\ \vdots & & SU(n-1) & & \\ 0 & & & & \end{pmatrix} \begin{pmatrix} e^{i\varphi} \cos \theta & -\sin \theta & 0 \\ \sin \theta & e^{-i\varphi} \cos \theta & 0 \\ 0 & 0 & \mathbb{1}_{n-2} \end{pmatrix} \begin{pmatrix} 1 & 0 & & \dots & 0 \\ 0 & & & & \\ \vdots & & SU(n-1) & & \\ 0 & & & & \end{pmatrix} \quad (3.74)$$

of the **FuR** $n \times n$ from [RSG99] is used. Acting with this decomposition on the vector $(1, 0, \dots, 0)^T$, we see that the number of parameters of one $SU(n-1)$ are irrelevant when describing the **CS**. Then the **CS** $|\psi_g\rangle_n$ of $SU(n)$ can be constructed from the **CS** $|\psi_g\rangle_{n-1}$ of $SU(n-1)$:

$$|\psi_g\rangle_n = \begin{pmatrix} e^{i\varphi} \cos \theta \\ 0 \\ \vdots \\ 0 \end{pmatrix} + \sin \theta \begin{pmatrix} 0 \\ |\psi_g\rangle_{n-1} \end{pmatrix}. \quad (3.75)$$

Per induction from the $SU(2)$ case we see that $2(n-1)$ parameters are enough to describe the **CS** of the **FuR** completely. Half of these parameters are phases and are enough for the **RoU** when considering **Thm. 3.2**.

When we then look at the tensor product of k **FuR**, we do not need more parameters as the tensor product $(1, 0, \dots, 0)^{T \otimes k}$ of our fixed vector will trivially be in our representation from the Clebsch-Gordan coefficients. This is due to the fact that our Fock states $|N_1 N_2 N_3\rangle$ are already a basis of the desired representation. The only thing we cannot proof at this stage is, if we can possibly get rid of even more parameters which will be discussed in **Sec. 3.3**.

Coherent states of the adjoint representation

The first problem that arises here is to move from the states $|_{M_1 M_2 M_3}^{N_1 N_2 N_3}\rangle$ to the eight basis states $|V_i\rangle$ of the **AdR**. For this representation we have $N = 1 = M$ and thus

$$|\mathbf{z}, \mathbf{w}\rangle = \sum_{i,j=1}^3 z_i w_j a_i^\dagger b_j^\dagger |0\rangle. \quad (3.76)$$

The sum of the coefficients of the states $|{}_{100}^{100}\rangle$, $|{}_{010}^{010}\rangle$ and $|{}_{001}^{001}\rangle$ vanishes. This is just due to our constraint $\mathbf{z} \cdot \mathbf{w} = 0$ which guarantees us the traceless condition. Thus we can move to the following eight linear independent states:

$$\begin{aligned} |V_1\rangle &= \frac{1}{\sqrt{2}} \left(|{}_{100}^{100}\rangle - |{}_{010}^{010}\rangle \right), & |V_2\rangle &= \frac{1}{\sqrt{6}} \left(|{}_{100}^{100}\rangle + |{}_{010}^{010}\rangle - 2 |{}_{001}^{001}\rangle \right), \\ |V_3\rangle &= |{}_{010}^{100}\rangle, & |V_4\rangle &= |{}_{100}^{010}\rangle, & |V_5\rangle &= |{}_{001}^{100}\rangle, \\ |V_6\rangle &= |{}_{100}^{001}\rangle, & |V_7\rangle &= |{}_{001}^{010}\rangle, & |V_8\rangle &= |{}_{010}^{001}\rangle. \end{aligned} \quad (3.77)$$

Be aware that these states $|V_i\rangle$ are the eigenstates of the Cartan operators but might not be directly related among each other via raising and lowering operators. Thus the signs we explicitly calculated in (3.61) are not included here. Now we define the CS as $|\mathbf{z}, \mathbf{w}\rangle = \sum_{i=1}^8 \lambda_i |V_i\rangle$ where the λ_i are derived from (3.77):

$$\begin{aligned} \lambda_1 &= \frac{1}{\sqrt{2}} (z_1 w_1 - z_2 w_2) \\ &= \frac{1}{\sqrt{2}} \sin \theta (e^{i\beta_2} \sin(2\varphi) \sin \chi + \cos^2 \varphi \cos \theta \cos \chi - \sin^2 \varphi \cos \theta \cos \chi), \\ \lambda_2 &= \frac{1}{\sqrt{6}} (z_1 w_1 + z_2 w_2 - 2z_3 w_3) = \sqrt{\frac{3}{2}} \sin \theta \cos \theta \cos \chi, \\ \lambda_3 &= z_1 w_2, & \lambda_4 &= z_2 w_1, & \lambda_5 &= z_1 w_3, \\ \lambda_6 &= z_3 w_1, & \lambda_7 &= z_2 w_3, & \lambda_8 &= z_3 w_2. \end{aligned} \quad (3.78)$$

Now we look at the RoU via (3.69) which takes the form

$$\mathbb{1} = D(1, 1) \int d\Omega \sum_{i,j=1}^8 \lambda_i \bar{\lambda}_j |V_i\rangle \langle V_j| \quad (3.79)$$

and we want to know which integrations are enough for the RoU. Taking the explicit form of the λ_i in (3.78) and considering each product $\lambda_i \bar{\lambda}_j$ in (3.79), we see that the integrations over α_2 , α_3 and β_2 leave only terms from $\lambda_1 \bar{\lambda}_2$ and its conjugate besides the diagonal terms $\lambda_i \lambda_i$. These remaining off-diagonal terms are of the form

$$\cos^3 \theta \cos^3 \chi \sin(4\varphi) \sin^5 \theta \sin \chi$$

and will vanish when we integrate over φ . Thus for the RoU there are four parameters enough and we can save two integrations when we are doing numerics. This gives us the following theorem after Thm. 3.1 and Thm. 3.2

Theorem 3.3. *The RoU of the AdR of $SU(3)$ CS can be written as*

$$\int d\alpha_2 d\alpha_3 d\beta_2 d\varphi \cos \varphi \sin \varphi \frac{D(1,1)}{4\pi^3} |\alpha_2, \alpha_3, \beta_2, \varphi\rangle \langle \alpha_2, \alpha_3, \beta_2, \varphi| = \mathbb{1},$$

$$\text{with } |\alpha_2, \alpha_3, \beta_2, \varphi\rangle = \frac{1}{\sqrt{D(1,1)}} \begin{pmatrix} \cos^2 \varphi - \sin^2 \varphi + 2 e^{i\beta_2} \sin \varphi \cos \varphi \\ 1 \\ \sqrt{2} \cos \varphi e^{-i\alpha_2} (\sin \varphi - e^{i\beta_2} \cos \varphi) \\ \sqrt{2} e^{i\alpha_2} \sin \varphi (\cos \varphi + e^{i\beta_2} \sin \varphi) \\ -\sqrt{2} e^{-i\alpha_3} \cos \varphi \\ e^{i\alpha_3} (\cos \varphi + e^{i\beta_2} \sin \varphi) \\ -\sqrt{2} e^{i(\alpha_2 - \alpha_3)} \sin \varphi \\ e^{i(\alpha_3 - \alpha_2)} (\sin \varphi - e^{i\beta_2} \cos \varphi) \end{pmatrix} \quad (3.80)$$

in the basis of the $|V_i\rangle$ from (3.77).

Again we also want to calculate the uncertainty of the CS of the AdR as in the case of the FuR above:

$$\frac{(\Delta \mathbf{T})^2}{\left| \begin{array}{c|ccc} \frac{1}{2}, \frac{\sqrt{3}}{2} \rangle & |0,0\rangle & |z\rangle_{\text{AdR}} & |\alpha_2, \alpha_3, \beta_2, \varphi\rangle \\ \hline 2 & 3 & 2 & 2.04 \end{array} \right.}.$$

The highest weight state $|T_3, T_8\rangle = \left| \frac{1}{2}, \frac{\sqrt{3}}{2} \right\rangle$ is our reference for the minimum uncertainty and we see that both states $|0,0\rangle$ in the middle of our hexagon of Fig. 3.1c have a higher uncertainty. From our construction with the vacuum state $|0\rangle$, also the CS of the AdR are states of minimum uncertainty. But however the states $|\alpha_2, \alpha_3, \beta_2, \varphi\rangle$ of the simpler RoU from Thm. 3.3 do not have minimal uncertainty as in the case of $SU(2)$ at page 28.

In this section we saw that we cannot reduce the number of parameters necessary to completely describe a CS. Recalling the case of the FuR we cannot achieve a construction similar to the one from Nemoto in (3.74), as the tensor product of the states $(1,0,0)$ from the 3 and $(1,0,0)$ from $\bar{3}$ is not in the AdR. Looking at the Clebsch-Gordan coefficients, we see that it is a linear combination of the basis states $|V_i\rangle$. This is the same as with some of the states $\left| \begin{smallmatrix} N_1 & N_2 & N_3 \\ M_1 & M_2 & M_3 \end{smallmatrix} \right\rangle$ which are neither in the AdR as we saw in (3.77). As we are not able to do a construction as in (3.75), we can not induce the AdR of $SU(3)$ from a representation of $SU(2)$ and thus we cannot get rid of more parameters. These bit heuristic arguments will be discussed in the next section with

more mathematical background and we will see that the statements made here hold true.

The only open question that remains is how to generalize the idea of [Thm. 3.3](#) to any $D(N, M)$ dimensional representation. But as we are mostly interested in the [FuR](#) and [AdR](#) for applications with quarks and gluons, we will not follow this track.

3.3 Finding the isotropy subgroup

The isotropy subgroup is defined in [Def. 2.2](#) as the maximum set of group elements which do not change our fixed state $|\psi_0\rangle$. The question that arises, is how large can the isotropy group be or equivalently how many parameters are at least necessary to completely describe the [CS](#). Our goal is to find all elements $h \in \mathcal{H}$ which is equivalent to finding all generators T_a of the Lie algebra for which $|\psi_0\rangle$ is an eigenstate. Then

$$\mathcal{H} = \{h = e^{i\theta_a T_a} | T_a \in \mathcal{H} \equiv \{T_b | T_b |\psi_0\rangle = \lambda_b |\psi_0\rangle\}\} \quad (3.81)$$

will be the isotropy subgroup and \mathcal{H} is the isotropy subalgebra of [Def. 2.5](#). Then it is only left, if we can decompose any group element into the form

$$e^{i\theta_a T_a} |_{T_a \notin \mathcal{H}} e^{i\theta_b T_b} |_{T_b \in \mathcal{H}} = g \in \mathcal{G}. \quad (3.82)$$

Acting with this onto $|\psi_0\rangle$, the right term will just give us a phase that we can ignore and we are left with only the parameters from the coset $\mathcal{X} = \mathcal{G}/\mathcal{H}$, which are sufficient to describe the [CS](#).

For the decomposition in [\(3.82\)](#) we need some terms from group theory as well as some assumptions. This detour is based on the book of Hermann [\[Her66\]](#) about Lie groups. The Lie group \mathcal{G} should be semisimple, connected and only has a finite center. In our case of $SU(n)$ this is fulfilled easily. We recall that \mathcal{G} is the corresponding Lie algebra. Let \mathcal{K} be a compact subgroup of the Lie group \mathcal{G} and \mathcal{G} has the so called Cartan decomposition $\mathcal{G} = \mathcal{K} \oplus \mathcal{P}$, i.e.

$$[\mathcal{K}, \mathcal{K}] \subset \mathcal{K}, \quad [\mathcal{K}, \mathcal{P}] \subset \mathcal{P}, \quad [\mathcal{P}, \mathcal{P}] \subset \mathcal{K}. \quad (3.83)$$

The first property is just due to the fact that \mathcal{K} is a subgroup. For our purpose it is enough to find such a decomposition but there exists a theorem that this is always possible, known as Cartan's theorem. Then we can formulate the following theorem

Theorem 3.4. *Let \mathcal{G} be a connected Lie group which only has a finite center and \mathcal{K} be a connected subgroup. Further \mathcal{G} and \mathcal{K} are the corresponding Lie algebras and \mathcal{G} admits a Cartan decomposition (3.83). Further \mathcal{P} be the image of \mathcal{P} in \mathcal{G} under the exponential map. Then the Lie group has the decomposition*

$$\mathcal{G} = \mathcal{P}\mathcal{K}. \quad (3.84)$$

The proof of this theorem is obtained via Riemann geometry and is of no particular interest for this work. This groundwork on Lie groups and algebras will enables us to fix the isotropy subgroup of the fixed vector $|\psi_0\rangle$ based on the ideas from the beginning of this section.

Before we move on, we want to mention the application of Thm. 3.4 when decomposing a group into subgroups. This procedure involves taking a maximal abelian subalgebra \mathcal{A} of \mathcal{P} . In the trivial case \mathcal{A} contains just one element but nevertheless \mathcal{P} can be written as $\mathcal{P} = \mathcal{K}\mathcal{A}\mathcal{K}$ [Her66]. Be aware that we now moved to the group and left the algebra. This fact enables us together with (3.84) to decompose \mathcal{G} as

$$\mathcal{G} = \mathcal{K}\mathcal{A}\mathcal{K}. \quad (3.85)$$

As \mathcal{K} is itself a group we can start this decomposition all over again. If \mathcal{A} always only consists of one element, this results in an algorithm where we can break down \mathcal{G} into a finite number of one-parameter subgroups in a specific order. In the case of $SU(n)$ this is always possible as the generators do not commute and thus the maximal abelian subalgebra \mathcal{A} only consists of one element. This gives the well known Euler-angle decomposition of $SU(2)$ which we already used in (3.6) and that can be generalized to $SU(n)$ based on this idea [Byr97, TS02, BCC06]. We want to show the $SU(2)$ and $SU(3)$ cases explicitly as they might also help to illustrate the following analysis. Considering $SU(2)$ we take $\mathcal{K} = J_3$ as the subalgebra and our conditions in (3.83) are clearly met and we can write

$$\mathcal{G} = e^{i(\theta_1 J_1 + \theta_2 J_2)} e^{i\theta_3 J_3} = \mathcal{P}\mathcal{K} \quad (3.86)$$

which is essentially nothing else than (3.8). Then for the maximal abelian subalgebra of $\{J_1, J_2\}$ we take J_2 , decompose \mathcal{P} as

$$\mathcal{P} = e^{i\alpha J_3} e^{i\beta J_2} e^{i\gamma J_3}. \quad (3.87)$$

In the case of $SU(2)$ it is fairly easy to show explicitly for the **FuR** that this is indeed an decomposition of \mathcal{P} but as stated above, this is always the case. Now we put (3.87) into (3.86) and we are at first left with four parameters. But the last two terms are both group elements with the generator J_3 in the exponential and this redundancy can easily be dealt with when we define $\gamma' = \gamma + \theta_3$. Then we have $\mathcal{G} = e^{i\alpha J_3} e^{i\beta J_2} e^{i\gamma' J_3}$, the Euler angle decomposition as in (3.6).

For $SU(3)$ we can start all over again and search for \mathcal{K} . Looking at the structure constants we see that $\{\lambda_1, \lambda_2, \lambda_3, \lambda_8\}$ is a good choice. As λ_8 commutes with the other three this is essentially a $SU(2)$ for which we already found the Euler decomposition. Then we choose one generator of the remaining ones, e.g. λ_5 and can decompose $\mathcal{P} = \mathcal{K}g(\lambda_5)\mathcal{K}$ equivalent to (3.87). Then we are left at a point where we have

$$\mathcal{G} = \mathcal{K}g(\lambda_5)\mathcal{K}\mathcal{K} \tag{3.88}$$

and the redundancies of the two \mathcal{K} terms on the right are easily dealt with. The only difficulty is the remaining λ_8 terms left to the λ_5 term but we still have one parameter too much in comparison to the rank of our group. Thus we finally arrive at the decomposition already done by Byrd [Byrd97]:

$$T(g) = e^{i\alpha\lambda_3} e^{i\beta\lambda_2} e^{i\gamma\lambda_3} e^{i\delta\lambda_5} e^{i\varepsilon\lambda_3} e^{iz\lambda_2} e^{i\eta\lambda_3} e^{i\theta\lambda_8} . \tag{3.89}$$

This is also one of the first works where the Euler decomposition was generalized to another $SU(n)$.

This idea then generalizes to any $SU(n)$: We can always take a $SU(n-1)$ subalgebra as before. If we choose a common generalization scheme, e.g the generalized Gell-Mann matrices [Geo99], this subalgebra will consist of the first generators and the single new Cartan generator. That one will completely commute with this algebra by definition. In the case of $n = 4$ this would be $\{\lambda_1, \dots, \lambda_8, \lambda_{15}\}$ and then we are at the already known case and just reproduce the scheme from above. For $n > 3$ we still need to put some thoughts in removing the already discussed redundancies as we have over-parametrized our group elements. But this can be done in a canonical way [TS02]. In this work it is also shown how to get the correct Haar measure for this parametrization if we want to construct a **RoU**.

After this little detour which firstly deepened the understanding of some points from above and secondly gave a nice outlook onto some applications of **Thm. 3.4**, we want to move on to discuss the consequence on the **CSS**. Therefore we want to find the isotropy subgroup, thus the maximal subgroup that leaves our fixed state $|\psi_0\rangle$ invariant. We

will exclusively work in the context of $|\psi_0\rangle$ being a canonical basis state vector of the representation as we can always do a unitary transformation into this system.

SU(2)

From the structure of $SU(2)$ (3.1) it is known that only one generator is diagonalizable at a time. Thus $|\psi_0\rangle$ can only be eigenstate to one which we have taken to be J_3 and the arguments from above justified the construction in Sec. 3.1.2: We are left with two parameters to completely describe the according CS and cannot reduce this further.

SU(3)

The rank of $SU(3)$ is two and as a result we have two Cartan operators and any state can be at least eigenstate to two generators, which are in general taken to be λ_3 and λ_8 . Then (3.89) already is of the form that the isotropy subgroup is acting first on $|\psi_0\rangle$. Thus in general we cannot get rid of more parameters.

Taking a look at the FuR, viz the Gell-Mann matrices (3.62), we see that any basis vector is also eigenvector of two more matrices, besides the Cartan operators, with the eigenvalue zero. Thus we can get rid of another two parameters and as stated before, four parameters are enough to describe the corresponding CS. This can also be seen when going to the complex algebra \mathcal{G}^c which is the linear combination of all generators with complex coefficients. Within this are the raising and lowering operators, e.g. $\lambda_1 \pm i\lambda_2$ which are equivalent to the roots. The six roots are shown in Fig. 3.1a with blue solid arrows.

Now we take a look at the FuR of $SU(3)$ which is shown in Fig. 3.1b where we placed the roots at the highest weight state and scaled them with a factor of $\frac{1}{2}$ for better visibility. The highest weight state is an eigenstate to the four solid roots with the eigenvalue zero. From these, only the two blue, thicker ones are a pair of raising and lowering operators. Thus also the two hermitian generators, those roots are composed of, must have the highest weight state as eigenstate, as they are only a linear combination of them. As a consequence the corresponding group elements of these two hermitian generators are also in the isotropy subgroup. The two red dotted roots do not have the highest weight state as eigenstates and eventually the corresponding four hermitian generators are needed to describe the CS. This can be done for each of the three states of the FuR with each pair of raising and lowering operators. Then we do a

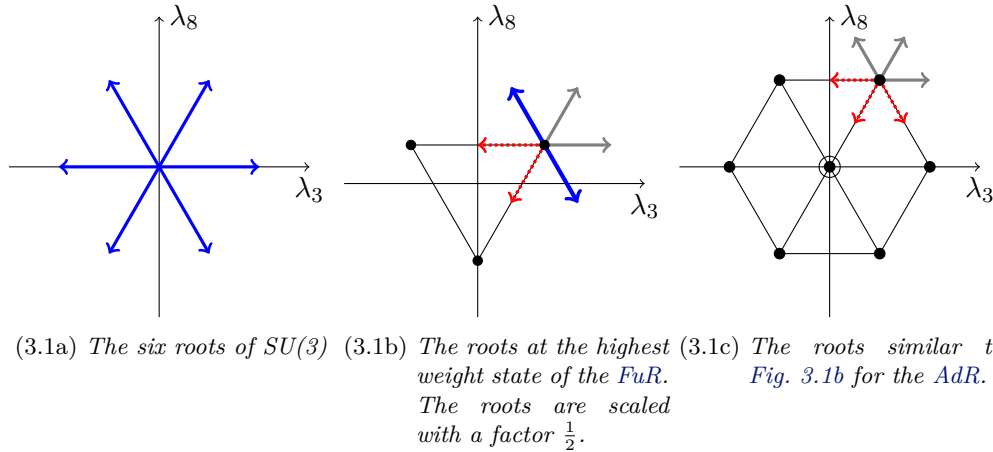


FIG. 3.1: The roots and weights for the FuR and AdR of $SU(3)$ [Geo99]. The axes are always labeled with the two canonical Casimir operators λ_3 and λ_8 . For description see the text.

decomposition similar to (3.89) where the generators for which $|\psi_0\rangle$ is an eigenstate are in \mathcal{K} . It is just about finding the corresponding $SU(2)$ subalgebra and then the scheme from above will lead us to the desired decomposition of (3.82). This leaves us with the four parameters as already discussed before.

When constructing higher dimensional representations as $3^{\otimes k}$ from the FuR , we do not change the shape of the triangle and the three maximum weight states have a four-dimensional isotropy subgroup. As already discussed with Thm. 2.8 we are anyways interested to take these states as they give us CS closest to the classical ones.

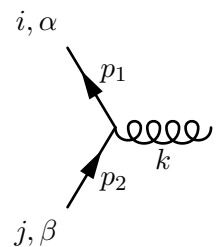
Now we turn our attention towards the AdR of $SU(3)$ as shown in Fig. 3.1c where we again put the roots onto the highest weight state with a factor $\frac{1}{2}$. The three solid gray roots have this state as an eigenstate and the three red dotted not. Thus we can not find a pair of raising and lowering operators which have both this state as an eigenstate and therefore it is not an eigenstate to any generator besides the two Cartan operators. This is true also for all the other states of the AdR and also for any representation which has at least one 3 and one $\bar{3}$ involved in its construction. Thus we need in total six parameters to describe our CSS as the isotropy subgroup is only two dimensional.

4 QCD cross sections

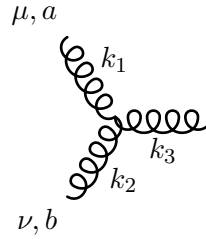
The goal of this chapter is to calculate QCD cross sections in the CSS and trying to find simplifications for calculating higher order processes. To see that our method indeed gives the correct results we will first calculate the cross sections in the color basis for comparison. We have chosen the process from quark and antiquark to two gluons as example. This chapter will give us the basis for the numeric calculation in the next one.

4.1 Feynman rules

We want to review quickly the Feynman rules we are using in the following which can be found in any textbook about QFT, e.g. [PS95]. First we look at the interactions, particularly between fermions and gluons:

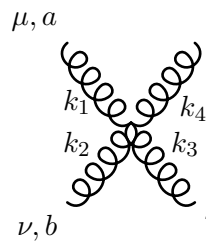

$$\mu, a = ig_s [\gamma^\mu]_{\alpha\beta} [T_a]_{ij}. \quad (4.1)$$

Here g_s is the QCD coupling constant, γ^μ are the Dirac matrices and T_a the generators of our color SU(n). Next we take a look at the three gluon vertex where it is important to specify the direction of the momenta: We use the convention of all momenta ingoing and we have:



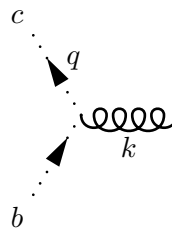
$$\eta, c = g_s f_{abc} (g^{\mu\nu} (k_1 - k_2)^\eta + g^{\nu\eta} (k_2 - k_3)^\mu + g^{\eta\mu} (k_3 - k_1)^\nu). \quad (4.2)$$

The structure constants f_{abc} of our color SU(n) are already known and $g^{\mu\nu}$ is the metric tensor of our Minkowski space. With the same convention of all momenta being incoming, the four gluon vertex is:



$$= -ig_s^2 (f_{abe} f_{cde} (g_{\mu\eta} g_{\rho\nu} - g_{\mu\rho} g_{\nu\eta}) + f_{ace} f_{dbe} (g_{\mu\rho} g_{\nu\eta} - g_{\mu\nu} g_{\eta\rho}) + f_{ade} f_{bce} (g_{\mu\nu} g_{\eta\rho} - g_{\mu\eta} g_{\rho\nu})). \quad (4.3)$$

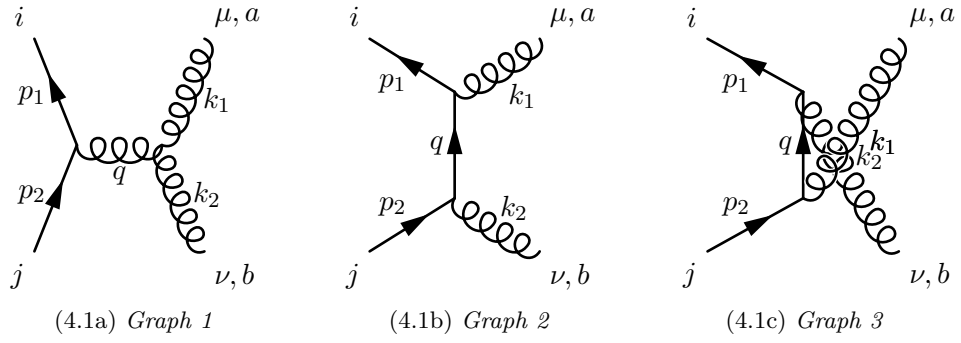
When we are not working with physical polarizations but instead with the simple polarization sum, used later in (4.14), we need to consider ghosts and their interaction term:



$$\mu, a = g_s f_{abc} q^\mu. \quad (4.4)$$

Lastly we need the propagators of gluons and fermions which are given via:

$$\mu, a \text{ (wavy line)} \nu, b = \delta_{ab} \frac{-ig^{\mu\nu}}{k^2} \quad (4.5)$$


 FIG. 4.1: Feynman graphs for the example process $q\bar{q} \rightarrow gg$.

and

$$i \xrightarrow{q} j = \delta_{ij} \frac{-i(\not{q} + m)}{q^2 - m^2}. \quad (4.6)$$

In all cases we are going to assume that we are at an energy scale where the quarks can be taken to be massless and then we have instead of (4.6):

$$\delta_{ij} \frac{-i\not{q}}{q^2} \equiv \delta_{ij} \frac{-i}{\not{q}}. \quad (4.7)$$

With these rules we can turn our attention to our example process next. For this one, the rules presented in this section are enough and we omitted the ones which are not needed in this thesis, e.g. the ghost propagator which we would need if we have four gluons in our final states.

4.2 Process example: $q\bar{q} \rightarrow gg$

As already mentioned, we are going to show the calculation of the cross section from a quark and an antiquark to two gluons. Therefore we need to consider the three Feynman graphs shown in Fig. 4.1. We take the momenta of the final gluons to be outgoing when calculating the Feynman amplitudes for these graphs:

$$\begin{aligned}
 M_1 &= \frac{g_s^2}{s} f_{abc} [T_c]_{ij} \bar{v}(p_1) \gamma^n u(p_2) \varepsilon^{*\mu}(k_1) \varepsilon^{*\nu}(k_2) \\
 &\quad \times (g_{\mu\nu}(k_2 - k_1)_\eta + g_{\nu\eta}(-k_2 - q)_\mu + g_{\eta\mu}(q + k_1)_\nu) \\
 M_2 &= -\frac{ig_s^2}{t} [T_a T_b]_{ij} \bar{v}(p_1) \gamma_\mu (\not{p}_2 - \not{k}_2) \gamma_\nu u(p_2) \varepsilon^{*\mu}(k_1) \varepsilon^{*\nu}(k_2) \\
 M_3 &= -\frac{ig_s^2}{u} [T_b T_a]_{ij} \bar{v}(p_1) \gamma_\nu (\not{p}_2 - \not{k}_1) \gamma_\mu u(p_2) \varepsilon^{*\mu}(k_1) \varepsilon^{*\nu}(k_2)
 \end{aligned} \tag{4.8}$$

where the subscript numbers i of M_i refer to the numbering of the graphs in Fig. 4.1. Further $u(p)$ and $v(p)$ are the spinors for the incoming fermions and the tensors $\varepsilon^\mu(k)$ are the polarization vectors of the outgoing gluons. Be aware that in this section we need to switch to the asterisk $*$ to mark complex conjugation to prevent confusion with the Dirac adjoint $\bar{u} = u^\dagger \gamma_0$. Moreover we use the Mandelstam variables

$$\begin{aligned}
 s &= 2p_1 p_2 &= 2k_1 k_2 \\
 t &= -2p_1 k_1 &= -2p_2 k_2 \\
 u &= -2p_1 k_2 &= -2p_2 k_1
 \end{aligned} \tag{4.9}$$

from the center-of-mass frame in the massless limit of the quarks and we can derive the following identity:

$$s + t + u = 0. \tag{4.10}$$

The intermediate momentum q in our graphs is given via momentum conservation at each vertex which results in:

$$\begin{aligned}
 \text{Graph 1: } q &= p_1 + p_2 &= k_1 + k_2 \\
 \text{Graph 2: } q &= p_2 - k_2 &= k_1 - p_1 \\
 \text{Graph 3: } q &= p_2 - k_1 &= k_2 - p_1.
 \end{aligned} \tag{4.11}$$

In order to calculate the total cross section, we need to compute

$$|M|^2 = |M_1 + M_2 + M_3|^2 = |M_1|^2 + |M_2 + M_3|^2 + M_1(M_2^\dagger + M_3^\dagger) + (M_2 + M_3)M_1^\dagger \tag{4.12}$$

which will be done in the way expressed in this equation. We will average over the incoming spins and the outgoing polarizations. The mainly interesting part for this work will be the calculation of the color terms from T_a and f_{abc} which will be later performed in the CSS. We leave still open any averaging over color indices, both incoming and outgoing. We will use the completeness relations for the quarks and the

simple polarization sum for the gluons:

$$\sum_s u_s(p)\bar{u}_s(p) = \not{p} = \sum_s v_s(p)\bar{v}_s(p) \quad (4.13)$$

$$\sum_x \varepsilon_{\mu,x}(k)\varepsilon_{\nu,x}^*(k) = -g_{\mu\nu} \quad (4.14)$$

In the first equation s is the spin of the fermion and in the second one is x the polarization of the gluon. As we use (4.14), we need to subtract the contributions from the ghosts in the end [PS95]. When we are considering the ghost graphs explicitly at page 58 we will discuss in detail how this is done. Further (4.13) induces that we average over the initial spins which gives us a factor $\frac{1}{2^2}$ and in the end we are further averaging over the color indices. Thus in the first part of this section we are only calculating (4.12) and there is no sum induced over the color indices a, b, \dots as well as i, j, \dots if they occur twice. Though this would not change the calculation, we just wanted to mention it for clarity. However there is still a sum over repeated Lorentz indices μ, ν, \dots implied.

Graph 1 We can rewrite the squared magnitude of graph 1 with (4.13):

$$\begin{aligned} \frac{1}{4} \sum_{\text{Spin}} |M_1|^2 &= \frac{g_s^4}{4s^2} A_\eta A_\lambda^* \text{tr}[\not{p}_1 \gamma^\eta \not{p}_2 \gamma^\lambda] f_{abc} f_{abd} [T_c]_{ij} [T_d]_{ji} \\ &= \frac{g_s^4}{4s^2} A_\eta A_\lambda^* 4(p_2^\lambda p_1^\eta - p_2 p_1 g^{\lambda\eta} + p_2^\eta p_1^\lambda) \Gamma_{abij}^1 \end{aligned} \quad (4.15)$$

where we used a trace identity of four Dirac matrices [PS95] and

$$A_\eta = \varepsilon^*(k_1)\varepsilon^*(k_2)(k_2 - k_1)_\eta - \varepsilon_\eta^*(k_2)(k_1 + 2k_2)\varepsilon^*(k_1) + \varepsilon_\eta^*(k_1)(2k_1 + k_2)\varepsilon^*(k_2).$$

The last line of (4.15) defines us the color term:

$$\Gamma_{abij}^1 \equiv f_{abc} f_{abd} [T_c]_{ij} [T_d]_{ji}. \quad (4.16)$$

Finally we plug in the polarization sum (4.14) and have to evaluate the following terms:

$$p_2 A p_1 A^* = 2s^2 - \frac{7}{4}(t^2 + u^2) - tu = p_1 A p_2 A^*$$

where the second equality can be derived from the first via an exchange of 1 and 2 which is equivalent to exchanging t and u . Finally

$$p_2 p_1 A^* A = \frac{9}{2} s^2$$

and in the massless limit we can use the following relation which we obtain from (4.10):

$$2tu = s^2 - t^2 - u^2.$$

Thus putting everything together in (4.15) we get:

$$\frac{1}{4} \sum_{\text{Spin}} |M_1|^2 = -g_s^4 \left(\frac{3}{2} + \frac{5}{2} \frac{t^2 + u^2}{s^2} \right) \Gamma_{abij}^1 = -\frac{g_s^4}{4} (11 + 5 \cos^2 \theta) \Gamma_{abij}^1 \quad (4.17)$$

where we introduced the scattering angle θ between p_1 and k_1 :

$$\cos \theta = 1 + \frac{2t}{s} = -1 - \frac{2u}{s} \quad \text{or} \quad u = -\frac{s}{2}(1 + \cos \theta), \quad t = -\frac{s}{2}(1 - \cos \theta). \quad (4.18)$$

Graph 2 + graph 3 We look at these two graphs together as the cross terms vanish in the high energy limit where we can neglect the masses of the quarks. Furthermore they are both related by an exchange of u and t and thus it is sufficient to calculate only one:

$$\begin{aligned} \frac{1}{4} \sum_{\text{Spin}} |M_2|^2 &= \frac{g_s^4}{4t^2} \text{tr}[\not{p}_1 \gamma_\mu (\not{p}_2 - \not{k}_2) \gamma_\nu \not{p}_2 \gamma_\eta (\not{p}_2 - \not{k}_2) \gamma_\lambda] g^{\mu\lambda} g^{\nu\eta} [T_a T_b]_{ij} [T_b T_a]_{ji} \\ &= \frac{g_s^4}{t^2} \text{tr}[\not{p}_1 (\not{p}_2 - \not{k}_2) \not{p}_2 (\not{p}_2 - \not{k}_2)] [T_a T_b]_{ij} [T_b T_a]_{ji} = 2g_s^4 \frac{u}{t} \Gamma_{abij}^2. \end{aligned}$$

In the last step we defined our second color term

$$\Gamma_{abij}^2 = [T_a T_b]_{ij} [T_b T_a]_{ji} \quad (4.19)$$

and then we get $|M_3|^2$ just via an exchange of the gluons, thus a and b as well as u and t and in total we have:

$$\frac{1}{4} \sum_{\text{Spins}} |M_2 + M_3|^2 = \frac{1}{4} \sum_{\text{Spins}} (|M_2|^2 + |M_3|^2) = 2g_s^4 \left(\frac{u}{t} \Gamma_{abij}^2 + \frac{t}{u} \Gamma_{ba ij}^2 \right). \quad (4.20)$$

At this stage, we need to keep track of the different color terms in this expression as they are not equal but will be in the end when we sum over the color indices.

Cross terms between 1 and 2/3 Going back to (4.12), we see that these are four terms in total but we will only calculate one term and the others are given by symmetries. Let's look at the term from graph 1 with the hermitian conjugation of the term from graph 2:

$$\frac{1}{4} \sum_{\text{Spins}} M_1 M_2^\dagger = \frac{ig_s^4}{4st} \text{tr}[\not{p}_1 \gamma_\eta \not{p}_2 \gamma_\nu (\not{p}_2 - \not{k}_2) \gamma_\mu] A^\eta \varepsilon^\mu(k_1) \varepsilon^\nu(k_2) f_{abc} [T_c]_{ij} [T_b T_a]_{ji}. \quad (4.21)$$

Considering the term with the polarization vectors, we can rewrite it as:

$$A^\eta \varepsilon^\mu(k_1) \varepsilon^\nu(k_2) = g^{\mu\nu} (k_2 - k_1)^\eta - g^{\nu\eta} (k_1 + 2k_2)^\mu + g^{\eta\mu} (2k_1 + k_2)^\nu.$$

And we are left with the trace

$$\begin{aligned} \text{tr}[\not{p}_1 (\not{k}_2 - \not{k}_1) \not{p}_2 \gamma^\mu (\not{p}_2 - \not{k}_2) \gamma_\mu - \not{p}_1 \gamma^\mu \not{p}_2 \gamma_\mu (\not{p}_2 - \not{k}_2) (\not{k}_1 + 2\not{k}_2) \\ + \not{p}_1 \gamma^\mu \not{p}_2 (2\not{k}_1 + \not{k}_2) (\not{p}_2 - \not{k}_2) \gamma_\mu] = -8t^2 \end{aligned}$$

which we put into (4.21):

$$\frac{1}{4} \sum_{\text{Spins}} M_1 M_2^\dagger = -\frac{2ig_s^4}{s} t \Gamma_{abij}^3 \quad (4.22)$$

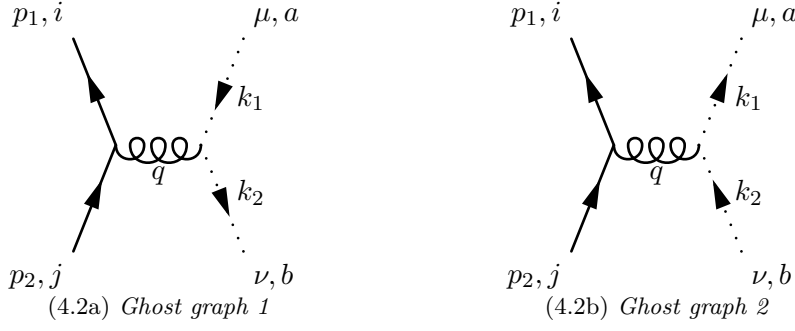
and we define our third color term

$$\Gamma_{abij}^3 = f_{abc} [T_c]_{ij} [T_b T_a]_{ji}. \quad (4.23)$$

Then $M_1 M_3^\dagger$ is just given by an exchange of the two gluons and the other terms are obtained via complex conjugation and we finally get:

$$\frac{1}{4} \sum_{\text{Spins}} (M_1 (M_2 + M_3)^\dagger + M_1^\dagger (M_2 + M_3)) = -\frac{4g_s^4}{s} \left(t \text{Re}(i\Gamma_{abij}^3) + u \text{Re}(i\Gamma_{baij}^3) \right). \quad (4.24)$$

Ghosts As we are only using the simple polarization sum (4.14) instead of the physical polarization, we need to subtract the ghost graphs to cancel the unphysical polarizations [PS95]. This means we need to look at the two graphs in Fig. 4.2 where we substituted each outgoing gluon with the corresponding ghost. As the ghosts only couple to the gluons we need to consider only the Feynman graph 1 from Fig. 4.1. It would be equivalent to first consider the symmetry factor of our Feynman graph which is $\frac{1}{2}$ here as we have two gluons in the final state. Then we only need to consider one


 FIG. 4.2: Ghost graphs for the example process $q\bar{q} \rightarrow gg$.

ghost graph since both give the same contribution as we will also see in our calculation. This equivalence can be understood from the following relation [PS95]:

$$\begin{aligned}
 \left| \begin{array}{c} \text{blob} \\ \text{blob} \end{array} \right|^2 &= \frac{1}{2} \left(\text{Im} \left(\begin{array}{c} \text{blob} \\ \text{blob} \end{array} \right) - \text{Im} \left(\begin{array}{c} \text{blob} \\ \text{blob} \end{array} \right) + \begin{array}{c} \text{blob} \\ \text{blob} \end{array} \right) \\
 &= \frac{1}{2} \text{Im} \left(\begin{array}{c} \text{blob} \\ \text{blob} \end{array} \right) - \text{Im} \left(\begin{array}{c} \text{blob} \\ \text{blob} \end{array} \right).
 \end{aligned}$$

Here the shaded blob just is a short notation for all the interactions and other external particles as only the gluons are relevant when we consider the ghosts. As we did not take the symmetry factor in account yet, we will stick to the first line of this relation and include it in the end.

Going back to the contribution of the ghost graphs from Fig. 4.2 we only need to calculate the matrix element for the first one and get the other one via an exchange of u and t :

$$M_{\text{ghost},1} = \frac{g_s^2}{s} f_{abc} k_{2\mu} \bar{v}(p_1) \gamma^\mu u(p_2) [T_c]_{ij}, \quad (4.25)$$

$$\begin{aligned}
 \frac{1}{4} \sum_{\text{Spins}} |M_{\text{ghost},1}|^2 &= \frac{g_s^4}{4s^4} \text{tr}[\not{p}_1 \not{k}_2 \not{p}_2 \not{k}_2] f_{abc} f_{abd} [T_c]_{ij} [T_d]_{ji} \\
 &= \frac{g_s^4}{4} \left(1 - \frac{u^2 + t^2}{s^2} \right) \Gamma_{abij}^1.
 \end{aligned} \quad (4.26)$$

We see that the occurring color term is the already known one from (4.16) and this (4.26) is symmetric in an exchange of t and u . Thus the second ghost graph gives the same contribution as already stated and in total we have:

$$\frac{1}{4} \sum_{\text{Spins}} |M_{\text{ghost}}|^2 = \frac{g_s^4}{2} \left(1 - \frac{u^2 + t^2}{s^2} \right) \Gamma_{abij}^1. \quad (4.27)$$

The complete matrix element and the cross section Now we take (4.12) and collect the individual terms from (4.17), (4.20) as well as (4.24) and subtract the ghost contribution (4.27):

$$\begin{aligned} \frac{1}{4} \sum_{\text{Spins}} |M|^2 = 2g_s^4 \left(- \left(1 + \frac{t^2 + u^2}{s^2} \right) \Gamma_{abij}^1 + \left(\frac{u}{t} \Gamma_{abij}^2 + \frac{t}{u} \Gamma_{baij}^2 \right) \right. \\ \left. - 2 \left(\frac{t}{s} \text{Re}(i\Gamma_{abij}^3) + \frac{u}{s} \text{Re}(i\Gamma_{baij}^3) \right) \right). \quad (4.28) \end{aligned}$$

Next we average over the external color indices which gives us a factor $\frac{1}{n^2}$ depending on our color $\text{SU}(n)$ as we have two quarks as initial particles which are in the **FuR**. This enables us to manipulate the third color term (4.23) due to the trace being invariant under cyclic permutations:

$$\begin{aligned} \sum_{a,b,i,j} f_{abc} [T_c]_{ij} [T_b T_a]_{ji} &= \frac{1}{i} \text{tr} [[T_a, T_b] T_b T_a] = -\frac{1}{2i} \text{tr} [[T_a, T_b] [T_a, T_b]] \\ &= \frac{1}{2i} \sum_{a,b,i,j} f_{abc} [T_c]_{ij} f_{abd} [T_d]_{ji}. \end{aligned}$$

This is the first color term and we can state that

$$\sum_{a,b,i,j} \Gamma_{abij}^3 = \frac{1}{2i} \sum_{a,b,i,j} \Gamma_{abij}^1 \quad (4.29)$$

which holds for arbitrary n only with the sums but in the $\text{SU}(2)$ case this equivalence is already given at the level of the individual elements. Then going back to (4.28), we replace $t + u$ in the last term with $-s$ (4.10) and get:

$$\frac{1}{4n^2} \sum_{\substack{\text{Spins} \\ a,b,i,j}} |M|^2 = 2 \frac{g_s^4}{n^2} \left(-\frac{t^2 + u^2}{s^2} \Gamma^1 + \left(\frac{u}{t} + \frac{t}{u} \right) \Gamma^2 \right) \quad (4.30)$$

where we use the notation $\Gamma^\alpha = \sum_{a,b,i,j} \Gamma_{abij}^\alpha$. This (4.30) will be the expression we will use in most cases below when we are calculating the color factors. In some cases we might also need (4.28). To compare our result to the literature we move on to $n = 3$ and calculate the differential cross section. For SU(3) the first color trace evaluates to 12 and the second to $\frac{16}{3}$ and we have the familiar result:

$$\frac{1}{4n^2} \sum_{\substack{\text{Spins} \\ a,b,i,j}} |M|^2 = \frac{32g_s^4}{27} \left(\frac{u}{t} + \frac{t}{u} - \frac{9}{4} \frac{t^2 + u^2}{s^2} \right). \quad (4.31)$$

For the cross section [PS95] we need to take into account the already mentioned symmetry factor because we have two final gluons which are indistinguishable. The QCD coupling constant can be expressed in terms of the strong coupling constant [O⁺14]:

$$g_s^4 = 16\pi^2 \alpha_s^2 \quad (4.32)$$

and in total we have:

$$\begin{aligned} \frac{d\sigma}{dt} &= \frac{1}{16\pi s^2} \frac{1}{2} \frac{1}{4n^2} \sum_{\substack{\text{Spins} \\ a,b,i,j}} |M|^2 = \frac{g_s^4}{27\pi s^2} \left(\frac{u}{t} + \frac{t}{u} - \frac{9}{4} \frac{t^2 + u^2}{s^2} \right) \\ &= \frac{16\pi\alpha_s^2}{27s^2} \left(\frac{u}{t} + \frac{t}{u} - \frac{9}{4} \frac{t^2 + u^2}{s^2} \right). \end{aligned} \quad (4.33)$$

With our definition of the scattering angle θ (4.18) we can evaluate the Jacobian determinant and get:

$$\frac{d\sigma}{d\Omega} = \frac{4\alpha_s^2}{27s} \left(\frac{u}{t} + \frac{t}{u} - \frac{9}{4} \frac{t^2 + u^2}{s^2} \right). \quad (4.34)$$

Comparing this with the result of the Particle Data Group [O⁺14], we see a difference of a factor of 2. This is due to the fact that they omit the symmetry factor and instead only integrate over half the domain of θ . But unfortunately they do not mention this very clearly but a comparison with [BP87] shows that our result (4.34) is indeed correct.

4.3 Calculation of the color terms

First we want to introduce the concept of primitiveness of invariant tensors from [Cvi08]. Cvitanovic uses a completely different approach to group theory as the tra-

ditional way: He defines a symmetry group via a list of primitive invariant tensors. These are tensors which are invariant under group transformations and cannot be decomposed into further invariants. In our example of $SU(2)$ these are the Kronecker-Delta δ and the generators T of the FuR and f of the AdR. For $SU(3)$ we also have the symmetric tensor d as an primitive invariant which is defined from the anticommutator instead of the commutator for f . Now the primitiveness says that each invariant tensor with a certain number of free indices must be proportional to a sum of all primitive tensors with the same number of free indices. As an example take the contraction $f_{abc}f_{bcd}$ which has only two free indices, viz a and d , and thus must be proportional to our only primitive tensor with two indices, i.e. δ_{ad} , which can be also shown via a direct calculation.

When we perform the calculations in the previous section of calculating cross sections of processes we need to evaluate the color factors in (4.28) or (4.30). Therefore we need to contract the tensors of our $SU(n)$ in the FuR and AdR. To generalize these calculations, we introduce a different notation: Let F be $\in \{T, f\}$, i.e. a generator in any representation. In addition N, O etc. is meant to be any combination of F via addition or multiplication. In this framework we do not have anymore the necessity to distinguish between indices from the FuR and AdR and we will use the roman letters a, b, c, \dots from the beginning of the alphabet for both. In the CSS we will use letters from the back of the alphabet, viz z, y, x, \dots to distinguish them from the color case. Be aware that in the CSS there is no summation but rather an integration with the correct measure, but we will still use the index notation. This is also known as the De-Witt-notation and used by Weinberg in [Wei96]. Further we do not need to take track of each individual index of a tensor and we will group them as $\{a_i\}$ or $\{z_i\}$ respectively.

To clarify this notation further, we look at the calculation of QCD cross sections as in Sec. 4.2 and we see that each Feynman graph has the following structure:

$$M_k = C_{\text{kinetic}}^k N_{\{a_i\}}^k \equiv C_{\text{kinetic}}^k N_{a_1 a_2 \dots}^k \equiv C_{\text{kinetic}}^k \prod_j F_{b_{j_1} b_{j_2} b_{j_3}}^j \quad (\text{no sum over } k). \quad (4.35)$$

Hence $N_{\{a_i\}}^k$ is the collection of all color generators of one Feynman graph. In the following we will use the first expression of this equation. The index k just distinguishes between the different graphs and consequently it is no index and to avoid confusion we added the remark that there is no sum over it implied. And the product over j after the last equivalence sign runs over all vertices of this graph. All the other terms which are not composed of generators of the color $SU(n)$, especially the kinetic ones,

are put into C_{kinetic}^k . Note that the group $\{a_i\}$ of indices are the indices of all the external particles.

A careful reader might have noticed that we cannot treat all Feynman rules in this manner, e.g. take a look at the four gluon vertex from (4.3). This one can not be factorized into a color and kinetic part as in (4.35). This is also the case if we include scalar particles in our theory. But we can treat each summand of (4.3) as two interaction of three gluons as each is composed of two f just with different factors than (4.2). Thus for each four gluon vertex in a Feynman graph we draw three times as many graphs which results in an equivalent description. Then we calculate the color factor for each of the new graphs and (4.35) is a valid decomposition if M_k is one of these new graphs.

The total matrix element is then the sum over all Feynman graphs, aka M_k . When calculating the cross section, we need the absolute square value of this sum which can be written as the sum over all combinations of the color tensors N^k :

$$\begin{aligned} |M|_{\{a_i\}}^2 &= \sum_{k,l} M_k^\dagger M_l = \sum_{k,l} (N_{\{a_i\}}^k)^\dagger N_{\{a_i\}}^l (C_{\text{kinetic}}^k)^\dagger C_{\text{kinetic}}^l \\ &\equiv \sum_{k,l} N^{k\{a_i\}} N_{\{a_i\}}^l (C_{\text{kinetic}}^k)^\dagger C_{\text{kinetic}}^l \quad (\text{no sum over } a_i). \end{aligned} \quad (4.36)$$

Be aware that the group of indices of N^k and N^l are exactly the same as they correspond to the external particles of our process. As in our example above we might want to average over all external colors which leads to a complete contraction of all indices of the tensors N^k and N^l . Further in the sum in (4.36) each contraction of these two tensors has a different kinetic coefficient which is also dependent on our particular process we are looking at. Thus we will look at each summand individually as we cannot make statements for the whole sum in the general case. This contraction of two tensors in each summand can either involve twice the same or two different tensors. In the first case we are actually calculating the absolute square of one Feynman graph:

$$\sum_{\text{external}} |M_k|^2 \equiv |C_{\text{kinetic}}|^2 \sum_{\text{external}} |N|^2 = |C_{\text{kinetic}}|^2 N^{\{a_i\}} N_{\{a_i\}} \quad (4.37)$$

and in the second case we have:

$$\sum_{\text{external}} M_k M_l \equiv C_{\text{kinetic}}^\dagger C'_{\text{kinetic}} N^{\{a_i\}} N'_{\{a_i\}}. \quad (4.38)$$

This is equivalent to (4.28) where we have already executed the calculation of the kinetic part and are only left with calculating the color factors T_i individually. Some-

times we might be able to use relations between different color factors like (4.29) and end up at a point equivalent to (4.30). Furthermore we might only have one Feynman graph for our process and the cross section is already proportional to (4.37). This also holds when we can neglect the other graphs, e.g. for collinear gluon radiation from a single quark as the graphs with crossed gluon lines are kinematically suppressed.

4.3.1 Color basis

First we start with the case of calculating the color factor of one Feynman graph thus starting at (4.37) without the kinetic terms. Now we decompose our graph at one internal line that it can be written in the form

$$N_{\{a_i\}} = O_{\{b_i\}d} P_{\{c_i\}}^d, \quad \{b_i\} \cup \{c_i\} = \{a_i\}. \quad (4.39)$$

Thus our graph is built of two subgraphs contracted over the one index d . This is only possible if we can find a cut which does not split up a loop. Then the grouped indices $\{b_i\}$ and $\{c_i\}$ only contain all the external particles.

Now calculating the color term, means to contract the free indices of the tensor N with all the indices of its hermitian conjugate and results in:

$$\sum_{\text{external}} |N|^2 = O_{\{b_i\}d} P_{\{c_i\}}^d P_e^{\{c_i\}} O^{e\{b_i\}} = \text{tr} OPP^\dagger O^\dagger. \quad (4.40)$$

Rearranging these terms, we can look at the terms $O^{e\{b_i\}} O_{\{b_i\}d}$ and $P_{\{c_i\}}^d P_e^{\{c_i\}}$ and see that they are invariant under group transformation as they are a composition of group invariant tensors, the generators F . We see that both these terms have only two free indices as we averaged over the external particles. Using the primitiveness introduced at the beginning of this Sec. 4.3 from [Cvi08] these terms must be proportional to δ_d^e and we have proved the following theorem:

Theorem 4.1. *The color factor of a Feynman graph is factorizable in the form*

$$\sum_{\text{external}} |N|^2 = \sum_{\text{external}} |OP|^2 = \sum_{\text{external}} |O_d|^2 |P^d|^2 \equiv \sum_d O^{d\{b_i\}} O_{\{b_i\}d} P_{\{c_i\}}^d P_d^{\{c_i\}} \quad (4.41)$$

if it can be cut at a single internal index d .

Remark 4.1. If our graph does not contain any loop this step can be iterated over all internal lines until we are only left with the generators F . This way we need to

perform the sum, and later the integral, over internal particles only once and not twice as in (4.40).

Remark 4.2. Moreover for the proof to work it is actually sufficient that only one of the two terms of (4.40) is proportional to a Kronecker-Delta.

Next we take a look at the color factor of a mixing term of two Feynman graphs as in (4.38). Now we need to split up N' similar to (4.39). But in general we cannot guarantee that $\{b_i\}$ of N and $\{b'_i\}$ of N' are the same set of external indices. Just take our example of Fig. 4.1 and the interference of the color terms of graph 1 and graph 2: They cannot be cut in such a way to fulfill equality of the two indices sets. Once we split into quarks and gluons and the other time we twice split into a quark and a gluon. This would also not work between graph 2 and 3 due to the exchange of the external gluons. For the proof to work we need to have two equivalent sets $\{b_i\}$ and $\{b'_i\}$ in order to be only left with two free indices which result in a Kronecker-Delta. Hence in this case we cannot formulate a theorem equivalent to Thm. 4.1.

4.3.2 Coherent state system

Moreover we can make a transformation from color basis to the CSS. This is done via an insertion of a RoU in the appropriate basis representation. Then D_a^z is the coefficient of the representation of a CS in the color basis or vice versa, thus written in bra-ket-notation:

$$D_a^z = \langle a|z \rangle. \quad (4.42)$$

We can also transform a group of indices to the CSS by transforming each index individually. In our notation this is written in the following way:

$$D_{\{a_i\}}^{\{z_i\}} = \langle \{a_i\} | \{z_i\} \rangle = \prod_i \langle a_i | z_i \rangle. \quad (4.43)$$

Invariants of the Coherent state system

When moving to the CSS we need to first think about the invariant tensors for the primitiveness argument. In particular the tensor with two indices equivalent to the δ_j^i of the color basis. This is not trivial and the problem can be seen from the following

consideration: Take the identity matrix which is a rank two tensor. In general any rank two tensor can be decomposed into the [CSS](#) hence also the identity:

$$\mathbb{1} = \int d\mu_z d\mu_y t_{yz} |y\rangle \langle z|. \quad (4.44)$$

Both $\delta(y - z)$ as well as $\langle y|z\rangle$ are valid for t_{yz} to obtain the known [RoU](#) in (2.34). Usually we are not working with an overcomplete system and we have in general the possibility to choose an orthogonal basis and then both solution are the same. But in our case of the [CSS](#) this is different as we saw in (3.19) that two different [CS](#) have a non-vanishing scalar product. However both solutions for t_{yz} are invariant under group transformations: The δ function just by the fact that different complex numbers z correspond to different [CS](#) and a group transformation does not alter this. The scalar product is invariant under group transformation due to it definition.

Already Glauber recognized this problem when he was working with the [CS](#). The choice can be made unique by demanding analyticity [[Gla63](#)]. To understand Glauber's proof consider an arbitrary state $|f\rangle = f(a^\dagger) |0\rangle$ in the Hilbert space and the [CS](#) of the [HWG](#). Then inserting the [RoU](#) one obtains

$$|f\rangle = \int d\mu_z |z\rangle \langle z|0\rangle f(\bar{z}) \quad (4.45)$$

where we just used the property of the [CS](#) that they are eigenstates of the annihilation operator. Then demanding that $f(z)$ is an analytic function one can show via an explicit calculation by using the power series of f , that $\langle z|f\rangle = f(\bar{z}) \langle z|0\rangle$. This shows the uniqueness also if z is multidimensional like in our case via the Schwinger representation. Moving from the Schwinger representation to the [CSS](#) of just one fixed dimension and the coset space \mathcal{X} , one has to take care of the following subtlety: To replicate Glauber's proof into this system one can not assume a general Taylor series for f and instead needs to take a series which does not exceed the dimension of our representation as well as the parameter space of \mathcal{X} . With these ideas the proof is done straight forward and can be found explicitly in [[Eis16](#)].

This proof can now be extended to rank two and higher operators [[Gla63](#)]. Therefore we use a decomposition like in (4.44) and then the calculation is analogous where we just have to evaluate one more integral than in (4.45).

Non-equality of $\langle y|z\rangle$ and $\delta(y-z)$ in the CSS We want to look at the operator

$$B = \int d\mu'_z |z_{\text{FuR}}\rangle \langle z_{\text{AdR}}| \quad (4.46)$$

with the CS $|z_{\text{FuR}}\rangle$ of the FuR and $|z_{\text{AdR}}\rangle$ of the AdR. This operator B transforms from the AdR to the FuR and its hermitian conjugate goes the other way. This is only possible as all CS of our $SU(n)$ can be described with the same angles over the same domain. Just be aware that for example in the case of the FuR of $SU(3)$ we need to take more parameters into account as would be actually necessary as they are redundant in the FuR but not in the AdR. The measure $d\mu'_z$ is the known measure from the construction above, viz (3.24) and (3.67), without the factor of the dimension of the representation as we consider two different representations. Now consider the operators $B^\dagger B$ and BB^\dagger : In the first case we have a transformation from the AdR onto itself but this is done via a lesser dimensional space, viz the FuR, and thus we are only left in a subspace of the AdR. This can be verified easily through an explicit calculation and the subspace has the same dimensionality as the FuR. Now we look at the second one, namely BB^\dagger , and the calculation shows that we are left with a diagonal operator in the color basis which is not proportional to the $\mathbb{1}$ as the diagonal entries are different. In both cases we have to evaluate a scalar product $\langle y|z\rangle$, where both y and z are from the same representation:

$$\int d\mu_z d\mu_y |z_\alpha\rangle \langle z_\beta|y_\beta\rangle \langle y_\alpha|, \quad (\alpha, \beta) \in \{(\text{FuR}, \text{AdR}), (\text{AdR}, \text{FuR})\}.$$

In both cases the final result is not proportional to $\mathbb{1}$. On the other hand this would be the case if $\langle y|z\rangle$ is equal to $\delta(y-z)$ but this is indeed not true, as we just saw.

Thus when in the CSS we can reduce ourself only to analytic decompositions of tensors and thus $\langle \alpha|\beta\rangle$ is the only invariant rank two tensor representation of the identity. This freedom in choice comes from the fact that our system of CS is overcomplete and fractions of $|\alpha\rangle$ in the decomposition of any state can be shifted to the other CS as they are linear dependent. In consequence as already mentioned above we have different equivalent decompositions of vectors and operators in terms of the CS and we can choose one. Then the proof of Glauber presented above guarantees us that our choice of analyticity will make the decomposition always unique and guarantees us its existence.

Averaging

Now we want to make the same calculation from the color basis also in the CSS and hopefully find an equivalent theorem to [Thm. 4.1](#). We start as in [\(4.40\)](#) with

$$\int_{\text{external}} |N|^2 = O_{\{z_i\}x} P_{\{y_i\}}^x P_w^{\{y_i\}} O^{w\{z_i\}} \quad (4.47)$$

but this time we do not get an δ_x^w as already discussed but we get a scalar product $\langle x|w \rangle$ and we define the constants of proportionality as c_O :

$$O^{w\{z_i\}} O_{\{z_i\}x} \equiv c_O \langle w|x \rangle \quad (4.48)$$

and for P the same way. Thus we can do the following calculation:

$$\begin{aligned} \int_{\text{external}} |N|^2 &= \int d\mu_w d\mu_x c_O \bar{c}_P \langle w|x \rangle \langle x|w \rangle \\ &= \int d\mu_w c_O \bar{c}_P \langle w|w \rangle \langle w|w \rangle \\ &= \int d\mu_w O^{w\{z_i\}} O_{\{z_i\}w} P_{\{y_i\}}^w P_w^{\{y_i\}} \end{aligned} \quad (4.49)$$

where we used the RoU of the CSS in the second line as well as the fact that the CS have unit norm: $\langle w|w \rangle = 1$. Then in the last step we used [\(4.48\)](#) the other way and we can state the following theorem equivalent to [Thm. 4.1](#):

Theorem 4.2. *In the CSS the color factor of a Feynman graph is factorizable as*

$$\int_{\text{external}} |N|^2 = \int_{\text{external}} |OP|^2 = \int_{\text{external}} |O_w|^2 |P^w|^2 \equiv \int d\mu_w O^{w\{z_i\}} O_{\{z_i\}w} P_{\{y_i\}}^w P_w^{\{y_i\}} \quad (4.50)$$

if it can be cut at a single internal index w .

This factorization can save us several integrations when we want to calculate the color factor. In the next section we are going to look at the differences between the color case in [Thm. 4.1](#) and the CSS in [Thm. 4.2](#) and the consequences of these.

4.3.3 Averaging over only a part of the external indices

We can make calculations for processes for which we know exactly the initial states and thus have no need of averaging over these. The goal of this section is to look at

[Thm. 4.1](#) and [Thm. 4.2](#) again and ask when they stay valid even if we are not summing over all external color indices. In the end we want to quickly discuss the implications from the results we obtain.

First we look at the color case and we see from (4.40) that already only a sum over $\{b_i\}$ or $\{c_i\}$ will result in a δ_d^e . Then it is not important if the other term is proportional to δ_d^e or not as only the diagonal terms can contribute anyways as we already noted in [Rmk. 4.2](#). Thus if e.g. only final indices are in $\{b_i\}$ they will be all summed over and [Thm. 4.1](#) still holds true. This is always possible as long as our cut through the internal line d separates our external indices in such a way that in one part are only indices from final particles as we almost always are averaging over these.

Now we look at the [CSS](#) and especially the step from (4.47) to (4.49): If we now only integrate over one group $\{y_i\}$ or $\{z_i\}$ we get still the scalar product $\langle w|x \rangle$ once. But as this is non-zero even if $x \neq w$ we get more contributions as in the case of our proof above. Thus now [Thm. 4.2](#) is not valid anymore.

To summarize, we can state that the calculation of the color terms in the color basis gives us more possibilities to factorize our terms and saving up single summations. The [CSS](#) is more complex in this regard due to the fact of the linear dependence of the [CS](#). In the case if we average over all external indices we can apply the same factorization in both systems. This is at least the case if all initial states are colorless because then all external color indices are from final particles over which we are averaging anyways.

5 Numeric calculations

5.1 Numeric tools

As already seen, we need to calculate integrals in higher dimensional spaces. For this purpose, we will use the numeric integration tool **VAMP** [Ohl99b]. As it was not clear from the beginning which integrations we are going to face in this thesis, we have chosen **VAMP** as it is one of the most powerful tools for numeric integration and it was at hand easily. In hindsight maybe **VEGAS** [Lep78, Lep80] or even the **METROPOLIS** algorithm [Met+53] would have sufficed but nevertheless **VAMP** gives a great insight in the subtleties of numeric integration.

5.1.1 VAMP basics

In this section we want to give a quick overview of **VAMP** and its advantages and disadvantages compared to other integration tools. The ideas in this section are from [Wei00] which also gives a quick overview of other numerical integration concepts. Furthermore [Ohl99a] also explains the basic feature of **MC** integration as well as the ideas leading to **VAMP**. First we start with a general discussion over **MC** integration.

Monte Carlo integration **MC** techniques¹ use random numbers to estimate the value of an integral

$$I(f) = \int_{\Omega} d\mu_x f(x) \tag{5.1}$$

of a function f over the domain Ω of a possibly multidimensional variable x with integration measure μ . This measure is in general chosen in such a way that $\int_{\Omega} d\mu_x = 1$.

¹For a first introduction into the history of Monte Carlo methods, take a look at [Met87].

The expectation value $\langle f \rangle$ converges to $I(f)$ by the law of large numbers:

$$\langle f \rangle = \frac{1}{N} \sum_{n=1}^N f(x_n), \quad \lim_{N \rightarrow \infty} \langle f \rangle = I(f). \quad (5.2)$$

Consequently the error for this estimation is the square root of the variance

$$\text{Var} \langle f \rangle = \frac{\langle f^2 \rangle - \langle f \rangle^2}{N} \quad (5.3)$$

and thus the error scales as \sqrt{N} independently of the dimension of our integration manifold. This is an improvement to classical methods like Gaussian quadrature where the error scales with the dimension of our integration. Now our goal is to minimize this error via various variance reduction methods where we want to highlight importance and stratified sampling.

Stratified sampling We can use the additivity of the integral to divide our integration manifold into smaller regions. Then if the number of **MC** points in each region is proportional to the variance in this region we minimize the total variance. This can be seen on the example of a one dimensional integral which we split up into two regions. Then the complete variance is the sum of the variances of the two regions which scale with their respective number of integration points. An explicit calculation shows that the total variance is minimized as stated above when the number of points is proportional to the variance in each region [Wei00].

Thus estimating these variances is the main bottleneck of this technique. The main advantage of this method is a good convergence and eventually higher precision integration. The higher precision is due to the fact that we are directly addressing to minimize the variance and thus the error.

Importance sampling Here we make use of a change of the integration variable via a function $p(x)$. Then we can rewrite our integral as

$$I(f) = \int_{\Omega} d\mu_{p(x)} \frac{f(x)}{p(x)} \quad (5.4)$$

and the measure $d\mu_{p(x)}$ contains the Jacobian determinant. Then we estimate the error via $\text{Var} \langle \frac{f}{p} \rangle$ which will be minimized if $\frac{f}{p}$ is constant. In general we put the

constraints

$$\int d\mu_p(x) p(x) = 1 \quad \text{and} \quad p(x) \geq 0 \quad (5.5)$$

onto p and can interpret it as a probability density function. But to know p exactly we need to know $I(f)$ which we are aiming to calculate. Thus we are generating events distributed according to p such that we mimic f best and thus minimizing our error for the estimation of $I(f)$. One problem occurs if p is very small and thus $\frac{f}{p}$ can be very large and thus our error.

Event generation The events generated with importance sampling are unweighted in the perfect case of $p \equiv f$: Then each random point contributes the same amount to the overall integral. In contradistinction to the case when we are integrating a function as in (5.2) where points with large $f(x)$ contribute more to $I(f)$ and hence each point is weighted with $f(x)$. The advantage of unweighted events is that we only obtain events in relevant regions. These events can then be used to test a real detector in the kinematically relevant region as they are not distributed completely randomly.

This event generation is done via a rejection algorithm, i.e. first we estimate the maximum of our function to be integrated and then we produce random events which will be rejected if they are larger than the maximum. Thus a wrong estimation of the maximum firstly leads to a wrong result as we reject events that would actually suit for our function. And secondly it takes longer to produce the events as we reject more. This is the limiting factor for the performance and depends on our estimation for f . In consequence our goal is to optimize this which means we are not directly minimizing the variance and thus the estimation for $I(f)$ from (5.4) will not be as good as with weighted events.

VEGAS To implement the mentioned methods we need to divide our integration manifold in smaller regions and distribute the MC points according to the concepts mentioned above. But this division of a manifold in more than one dimension is causing problems as we also reshape the regions which lead to numerical instabilities. The ansatz of VEGAS thus is to assume that our function $f(x)$ can be factorized into one dimensional functions. VEGAS is trying to find an adequate coordinate system for this factorization. But the integrals we are facing in high energy physics are not factorizable only in one coordinate system. The motivation for VAMP is to handle these kind of problems.

VAMP The idea behind **VAMP** is to find a mapping from the multidimensional hypercube on to our integration manifold such that we can factorize our singularities. This problem can then be handled by **VEGAS**. For a concrete description and realization of this technique we refer to [Ohl99a]. In the case of such problems which are not factorizable in one coordinate system, **VAMP** shows a better error in comparison to **VEGAS** besides the losses due to the effort of finding such a mapping.

5.1.2 Missing features of VAMP

Looking at the integrations we are facing in the case of the **CSS** we can look at an example of a quark and an antiquark into two gluons as also considered above in [Sec. 4.2](#). Even with all the simplifications discussed above, we are still facing a 20-dimensional integration for the one color factor with only a quark in the intermediate state and only integrating over all external colors. In the last section we saw we need to divide our integration manifold into smaller regions to optimize the result. Just bisecting each dimension will result in 2^{20} regions. Then to get some statistics each region must be filled with several **MC** points which easily surpasses the capacity of a normal integer type in **FORTRAN**.

Thus the idea was to rewrite the according **VAMP** variables and routines to handle long integer type number of points. When we tried to attempt this we had one major problem: It is not clear which variables need to be changed to long integer type. E.g. the number of points in each dimension can still be a normal integer but this leads to integer overflow if we try to assign the product of them to another variable which is also normal integer type. In **FORTRAN** there is no runtime check if a calculation causes an integer overflow; **FORTRAN** only checks at compilation the assignment between variables based on their given type. Hence we could not guarantee the correctness of the rewritten **VAMP** even in lowest order. Another way to circumvent this problem is to use the **FORTRAN** compiler option `-finteger-4-integer-8` which converts all normal integers to long integers which will do the job in our case but is not a very elegant solution.

5.2 Numeric results

In this section we are looking at the numeric results of the previously discussed color terms in [Sec. 4.3](#). The main idea is to start at a point equivalent to (4.37) and (4.38) in

the **CSS**. Instead of executing the sum in the color basis we calculate the integral over the **CS**. For this purpose we have written a short **FORTRAN** program using **VAMP** which will be introduced now. In all calculations, if not stated otherwise, our setup will be six iterations and 1000 **MC** points for the grid adaptation and then four iterations over various number of integrations points for the actual integration. This actual means we are solely using the **VEGAS** parts of **VAMP** which is enough due to the non-singular functions we are facing currently.

When talking about the program and its features, we stay always in the scope of mathematics and pseudocode and will not mention any particular code if not absolutely needed. This thesis, and in particular this section, is much more a description of how to implement the ideas presented into a functional program. And we are not aiming at completely describing our program here, rather together with the comments in the code the program should be comprehensible. Furthermore the program is written to show a validation of the statements made in this thesis and to play with the different settings. In addition it is meant to analyze advantages and disadvantages of the **CSS** over the color basis. Hence it is not written in a way to easily calculate total cross sections and highly precise predictions for **QCD** processes. Consequently an integration into another tool would require some recoding. Furthermore it is solely written to test the scope of the **CSS** for color $SU(n)$, a first basic analysis and understanding. Thus to move on this path, there is a big room for improvement and deeper research.

5.2.1 Features of our program

The main task of the program is to calculate complete contractions of two color tensors N and N' . The calculation of the kinetic terms C in (4.36) are not our focus of interest as there are refined tools available to do such tasks. This complete contraction of two tensors N and N' are the color factors we already encounter on our example process in Sec. 4.2. The first possibility of calculating this contraction is via calculation of the tensors N in the color basis, i.e. the contraction over all internal indices is performed in this basis. Then we transform this quantity to the **CSS** and execute only the contraction over the external indices in this system. The main purpose of this approach is more to verify that this method of **CS** indeed works and won't give any particular insight into the color-flow. The next step is to calculate the tensor N from the Feynman rules in the **CSS** and then contracting the two tensors. Hence we are performing the contraction of the internal and the external indices with the **CS**. When we have twice

the same tensor and are thus calculating the absolute square value of it, we can use the factorization as stated in [Thm. 4.2](#) to save some integrations. Furthermore we can save even more integration if we use the simpler [RoU](#) of [Thm. 3.1](#), [Thm. 3.2](#) or [Thm. 3.3](#). We want to sum up these three possibilities again:

- Calculation of the tensor N via the Feynman rules in the [CSS](#)
- Factorizing the color factor
- Using the simpler [RoU](#)

For brevity we will just state the boolean value of these three options. Thus false for the first one with the Feynman rules means, we calculate the contraction over the internal indices in the color basis and only the contraction over the external indices will be performed in the [CSS](#). Further the factorization can only be done if we use the Feynman rules in the [CSS](#) and thus we have six different possibilities to choose from. Finally all calculations can be done in $SU(2)$ and $SU(3)$.

The [VAMP](#) interface is written that it is not possible to pass allocatable objects to it, e.g. when specifying the borders of our integration domain. Thus we need to know the length of certain arrays already at compilation as the dimension of our integration depends on the considered graphs as well on our parameters, i.e. the $SU(n)$, using the simpler [RoU](#), factorization and using Feynman rules. Hence we opted for using the C-preprocessor to set these parameters and allowing an easy switch between them.

As an example case, we are always looking at the color terms of the example in [Sec. 4.2](#) and compare the precision, calculation time and different graphs. Our program is written to handle any Feynman graph but the given examples should be enough for general statements at the first level.

5.2.2 Results

Proof of consistency

In this section we are going to see that the methods explained above indeed work. As a consequence all results presented here are confirming what we already expect. Thus we will not point this out every time.

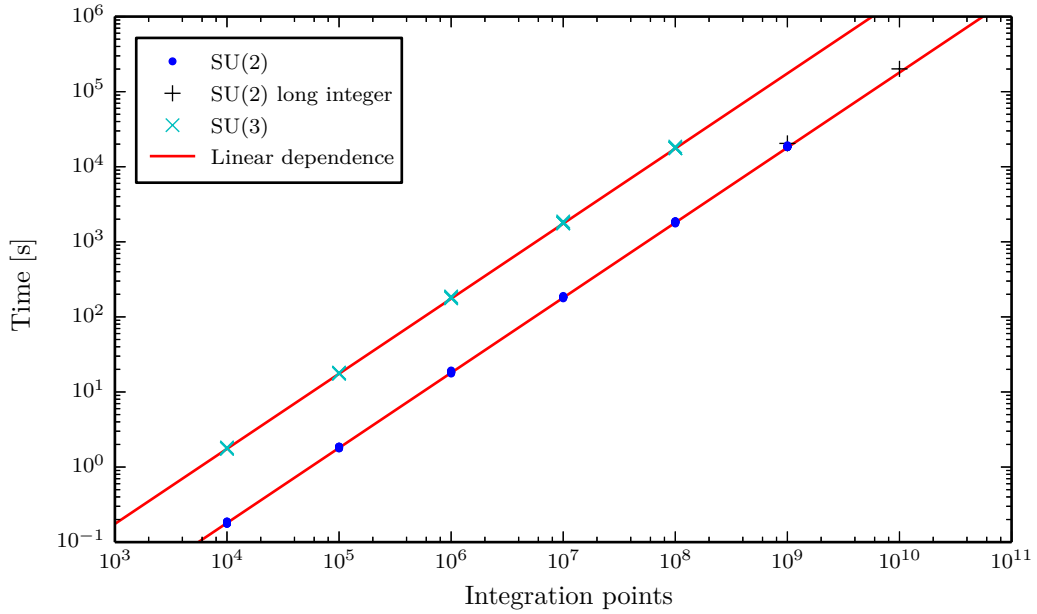


FIG. 5.1: *The times for runs with different number of MC points.*

First in Fig. 5.1 we see the dependence of the integration time on the number of integration points. For $n = 2$ the times are shown with blue dots and we did ten runs for each number of MC points. For $n = 3$, we only did five runs and the results are plotted with cyan 'x's and in both cases all runs are plotted individually. When we are doubling the number of points the program also takes double the time, thus the runtime is linear dependent on the integration points [Ohl99b]. This is as expected for a MC method and this dependence is shown in Fig. 5.1 with red, solid lines for each case respectively. There is also no apparent variation between the different runs. In the case of SU(2), we also did two runs with the long integer implementation which are shown with black crosses. We see that this only takes a marginal time longer than with normal integers. This might just be due to the larger data type but it does not alter our main statement.

Next we are looking at the error between the MC integration and the exact value and in the following we always look at the color factor of graph 2 in Fig. 4.1b as example. First we are looking at the improvement of our result when we are increasing the number of MC points. In Fig. 5.2 we see the result: The same color factor with blue dots for $n = 2$ in Fig. 5.2a and for $n = 3$ in Fig. 5.2b. This time for each number of integration points we did 100 runs except for 10^9 and more MC points in case of

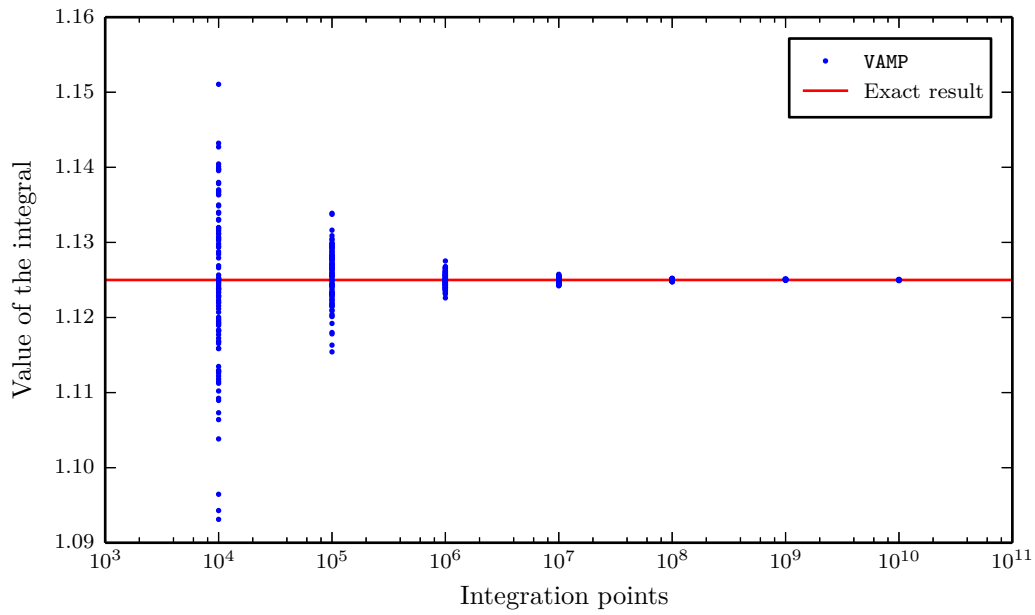
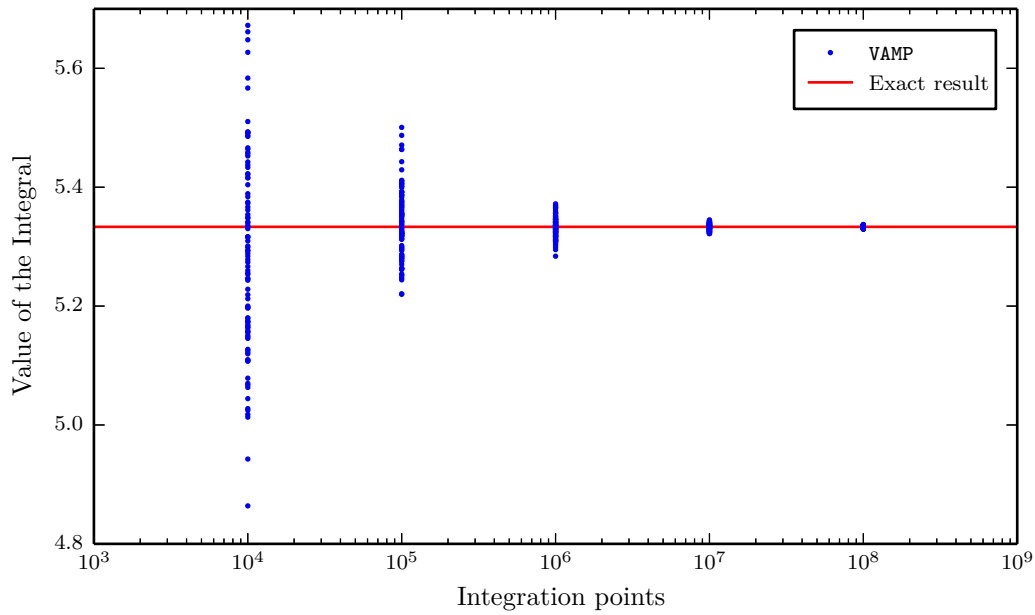
(5.2a) *The SU(2) case.*(5.2b) *The SU(3) case.*

FIG. 5.2: Value of the integral for the color factor of graph 2 in Fig. 4.1b from 100 runs for different number of MC points.

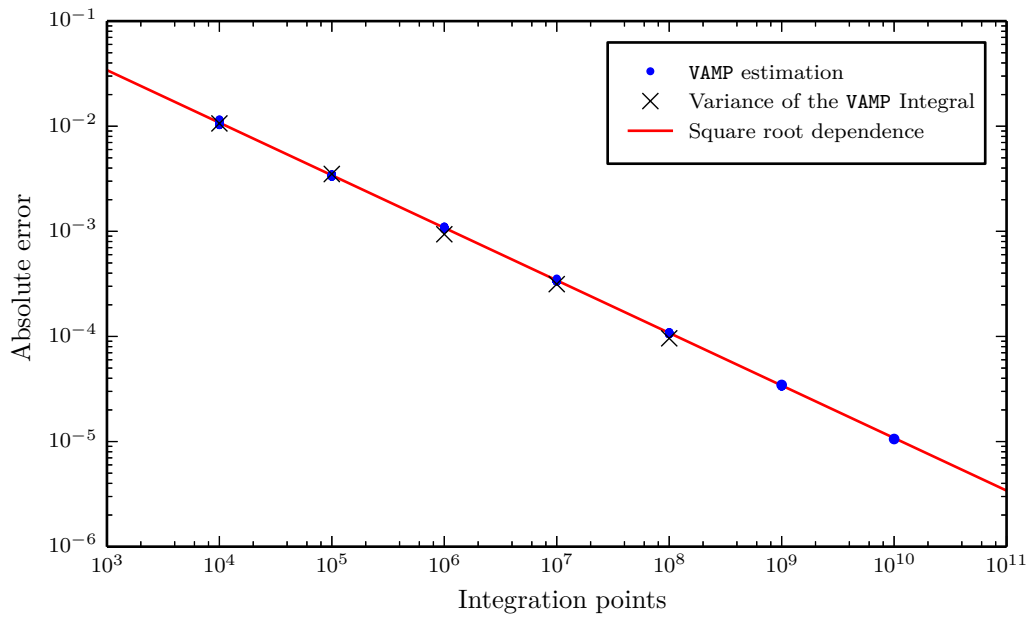
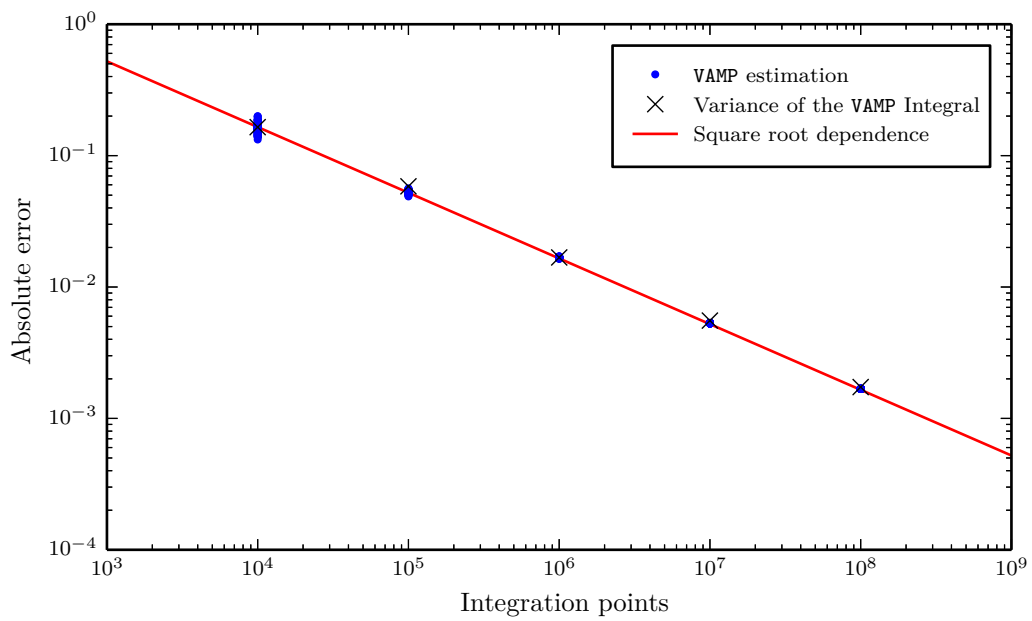
(5.3a) *The $SU(2)$ case.*(5.3b) *The $SU(3)$ case.*

FIG. 5.3: Comparison of the VAMP estimation for the error with the error from the variance over 100 runs. This is shown for setups with different number of MC points.

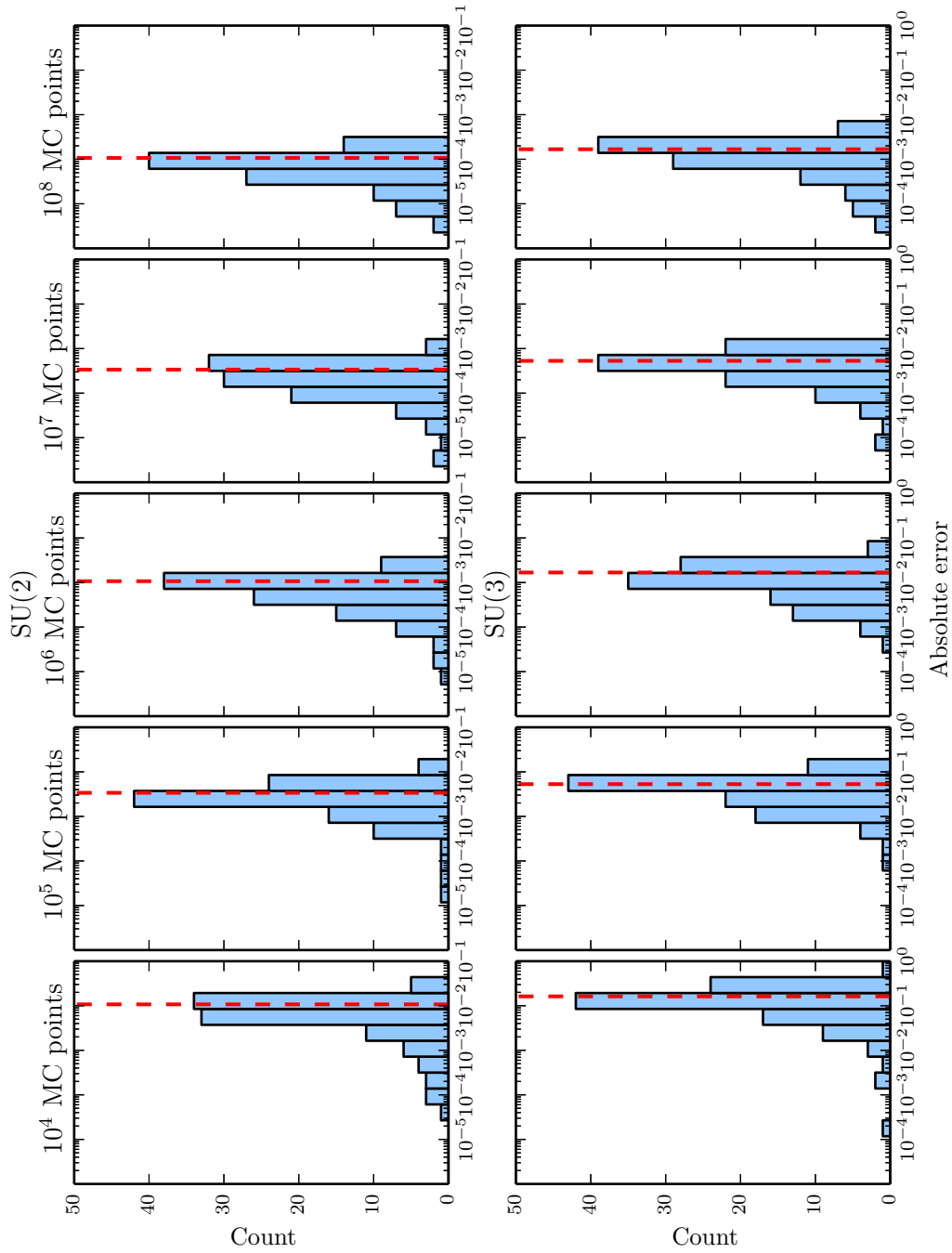


FIG. 5.4: Distribution over 100 runs of the deviation from the exact value of the integral from Fig. 5.2 compared with the average of the VAMP error estimation from Fig. 5.3. The top row is for $SU(2)$, the bottom row for $SU(3)$ and each column is the data with the number of MC points shown on top.

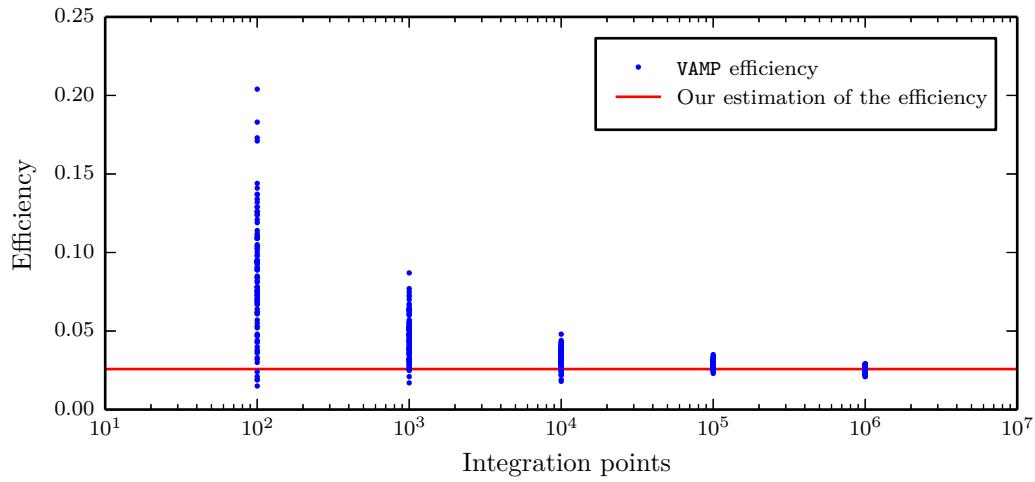
SU(2). For these high number of integration points the time for each run is just too long to do several runs and as we see on the plots this cases already give really good results. The red, solid line symbolizes the exact value calculated via the color basis. When increasing the number of integration points, the distribution gets more narrow around the exact value.

A measure for this is the sample variance of each integration as defined in (5.3) and which is estimated by VAMP itself based on the values of the individual MC points. The square root of this variance, viz the error of our integration, is shown in Fig. 5.3 with the same data set as the previous plot with blue dots for $n = 2$ in Fig. 5.3a and for $n = 3$ in Fig. 5.3b. We see that the estimation of the error for the different integrations is always almost the same over the 100 runs. Only in the case of 10^4 MC points for SU(3) we have a spread. This might just be due to the high number of dimensions, thus the large integration domain and the small number of integration points in relation to it. The VAMP error as square root of the sample variance should scale with \sqrt{N} [Ohl99a] just from its definition in (5.3). This behavior is shown by the red, solid line in each figure. Further the variance of the integral of Fig. 5.2 over the 100 runs for less than or equal to 10^8 MC points should coincide with the estimation from VAMP just by the law of large numbers. This variance is shown with black 'x's in both cases of SU(n) and there is a very good agreement. For the SU(2) cases with 10^9 and more integration points we only had a couple or just a single run and thus not enough statistics to give the variance over these runs any significant meaning. Hence there are no 'x's for these cases.

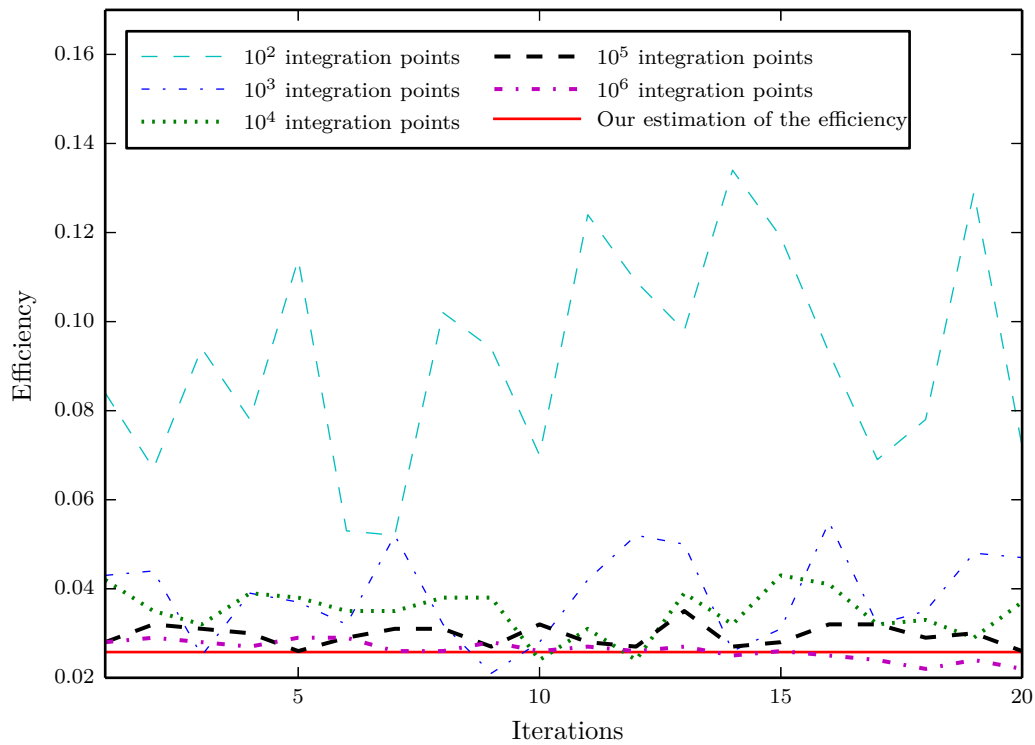
The last plot analyzing our error of the integration is shown in Fig. 5.4: Here we take the integral of the 100 runs and calculate its deviation from the exact value and plotted this distribution. This is essentially the data that lead to the black 'x's in Fig. 5.3. We compare this distribution to the average of the VAMP estimation of the error from this figure. There we saw that these errors are always almost the same and thus we can just take the average. This average is plotted with red dashed lines in each individual case. We can state that the VAMP estimation reflects very well the mode of each distribution and is a very good approximation for the real error.

Next we want to look at the grid adaptation and thus the event generation. We will analyze these through the efficiency of VAMP which is a measure for rejection criteria mentioned on page 72. The efficiency is calculated via [Ohl15]

$$\text{efficiency} = \frac{\int_{\Omega} dx f(x)}{\text{Vol}(\Omega) \max_{\Omega} f(x)} \quad (5.6)$$



(5.5a) The VAMP estimation of the efficiency for different number of MC points. The points are always from five runs as well as from 20 iterations each.



(5.5b) The VAMP estimation of the efficiency of one run for each number of MC points.

FIG. 5.5: The analysis of the efficiency (5.6).

where Ω is the integration domain. We know the exact value of the integral already from the color basis. Further we can estimate the maximum value of f on our domain easily from just calculating $f(x)$ for a high number of random points x and take the maximum. This should be very close to the actual maximum especially if f has no singularities and is thus not very localized. Further this is much faster with a higher accuracy than VAMP, as VAMP only takes the maximum of the set of MC points from the integral calculation. We can then compare our almost exact result to the estimation of the efficiency from VAMP.

We took five different runs and in each we let adapt the grid over 20 iterations. Then we repeated this for different number of MC points. We want to emphasize here that we changed the setup mentioned in the first paragraph of Sec. 5.2 here: We manipulated the number of iterations and MC points for the grid adaptation and did not look at the integration afterwards. The result of this analysis is shown as blue dots in Fig. 5.5a where we omitted the distinction between the five runs with the same number of integration points. The red, solid line is our more accurate estimation of the efficiency. The main result is that the distribution of the VAMP efficiency gets closer to this exact value with more points. Taking in account the results of the previous paragraphs we see that the large deviations in the efficiency cannot be from wrong estimation of the integral. As already mentioned VAMP fails to estimate the maximum of f by a large margin which is naturally biased. This results in mostly too large efficiencies. We assume with around 10^6 MC points the maximum should be approximated very well as this is the same magnitude of points we needed to use when finding the maximum. In addition the distribution in this last case around the exact value is very symmetric but an error in the maximum can only lead to a larger efficiency and thus an uneven distribution around the red line.

Fig. 5.5b shows the efficiency over the 20 iterations. We have chosen just one sample of the five runs from each number of integration points. The different runs are plotted with different colors and linestyles and the red, solid line shows the exact value from our estimation. We do not see any improvements over the number of iterations which indicates that our function f is very smooth and constant, particularly it does not have any singularities. This is as expected as we are dealing essentially with products and sums of sine and cosine functions which have a limited range. Thus there is no particular grid configuration which improves the integration as there are no regions which contribute far more to the integral than others.

This finishes this section: We saw that the VAMP integration produces the results we expect and also confirmed that VAMP has a good estimation of its error. In the end we

also saw that our function in the integral behaves just as we would expect from the structure of the CS from (3.16) and (3.68). Now after confirming that our approach as well as VAMP are yielding the results we expect, we can move on to analyze the CSS in more depth and look for any insight into the color-flow of QCD.

Observations

Now we are going back to the possibilities of different calculation we have which we have already mentioned in Sec. 5.2.1: We can use the Feynman rules in the CSS, the factorization theorems and the simpler RoU. We want to examine how these different possibilities influence our result. Our first observation is that all give us the correct value for a color factor within their respective error as we expect. A comparison between the different times of the runs for these setups is not meaningful as they differ quite strong in the amount of calculation steps performed at each evaluation of the integrand. These numbers of steps are the dominating part of the complete integration time.

However it is more interesting to look at the error estimation of VAMP which is a good measure for the actual error as we saw. If we choose one of the different possibilities mentioned above, our function to be integrated can be more flat or more oscillating. Functions which are almost constant will automatically give a smaller variance. Further the different possibilities also change our dimension of the integration domain. Lower dimensionality means we need less MC points for the same accuracy. That is the idea of Fig. 5.6: For the same number of integration points we look at the error estimation of VAMP dependent on the dimension of our integration. In the plot we see this for SU(2) with blue dots and with cyan crosses for SU(3). As mentioned above we have six different possibilities to choose the boolean values of the different setups as we cannot factorize anything if we do not use the Feynman rules in the CSS. The different setups lead to different dimensions shown on the bottom horizontal axes and the top horizontal axes is labeled with the respective boolean values. These are shown according to the data points with blue font for SU(2) and cyan, italic font for SU(3) and 'T' means true and 'F' false for the respective value. We see that higher dimensional integrals give in general a larger error as expected.

The structure of the data in this semilogarithmic plot lets assume an exponential dependency of the error on the dimension. Thus we make a fit of the form

$$\Delta = C e^{\alpha d} \tag{5.7}$$

where Δ is the error and d the dimension of our integration. The two parameters C and α are obtained from the fit. The fit is done for SU(2) and SU(3) individually and respectively plotted with a red line. The fit gives us the following values:

	SU(2)	SU(3)
C	$(1.14 \pm 0.38) \times 10^{-5}$	$(5.1 \pm 1.4) \times 10^{-5}$
α	0.150 ± 0.036	0.173 ± 0.012

and, as we can already see in Fig. 5.6, the SU(3) case gives the better fit. The value of α is the more interesting one as it describes how fast the error is growing with the dimension. As we already see on the plot itself, the values of α for $n = 2$ and $n = 3$ are roughly the same. This is also the conclusion from our fit where both values of α coincide very well. Moreover with α we can estimate our error if we change the dimension of our integration for other color factors and processes.

Next we want to discuss the event generation. We are looking at unweighted events which are distributed with a probability function $p(x)$ which should mimic our integrand $f(x)$ as discussed on page 72. We saw that we are dealing with high dimensional integrations and thus we can only plot a projection of the events onto a one or two dimensional subspace. For example looking at the one dimensional case, we want to know how many events we created in a given interval Δx_i which means we sum over all the other dimension. The index i just labels the different dimensions of our integration manifold. Analytically this sum over the other dimensions corresponds to an integration over all these. The result for each integration variable is shown in Fig. 5.7, for the SU(2) CS in Fig. 5.7a and for SU(3) in Fig. 5.7b. For each case, one can calculate the covering function by just executing the integration in the other dimensions. These results are shown with the red, solid curves. Due to different integration domains we opted to norm the area under the curves to be equal the volume of the respective domain.

For the both cases $n = 2$ and $n = 3$ we only show the plot for one particle each as they are the same for internal and external particles as well as CS from the FuR and AdR. Further it is also independent from the particular color factor we are calculating and also the absolute square matrix element of any given process will produce the same distributions. We can understand this fact from a theoretical point of view: Looking at (4.37) and (4.38) in the CSS, we see, we need to calculate an object like $N^{\{z_i\}} N'_{\{z_i\}}$ where N' is not necessary unequal to N . Then when integrating out all parameters except one we can first integrate out all other particles except the one which carries

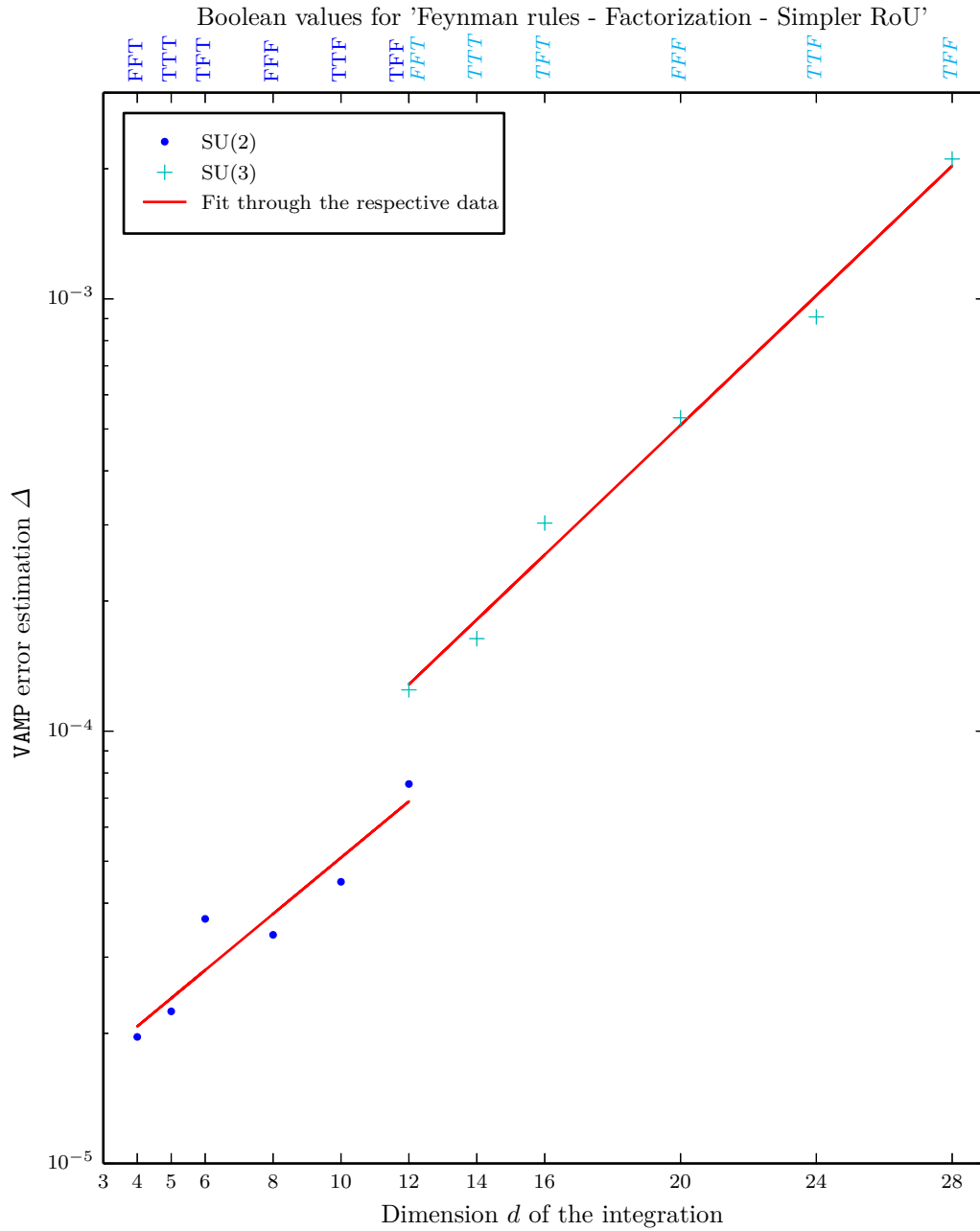
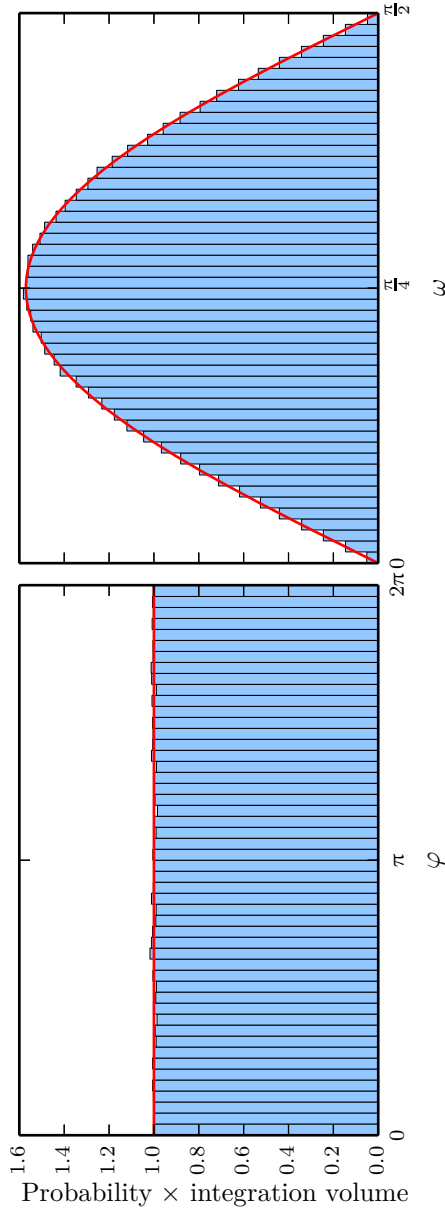
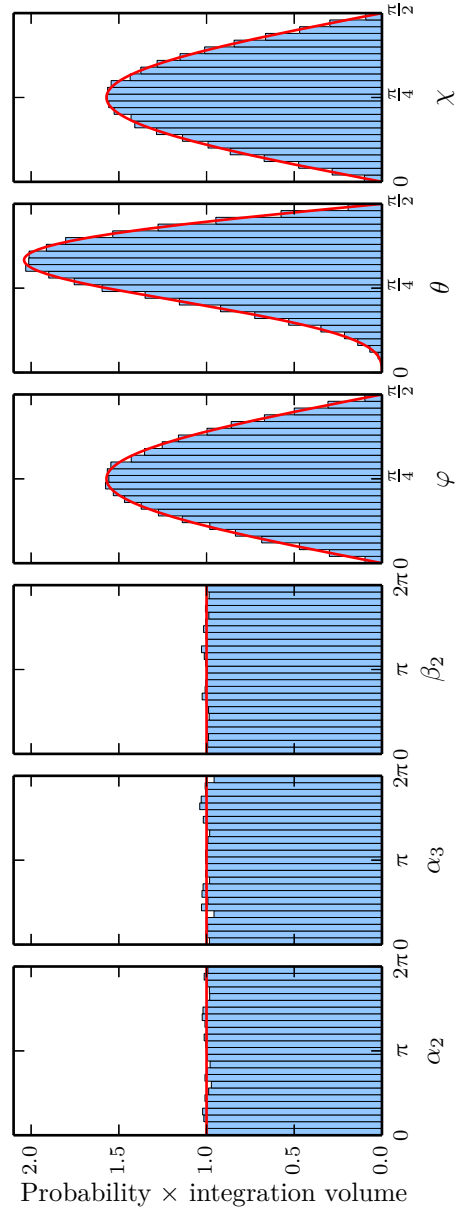


FIG. 5.6: The VAMP estimation for the error compared for different setups always for one integral and fixed number of MC points. The boolean values on the top horizontal axes label refer to: Usage of the Feynman rules in the CSS, factorization according to Thm. 4.2 and usage of the simpler RoU from Thm. 3.1, Thm. 3.2 and Thm. 3.3. Both horizontal axes are always only labeled where there is a respective data point.



(5.7a) The $SU(2)$ case.



(5.7b) The $SU(3)$ case.

FIG. 5.7: The event generation marginalized over all other parameters except the one shown. The red, solid line is the analytic result for each plot.

our parameter we want to look at. Let us rearrange the tensors in N and in N' that we explicitly write the integration over the one particle we do not integrate at first:

$$N^{\{z_i\}} N'_{\{z_i\}} = O^{\{y_i\}x} O'_{x\{y_i\}}, \quad \{y_i\} \cup \{x\} = \{z_i\}. \quad (5.8)$$

Then our statements from above, i.e. [Sec. 4.3.2](#), tells us that the expression in [\(5.8\)](#) integrated over all $\{y_i\}$ must be proportional to $\langle x|x \rangle$ and we can write:

$$O^{\{y_i\}x} O'_{x\{y_i\}} = c_{OO'} \int d\mu_x \langle x|x \rangle = c_{OO'} \int d\mu_x 1. \quad (5.9)$$

The proportionality constant $c_{OO'}$ is defined as in [\(4.48\)](#) and our **CS** are normalized by definition. Thus we are only left with an integral over the measure of our **CSS** independent of our color factor. When we consider the squared absolute value of a matrix element when calculating the cross section of a process, we have the sum over several color factors with different coefficient as in [\(4.36\)](#). When we integrate out all particles except one, then each color factor is just an integration over the measure. Thus also $|M|^2$ as a sum of these terms is only this integral and consequently the distribution of the events marginalized over all except one parameter is always the same regardless of the representation of the particle and the specific process: As the histograms represent an probability distribution an overall prefactor has no influence on it. From this we also see that any correlation of two parameters of the same particle is always the same. This we will see later when we look at the projection of our events onto two dimensional subspaces. This also holds true when we use the simpler **RoU** as well as when we factorize our color factors as both these concepts do not change our integrations measure of the parameters still involved in the integral.

Now that we have understood why all histograms for one parameter always look like in [Fig. 5.7](#), we can further analyze this plot. As these distributions are over different domains, viz $[0, \frac{\pi}{2}]$ and $[0, 2\pi]$, we normed the total area of all histograms, i.e. the integral over the curve to the volume of the integration domain. For all the phases, i.e. φ for $SU(2)$ and α_2, α_3 as well as β_2 for $SU(3)$, the result is a constant histogram. This is just due to the fact that there is no dependence of these parameters in our measures, viz [Eq. 3.24](#) and [Eq. 3.67](#). Looking at these, we see that for ω of $SU(2)$ and φ, χ of $SU(3)$ we have a $\sin 2x$ dependency, $x \in \{\omega, \varphi, \chi\}$, when we use [\(3.21\)](#). The last parameter left is θ of $SU(3)$ where we have $\sin^3 \theta \cos \theta$ and all these functions are shown in the respective plot with red lines. Lastly we want to mention that the **CS** of the **FuR** of $SU(3)$ can be described with less parameters than of the **AdR**. Nevertheless

the case of SU(3) we can also compare it with WHIZARD [KOR11, MOR01]. We get the following results:

$\sigma[\text{fb}]$	CSS	Analytic	WHIZARD
SU(2)	$(5.1665 \pm 0.0043) \times 10^6$	5.166326×10^6	-
SU(3)	$(1.1241 \pm 0.0040) \times 10^7$	1.122843×10^7	$(1.1217 \pm 0.0012) \times 10^7$

which are in good agreement with each other. In addition the result with the CS is always the same if we use the Feynman rules, the simpler RoU or the factorization as we expect. In the case of WHIZARD we also tried to change the model file to color SU(2) but we still obtained the SU(3) result. The reason for this is that the color-flow is hard coded in WHIZARD and there is no check for the values set in the model file. However as we are always working in the framework of color SU(3), this is not a problem in general but could be addressed if more analysis for different SU(n) is needed. We only did all calculations in the SU(2), too, as it facilitated the understanding of the CS of SU(3) but there is currently no physical reason to look at any SU(n) for $n \neq 3$.

For the total cross section we already discussed the event generation for one dimensions and saw that we end up only with an integration over the measure and thus we get indeed the same plots as in Fig. 5.7. For the total cross section we also need to integrate over our scattering angle of the kinematic as we already did in the previous paragraph. We will use the differential cross section (4.33) and integrate over the dimensionless variable $-\frac{t}{s}$. The event generation of this is shown in Fig. 5.8 and we see the familiar distribution as well as the comparison to the analytic result with a red, solid line. The SU(2) Fig. 5.8a and SU(3) Fig. 5.8b only differ slightly in the flat region in the middle due to the different color factors. Therefore we also included an inset in each case to specially show this part. Otherwise the difference is too marginal to see in our plots and further an overall factor has, as always, no influence on our histograms. We want to remark that these histograms are obtained from weighted events. We saw that the quality of unweighted events is related to the estimation from VAMP of the maximum of the functions to be integrated. But in this case we have two singularities at the borders where the function has its maximum value. Thus an estimation of it via random points will normally miss it. Then we will miss some events at the singularities which will get distributed over the whole interval. In the middle where we only have a small number of events these added ones have a large influence and we have a significant deviation from the theoretic prediction. Thus we used weighted events in this case to obtain the

better plots as the ones with unweighted events are biased in the middle like we just discussed.

Now we look at the marginalization over all parameters except two. This is most interesting for the cross section as it shows the correlation of the particles from our process. Thus all the following results are taken from the cross section and not only from a single color factor as mostly above. Then we have two possibilities: Both parameters can be from one particle or they can be from different particles. Let us look at the first case when both parameters are only from one *CS*. We already saw in the one dimensional case above that we will always get the same distribution, independent of the particle and its representation. Thus we only get a product of two different plots of Fig. 5.7. Then we have only one possibility in the $SU(2)$ case and in the $SU(3)$ case we would have 15 but only five are different. These different cases are shown in Fig. 5.9 in comparison to the analytic prediction. The distributions of $SU(2)$ are shown in Fig. 5.9a and of $SU(3)$ in Fig. 5.9b and again we normed the plots in such a way that the integration over the complete domain is equal to the volume of this domain. We see that the event generation has the expected distribution and for a better three dimensional perception of the plots, one can just imagine the products of Fig. 5.7 as already stated. There is nothing special to note about these plots after we have already seen these one dimensional cases.

Next we look at the second case where the two parameters are from two different *CS*. This is the most interesting part as it gives us an insight into the quantum correlation between two particles. This can enable us to understand the mechanics of color-flow and obtain an insight into the *QCD* mechanics. But for this we need to understand the relation of the parameters of the *CS* to the physical quantities we can measure. However this is still a largely unexplored area where we cannot make any statements right now and for any conclusion of our results more analysis in this topic is needed. Nevertheless we can list the different distribution we encounter at least on our example process from Sec. 4.2. Thus we will not list all various distributions we found but only one example for each different main structure we encounter. The first idea might be to look if we can associate any substructure to a certain color factor of the three we considered above, aka (4.16), (4.19) and (4.23). But looking at (4.28) we see that they contribute with various coefficients given by the kinetic terms and a quick calculation shows that the dominant contribution is from the first color term. Thus if this color factor has any structure, this one will give the main structure of our two dimensional distributions. Further there might be distributions which deviate from others only slightly either due to additional terms with smaller coefficients or because these terms

have a similar shape. We cannot resolve these small differences and in addition at our current stage, these details do not give us any meaningful information as we cannot utilize them further. Hence we will only show one plot for each dominating structure to give a first overview but for a deeper analysis one needs to also consider the small deviations. Further the results are taken essentially at the basis of (4.30) where we have used the equivalence of Γ^1 and Γ^3 from (4.29) but we still implemented the explicit terms from (4.20) with Γ^2 . This might look a bit artificial at first but these were the first results at hand and a inclusion of Γ^3 gives essentially the same structures as the main contribution is from Γ^1 anyways as already discussed. For further work on this subject, especially including Γ_3 , one needs more discussion and research to make any conclusions: This is due to the fact that the terms $\frac{t}{s}$ and $\frac{u}{s}$ of (4.28) are not symmetric under an exchange of t and u . Thus the coefficients of Γ_3 are the only ones, different under such an exchange which leads to slightly different correlations between quark-gluon and antiquark-gluon, viz a difference of t - and u -channel. As we want to give here only a overview of the structures of correlations we encounter, we omit the third color term and work with the setup mentioned above where we express Γ^3 via Γ^1 .

For SU(2) the different distributions are shown in Fig. 5.10 which we will discuss now column by column where we indicate on top of each column to which pair of particles, i.e. quark (q), antiquark (\bar{q}) and gluon (g), the correlation corresponds. If there is no symmetry in the exchange of the two axes, the order of the particles is abscissa first and ordinate second and we generated a total of 10^6 events for these plots. The first column is just nothing else than a product of two ω distributions we already know from the measure in Fig. 5.7a. The second correlation is almost the one from Fig. 5.9a but just a bit curvy due to a $\sin \varphi \cos 2\omega$ contribution. We have chosen this correlation because there we can actually recognize the small deviation from the main structure and we see that they do not alter the overall correlation. The most interesting plots are from the correlation of the phase φ between two different particles. Thus between quark and antiquark shown in the third, between a fermion and a gluon in the fourth and two gluons in the last column. In all cases the structure lies on top of a constant distribution due to the product of two φ histograms of Fig. 5.7a. Thus in the first and second case of the φ - φ correlations we need to change the range of the color shading for better visibility of the pattern. This is indicated with blue color and diagonal solid lines. Here we see that the deviation from the constant is roughly of the order of 10% and this is why they can be best seen in the case of a correlation between two φ as they lie on top of a constant distribution. In the case where one ω angle is involved, we cannot resolve the additional contributions and a further analysis would need to

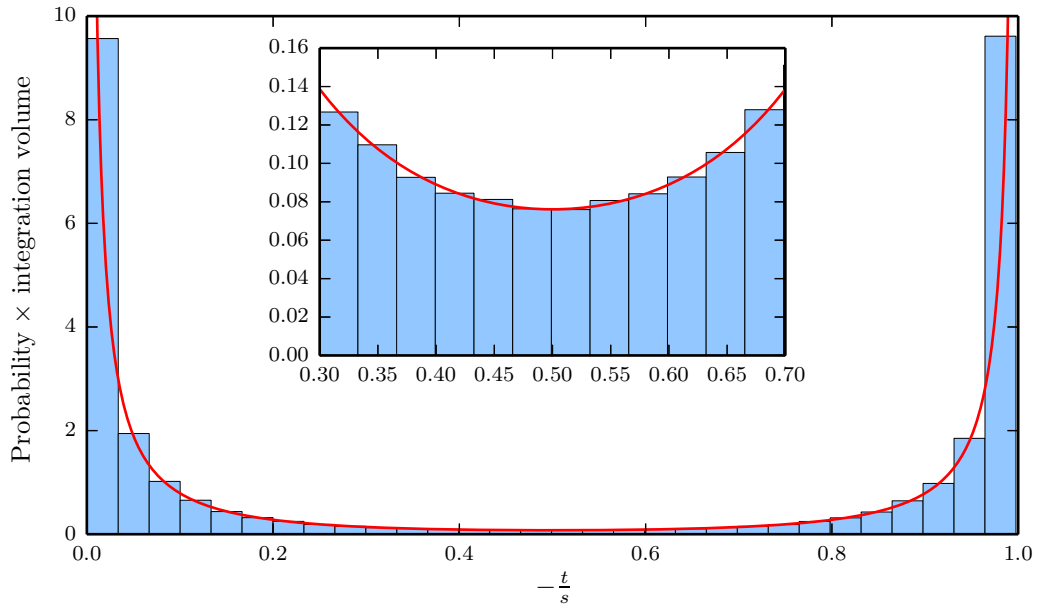
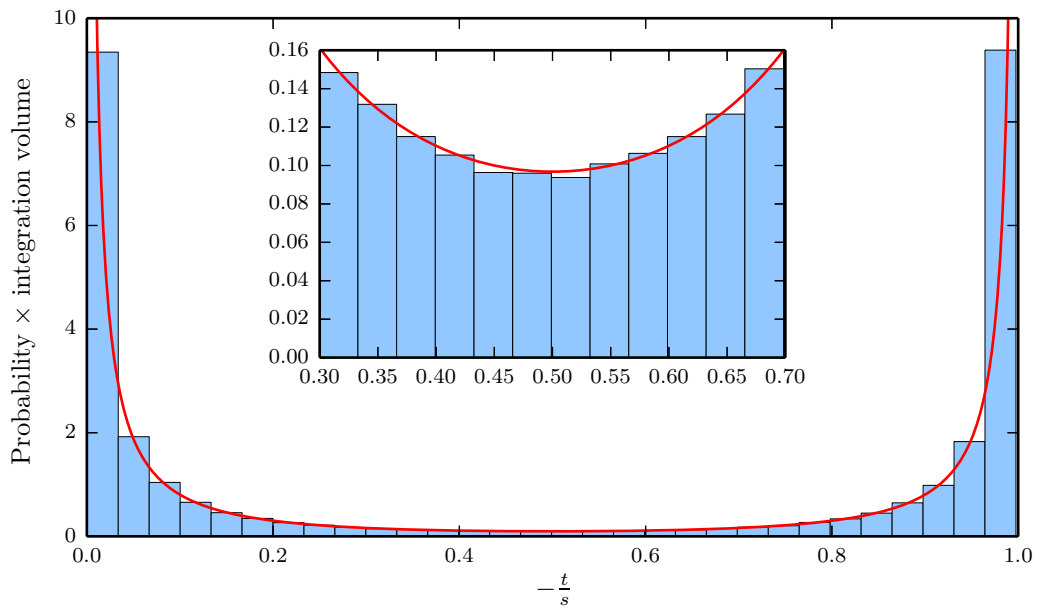
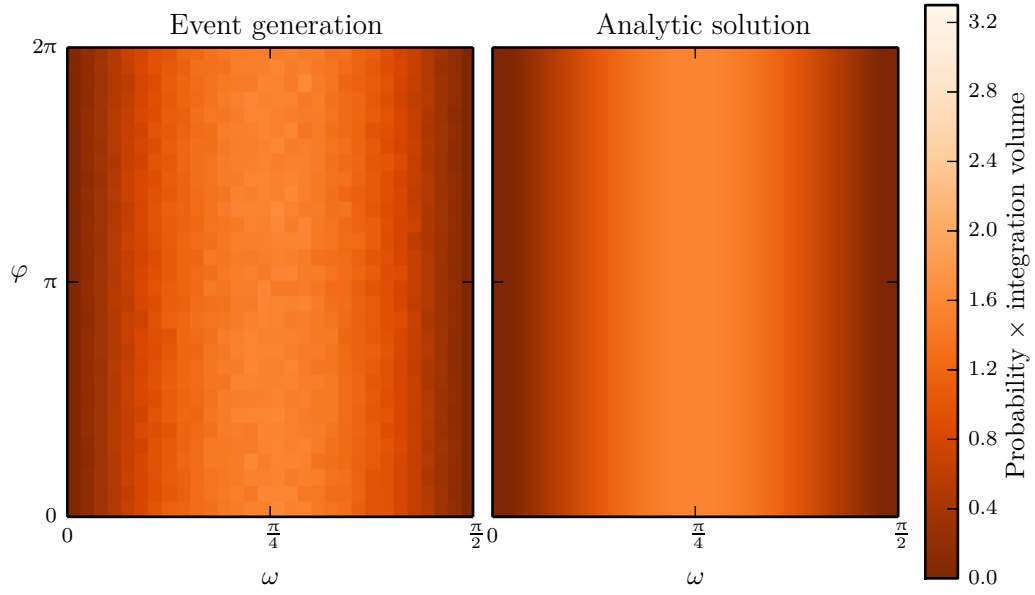
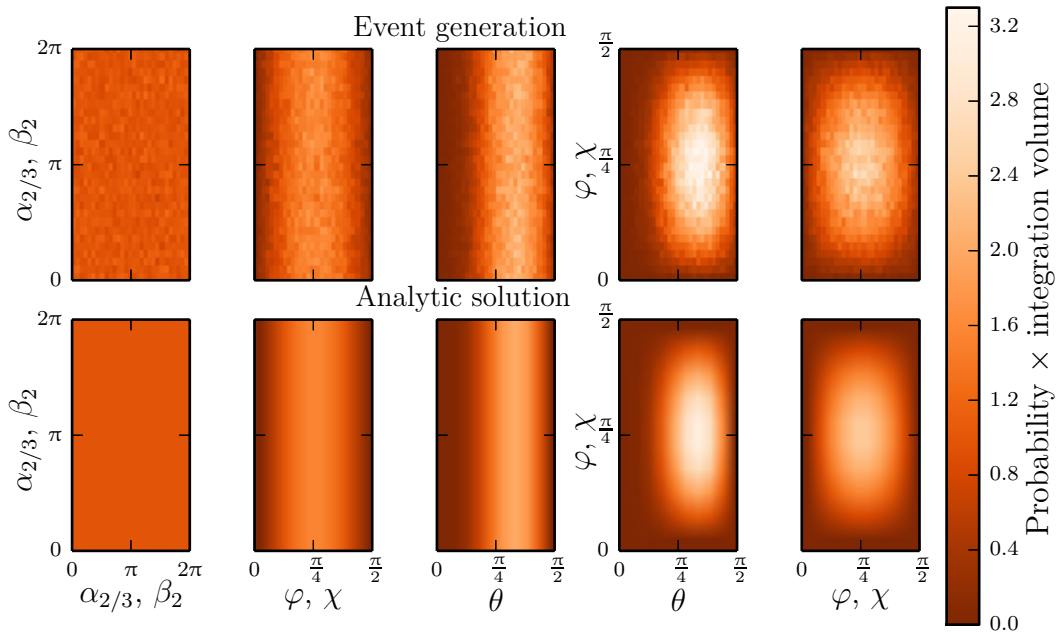
(5.8a) *The SU(2) case.*(5.8b) *The SU(3) case.*

FIG. 5.8: *The distribution of the events from the total cross section of our example process, marginalized over all parameters except the dimensionless quantity $-\frac{t}{s}$. The inset shows the same plot zoomed into the range $-\frac{t}{s} \in [0.3, 0.7]$.*



(5.9a) The $SU(2)$ case.



(5.9b) The $SU(3)$ case. Be aware that the ordinate changes after the third column.

FIG. 5.9: Correlation of the parameters of the CS of just one particles and marginalized over all other particles and remaining parameters. Shown are just all different combinations of the respective $SU(n)$ of Fig. 5.7 and the corresponding analytic solution.

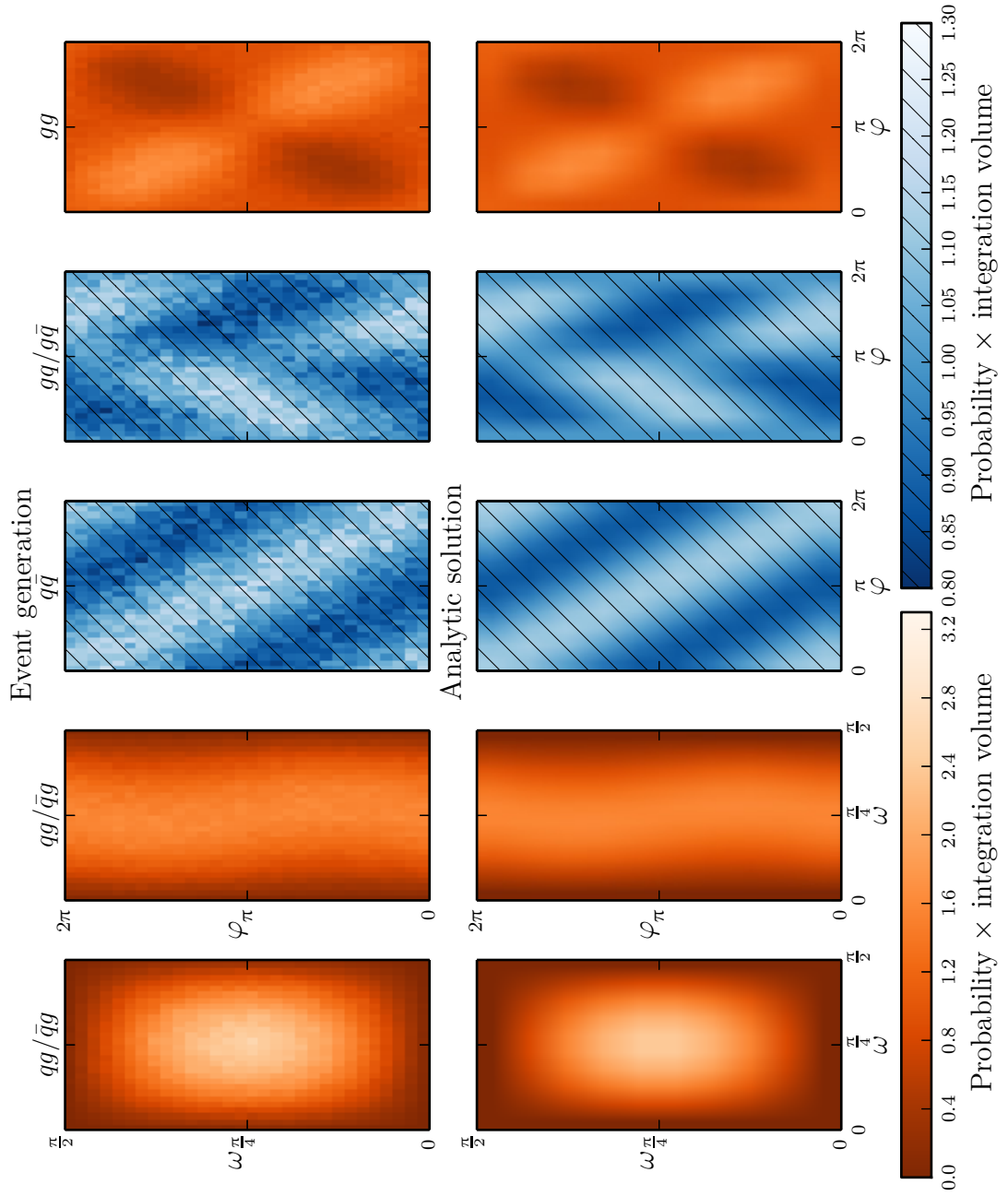


FIG. 5.10: *The different structures of correlations of two parameters of different particles for the case of $SU(2)$ except the one already shown in Fig. 5.9a. They are labeled on top whether it is a correlation between a quark (q), antiquark (\bar{q}) or gluon (g) in the order abscissa-ordinate where it is not symmetric under an exchange of the axes. Below we see the corresponding analytic solution and the third and fourth column has a different color mapping to recognize the structure.*

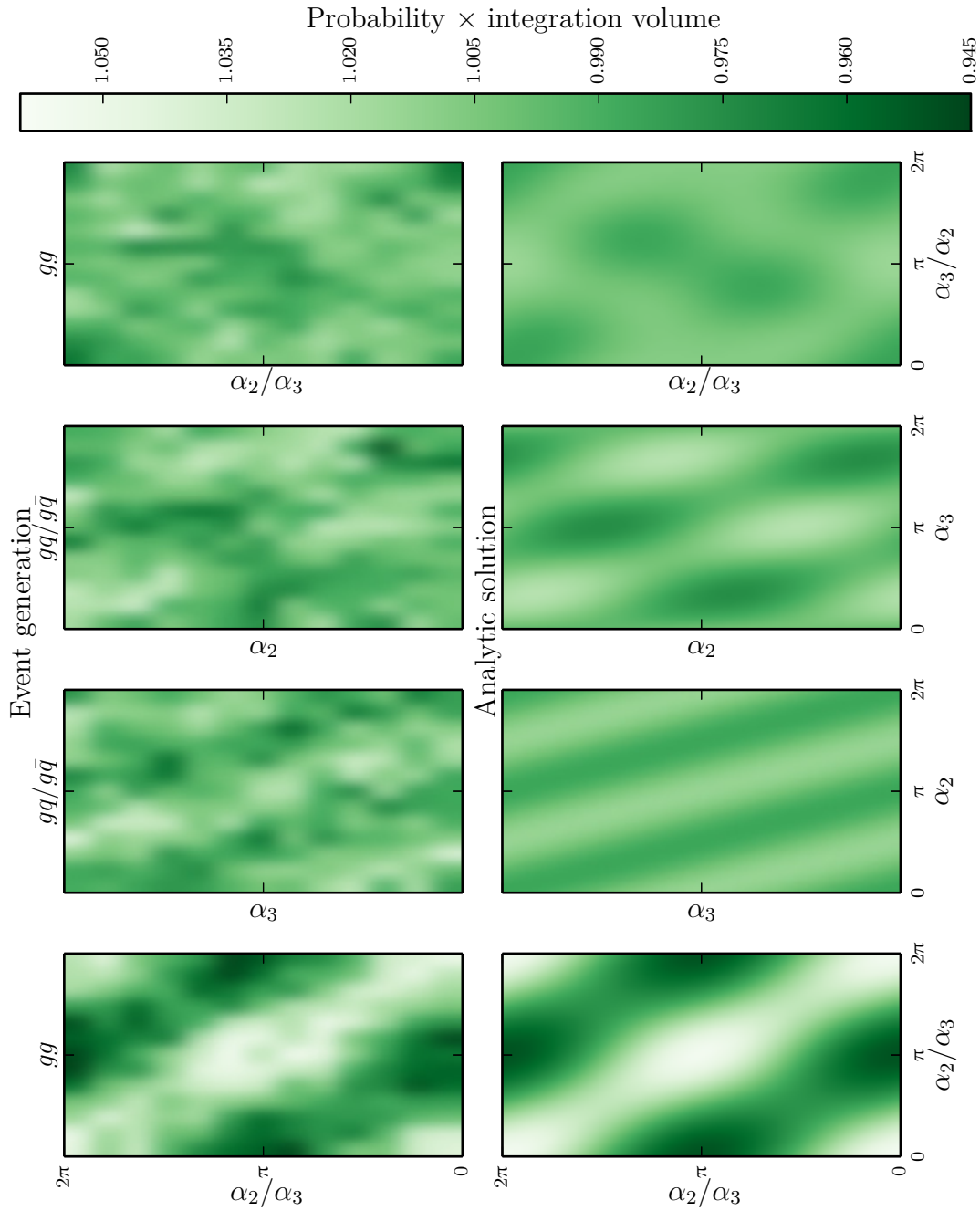


FIG. 5.11: The same plot as Fig. 5.10 for $SU(3)$ where we only show the structures different to the ones shown in this and to the ones from the measure in Fig. 5.9b. The labeling is according to Fig. 5.10 but due to the small structure we have chosen another color mapping. Further we have interpolated the event generation to better recognize the structure.

subtract the main distribution to view the underlying structure. Moreover we cannot discuss these distribution in more depth at our stage due to the lack of understanding the physical consequences of the parameters of the CS. Nevertheless we see a good coincidence with the analytic prediction.

Next we look at the SU(3) case and we have again the structure we already encountered from the measure in Fig. 5.9b and small deviations to it. We will see that these differences from the structure of the measure are of the order of 1% or less and we are again facing the problem that we can only recognize them on top of a constant distribution. We could also subtract the underlying main structure from the correlations but as the plots will show, the distribution from our 10^6 events is not very smooth. Thus it is already hard to recognize any patterns in the plots with a constant structure and it gets even worse if we subtract the main structure. This is also due to the fact that we have a 21 dimensional integral and hence we need more events than for SU(2) to get the same smooth distributions. But the 10^6 events took already several days to generate which limited to use more events. As a result we only look at the structure between the phases α_2 , α_3 and β_2 as the other correlations do not have a constant structure from the measure. Besides the structures we already know from the measure in Fig. 5.9b we also find again the same plots as the third and last column of Fig. 5.10 for quark-antiquark and gluon-gluon correlation respectively. Furthermore we have structures which only deviate of the order of 0.1% from the constant and thus we can not distinguish them in the event generation and can only recognize them in the analytic case. Except all these cases we have the correlations shown in Fig. 5.11 where we have chosen a different colormap in green due to the small deviations. In addition we have chosen to interpolate in the case of the event generation as this facilitates to recognize the structure. Again we discuss the four plots column by column: The first is the third column of Fig. 5.10 with some deviations. The next two columns have a similar relation to each other just with more stripes. The last column is something completely different as well as the last distribution where the correlation pattern can still be recognized in the event generation at least with the help of the analytic solution. We haven chosen these four plots in Fig. 5.11 as the first three show very good how already known correlations occur differently because the structure is repeated more often. Further we see how these distributions then get altered twice the same way.

This finishes the discussion on our numeric results. First we proofed that the calculation of the color factors in the CSS indeed work and analyzed the VAMP error estimation in detail. Then we saw that the grid adaptation is not very fruitful as we are facing

a relatively flat integrand. Furthermore we found an exponential dependency between the error of our integration and the dimension of the integral. We also verified that the theorems for the simpler **RoU** and the factorization are correct in our example and explored their scope. The last part was deviated towards the event generation and in special the correlation between two parameters for the cross section of our example process of quark and antiquark into two gluons. There we were only able to present the various structures we encounter and a further analysis needs to first discuss the meanings of the different angles which describe our **CS**. In addition one can also investigate the structure lying under the main structures from the measure when this one is subtracted from the distributions. And further a closer analysis of the event generation with the simpler **RoU** could enable to understand the difference between the two cases because at first order both give the same distributions.

6 Conclusion

In this thesis the coherent state system (CSS) especially for $SU(n)$ was analyzed in great detail. We saw that a coherent state (CS) is not only connected to the harmonic oscillator in which context most physicists first learn about it. We generalized the CS from the Heisenberg-Weyl group (HWG) to any group based on the concepts of Perelomov [Per86]. First we reviewed the CS of the harmonic oscillator and discussed them in more depth than usually in a first quantum mechanics course. Notably we introduced a construction scheme of the CSS that we could generalize to any group afterwards based on a fixed vector $|\psi_0\rangle$. There we found that a point in the coset space of the isotropy group of our vector $|\psi_0\rangle$ is enough to completely describe a CS. Despite the overcompleteness and thus linear dependence of the CS we can construct a resolution of unity (RoU) of the form $\int d\mu_\alpha |\alpha\rangle\langle\alpha|$. It is this overcompleteness which makes working with the CSS at first very unfamiliar. But we saw that this property enables the CS to be such a versatile tool and we can even find a unique representation of any state and operator in the CSS with the help of Glauber's work [Gla63]. Our idea is to understand in more depth the color-flow of Quantum Chromodynamics (QCD) which is currently described very well via the Lund string model [And+83] of quark and gluon confinement. This theory has a very classical concept of the color carrying particles and thus we need CS closest to the classical states similar to the case of the harmonic oscillator. In order to achieve this, we first needed to introduce a universal concept of uncertainty for the eigenstates of our group generators as minimizing the Schrödinger uncertainty relation is not as straightforward as minimizing the Heisenberg uncertainty relation like in the case of the harmonic oscillator. The states with minimal uncertainty are the maximum weight states, i.e. $h_k h_k$ is maximal where h_k are the eigenvalues of the eigenstates $|\mathbf{h}\rangle$ of the Cartan operators H_k .

After this discussion of the general case we moved on to the CS of $SU(2)$ and $SU(3)$. First we presented the construction of the CSS of $SU(2)$ from Perelomov [Per86] which is easy to understand. Next we used the Schwinger representation [Sch52, Mat81] of $SU(n)$ to construct it again. This enables us to generalize the CS to $SU(3)$ and even all $SU(n)$ [MS01, MM02] if necessary. On the basis of the construction from Perelomov

and the SU(2) Schwinger representation, the SU(3) CS were better comprehended. We presented all these steps in great detail as they are very concise in the mentioned references and not easy to grasp for somebody relatively new to this subject. Thus we highlighted the important steps precisely and omitted the subtleties which are only important for the general or some special cases. Moreover we explicitly showed the CS for the fundamental representation (FuR) and adjoint representation (AdR) of SU(2) and SU(3). As always the easy SU(2) case facilitated the understanding of the difficulties we faced for SU(3). One of these is that the Fock states of a tensor product of the FuR and its conjugate representation are not in a irreducible representation of SU(n). Thus one has to consider the CS as a linear combination of the canonical basis states for such representations individually for each. As we are interested in calculating color factors of QCD in the CSS numerically together with the total cross section of a process, it is helpful if our integration is less dimensional. Thus on the one hand we found a simpler RoU which facilitates the integration but which also involves states which are no longer closest to the classical one. This concept is a nice mathematical and technical trick but might not help us in understanding the theory of color-flow. On the other hand we want the isotropy group to be as high-dimensional as possible thus its coset space is described by lesser parameters and in consequence also the CS. Here we could verify that our constructions from before already had the least number of parameters. Therefore we used the Cartan decomposition of elements of a Lie group which also enabled us to motivate the Euler decomposition of SU(2) and to generalize it to any SU(n).

With this groundwork we applied the concept of CS to the color of QCD where we looked at the process example of quark and antiquark into two gluons. Therefore we calculated the differential cross section without evaluating the traces in the color basis as this one is left for the CSS. Then we first analyzed the calculation of the individual color factors first in the color basis and afterwards in the CSS: We found that we can factorize them, if we cut our Feynman graphs on a single internal index and average over all external particles. But if we cut in a loop or consider a color factor from the mixing of two different Feynman graphs, viz not the square absolute value of one graph, this factorization should fail in general. At this point the overcompleteness of the CS was hindering in contrast to the color basis as two different CS are not orthogonal. In consequence one can apply the factorization in the color basis also if one does not average over all external color indices. Here we recognized that the CSS will not facilitate the calculation of the color factors but nevertheless it can still help us to understand the inner mechanics of the QCD confinement.

In the last chapter about the numeric evaluation with the CS, we also concluded that

these are not suited for exact calculation. Here we first introduced the concepts of Monte Carlo (MC) integration and discussed the various methods to obtain better results. The results showed us that the statements made before are valid on the basis of our example and we also analyzed the VAMP error estimation in great depth which is a very good estimation. In the end we put a lot of emphasis into the event generation and its discussion. Here we found that the one dimensional distribution as well as the correlation of two parameters of the same particle are just given by the integration over the measure. Different distributions were obtained from the correlation between different particles. As we have not yet understood the physical meaning of the parameters of the CS, a discussion of the consequences of our results on the physics of QCD color-flow is currently not possible. This is left for further research as well as a deeper analysis of our results. Nevertheless we could present the different main structures we encountered. This resulted in some interesting plots up to the subtleties we could resolve. Besides the open question in the numeric section also more depth is needed in fully understanding the CS.

Bibliography

- [Ale⁺] A. ALEX ET AL. *SU(N) Clebsch-Gordan coefficients*. <http://homepages.physik.uni-muenchen.de/~vondelft/Papers/ClebschGordan/>
- [And⁺83] B. ANDERSSON ET AL. *Parton Fragmentation and String Dynamics*. *Physics Reports* **97** (1983), 2-3: pp. 31. [doi:10.1016/0370-1573\(83\)90080-7](https://doi.org/10.1016/0370-1573(83)90080-7)
- [Bak05] H. F. BAKER. *Alternants and Continuous Groups*. *Proceedings of the London Mathematical Society* **s2-3** (1905), 1: pp. 24. [doi:10.1112/plms/s2-3.1.24](https://doi.org/10.1112/plms/s2-3.1.24)
- [Bar61] V. BARGMANN. *On a Hilbert space of analytic functions and an associated integral transform. 1*. *Communications on pure and applied mathematics* **14** (1961), 3: pp. 187. [doi:10.1002/cpa.3160140303](https://doi.org/10.1002/cpa.3160140303)
- [BCC06] S. BERTINI, S. L. CACCIATORI and B. L. CERCHIALI. *On the Euler angles for SU(N)*. *Journal of Mathematical Physics* **47** (2006), 4: p. 043510. [arXiv:math-ph/0510075](https://arxiv.org/abs/math-ph/0510075), [doi:10.1063/1.2190898](https://doi.org/10.1063/1.2190898)
- [BD65] L. BIEDENHARN and H. V. DAM. *Quantum Theory of Angular Momentum* (Academic, New York, 1965)
- [BP87] V. D. BARGER and R. J. N. PHILLIPS. *Collider Physics*, vol. 71 of *Frontiers in Physics* (Addison-Wesely, Redwood City, USA, 1987)
- [Byr97] M. BYRD. *The Geometry of SU(3)* (1997). [arXiv:physics/9708015](https://arxiv.org/abs/physics/9708015)
- [Cam96] J. E. CAMPBELL. *On a Law of Combination of Operators bearing on the Theory of Continuous Transformation Groups*. *Proceedings of the London Mathematical Society* **s1-28** (1896), 1: pp. 381. [doi:10.1112/plms/s1-28.1.381](https://doi.org/10.1112/plms/s1-28.1.381)

- [Cam97] J. E. CAMPBELL. *On a Law of Combination of Operators (Second Paper)*. Proceedings of the London Mathematical Society **s1-29** (1897), 1: pp. 14. [doi:10.1112/plms/s1-29.1.14](https://doi.org/10.1112/plms/s1-29.1.14)
- [Che⁺87] J.-Q. CHEN ET AL. *Tables of the Clebsch-Gordan, Racah and Subduction Coefficients of $SU(n)$ Groups* (World Scientific Publishing, Singapore, 1987). [doi:10.1142/9789814415439_0003](https://doi.org/10.1142/9789814415439_0003)
- [Cvi08] P. CVITANOVIC. *Group theory: Birdtracks, Lie's and exceptional groups* (Princeton University Press, New Jersey, 2008). The author makes the current version of the book on-line available at <http://www.birdtracks.eu/version9.0>
- [Del77] R. DELBOURGO. *Minimal uncertainty states for the rotation and allied groups*. Journal of Physics A: Mathematical and General **10** (1977), 11: pp. 1837. [doi:10.1088/0305-4470/10/11/012](https://doi.org/10.1088/0305-4470/10/11/012)
- [DF77] R. DELBOURGO and J. R. FOX. *Maximum weight vectors possess minimal uncertainty*. Journal of Physics A: Mathematical and General **10** (1977), 12: pp. L233. [doi:10.1088/0305-4470/10/12/004](https://doi.org/10.1088/0305-4470/10/12/004)
- [Dui00] DUISTERMAAT. *Lie Groups*. Universitext (Springer, Berlin/Heidelberg, 2000). [doi:10.1007/978-3-642-56936-4](https://doi.org/10.1007/978-3-642-56936-4)
- [Dyn50] E. B. DYNKIN. *Normed Lie algebras and analytic groups*. Uspekhi Matematicheskikh Nauk **5** (1950), 1(35): pp. 135. In Russian; English translation in [Dyn62]
- [Dyn62] E. B. DYNKIN. *Normed Lie algebras and analytic groups*. American Mathematical Society Translations (Series 1) **9** (1962): pp. 470
- [Eis16] K. EISENHUT. *$SU(3)$ kohärente Zustände in der QCD*. Masterthesis, University Würzburg (2016). Supervision also from Prof. Dr. Thorsten Ohl (<http://thorsten-ohl.info>). Not yet published.
- [Foc32] V. FOCK. *Konfigurationsraum und zweite Quantelung*. Zeitschrift für Physik **75** (1932), 9: pp. 622. [doi:10.1007/BF01344458](https://doi.org/10.1007/BF01344458)
- [Geo99] H. M. GEORGI. *Lie algebras in particle physics*, vol. 54 of *Frontiers in Physics* (Perseus Books, Reading, MA, 1999), 2nd ed.

- [Gla63] R. J. GLAUBER. *Coherent and Incoherent States of the Radiation Field*. Physical Review **131** (1963), 6: pp. 2766. doi:10.1103/PhysRev.131.2766
- [GR94] I. S. GRADSHTEYN and I. M. RYZHIK. *Table of Integrals, Series, and Products* (Academic Press, 1994), 5th ed.
- [Hau06] F. HAUSDORFF. *Die symbolische Exponentialformel in der Gruppentheorie*. Berichte über die Verhandlungen der Königlich Sächsischen Gesellschaft der Wissenschaften zu Leipzig **58** (1906): pp. 19
- [Her66] R. HERMANN. *Lie Group for physicists* (W. A. Benjamin, Inc., New York, 1966)
- [Jac62] N. JACOBSON. *Lie algebras* (Interscience Publishers, New York, 1962)
- [Kla60] J. R. KLAUDER. *The Action option and a Feynman quantization of spinor fields in terms of ordinary C numbers*. Annals of Physics **11** (1960), 2: pp. 123. doi:10.1016/0003-4916(60)90131-7
- [KOR11] W. KILIAN, T. OHL and J. REUTER. *WHIZARD: Simulating Multi-Particle Processes at LHC and ILC*. The European Physical Journal C **71** (2011), 9: 1742. arXiv:0708.4233, doi:10.1140/epjc/s10052-011-1742-y. Software available on their website: <http://whizard.hepforge.org/>
- [Lep78] G. P. LEPAGE. *A New Algorithm for Adaptive Multidimensional Integration*. Journal of Computational Physics **27** (1978), 2: pp. 192. doi:10.1016/0021-9991(78)90004-9
- [Lep80] G. P. LEPAGE. *VEGAS - An Adaptive Multi-dimensional Integration Program*. CLNS-80/447 (1980). On-line version available at <http://cds.cern.ch/record/123074/files/clns-447.pdf?version=1>
- [Mat81] D. C. MATTIS. *The Theory of Magnetism I* (Springer, Berlin/Heidelberg, 1981). doi:10.1007/978-3-642-83238-3
- [Met⁺53] N. METROPOLIS ET AL. *Equation of state calculations by fast computing machines*. The Journal of Chemical Physics **21** (1953), 6: pp. 1087. doi:10.1063/1.1699114

- [Met87] N. METROPOLIS. *The Beginning of the Monte Carlo Method*. Los Alamos Science **15** (1987), special issue dedicated to Stanislaw Ulam: pp. 125. On-line version available at <http://library.lanl.gov/cgi-bin/getfile?00326866.pdf>
- [MM02] M. MATHUR and H. S. MANI. *SU(N) coherent states*. Journal of Mathematical Physics **43** (2002), 11: pp. 5351. [arXiv:quant-ph/0206005](https://arxiv.org/abs/quant-ph/0206005), [doi:10.1063/1.1513651](https://doi.org/10.1063/1.1513651)
- [MOR01] M. MORETTI, T. OHL and J. REUTER. *O'Mega: An Optimizing matrix element generator*. At *2nd Workshop of the 2nd Joint ECFA / DESY Study on Physics and Detectors for a Linear Electron Positron Collider*, pp. 1981–2009 (Lund, Sweden, 2001). [arXiv:hep-ph/0102195](https://arxiv.org/abs/hep-ph/0102195)
- [MS01] M. MATHUR and D. SEN. *Coherent states for SU(3)*. Journal of Mathematical Physics **42** (2001), 9: pp. 4181. [arXiv:quant-ph/0012099](https://arxiv.org/abs/quant-ph/0012099), [doi:10.1063/1.1385563](https://doi.org/10.1063/1.1385563)
- [Nem00] K. NEMOTO. *Generalized coherent states for SU(n) systems*. Journal of Physics A: Mathematical and General **33** (2000), 17: pp. 3493. [arXiv:quant-ph/0004087](https://arxiv.org/abs/quant-ph/0004087), [doi:10.1088/0305-4470/33/17/307](https://doi.org/10.1088/0305-4470/33/17/307)
- [Neu31] J. v. NEUMANN. *Die Eindeutigkeit der Schrödingerschen Operatoren*. Mathematische Annalen **104** (1931), 1: pp. 570. [doi:10.1007/BF01457956](https://doi.org/10.1007/BF01457956)
- [O⁺14] K. A. OLIVE ET AL. (Particle Data Group). *Review of Particle Physics*. Chinese Physics C **38** (2014), 9: pp. 090001. [doi:10.1088/1674-1137/38/9/090001](https://doi.org/10.1088/1674-1137/38/9/090001). Visit their website <http://pdg.lbl.gov> for latest data and to stay up to date
- [Ohl99a] T. OHL. *Electroweak gauge bosons at future electron positron colliders*. At *2nd Workshop of the 2nd Joint ECFA / DESY Study on Physics and Detectors for a Linear Electron Positron Collider*, pp. 55–204 (Lund, Sweden, 1999). [arXiv:hep-ph/9911437](https://arxiv.org/abs/hep-ph/9911437)
- [Ohl99b] T. OHL. *Vegas revisited: Adaptive Monte Carlo integration beyond factorization*. Computer Physics Communications **120** (1999), 1: pp. 13. [arXiv:hep-ph/9806432](https://arxiv.org/abs/hep-ph/9806432), [doi:10.1016/S0010-4655\(99\)00209-X](https://doi.org/10.1016/S0010-4655(99)00209-X). The software can be found on the WHIZARD [KOR11, MOR01] website including an almost complete documentation [Ohl15].

- [Ohl15] T. OHL. *VAMP, Version 1.0: Vegas AMPlified: Anisotropy, Multi-channel sampling and Parallelization* (1999-2015). On-line available at <https://whizard.hepforge.org/vamp.pdf>
- [Per77] A. M. PERELOMOV. *Generalized coherent states and some of their applications*. Soviet Physics Uspekhi **20** (1977), 9: pp. 703. [doi:10.1070/PU1977v020n09ABEH005459](https://doi.org/10.1070/PU1977v020n09ABEH005459)
- [Per79a] A. M. PERELOMOV. *Description of generalized coherent states closest to classical*. Yadernaya Fizika **29** (1979): pp. 1688. In Russian; English translation in [Per79b] which is also equivalent to chapter 2.4 in [Per86].
- [Per79b] A. M. PERELOMOV. *Description of generalized coherent states closest to classical*. Soviet journal of nuclear physics **29** (1979), 6: pp. 867
- [Per86] A. M. PERELOMOV. *Generalized Coherent States and Their Applications*. Theoretical and Mathematical Physics (Springer, Berlin/Heidelberg, 1986). [doi:10.1007/978-3-642-61629-7](https://doi.org/10.1007/978-3-642-61629-7)
- [PS95] M. E. PESKIN and D. V. SCHROEDER. *An Introduction to Quantum Field Theory* (Addison-Wesely Publishing Company, Reading, MA, 1995)
- [Ram10] P. RAMOND. *Group theory: A physicist's survey* (Cambridge University Press, Cambridge, UK, 2010)
- [RSG99] D. J. ROWE, B. C. SANDERS and H. DE GUISE. *Representations of the Weyl group and Wigner functions for $SU(3)$* . Journal of Mathematical Physics **40** (1999), 7: pp. 3604. [arXiv:math-ph/9811012](https://arxiv.org/abs/math-ph/9811012), [doi:10.1063/1.532911](https://doi.org/10.1063/1.532911)
- [Sch91] F. SCHUR. *Zur Theorie der endlichen Transformationsgruppen*. Mathematische Annalen **38** (1891), 2: pp. 263. [doi:10.1007/BF01199254](https://doi.org/10.1007/BF01199254)
- [Sch93] F. SCHUR. *Ueber den analytischen Charakter der eine endliche kontinuierliche Transformationsgruppe darstellenden Functionen*. Mathematische Annalen **41** (1893), 4: pp. 509. [doi:10.1007/BF01443741](https://doi.org/10.1007/BF01443741)
- [Sch26] E. SCHRÖDINGER. *Der stetige Übergang von der Mikro- zur Makromechanik*. Naturwissenschaften **14** (1926), 28: pp. 664. [doi:10.1007/BF01507634](https://doi.org/10.1007/BF01507634)

- [Sch30] E. SCHRÖDINGER. *Zum Heisenbergschen Unschärfeprinzip*. Sitzungsberichte der Preussischen Akademie der Wissenschaften, Physikalisch-mathematische Klasse **19** (1930): pp. 296. Reprinted in [Sch84] and an English translation can be found in [Sch99]
- [Sch52] J. SCHWINGER. *On Angular Momentum*. U.S. Atomic Energy Commission **NYO-3071** (1952). Reprinted in [BD65]
- [Sch84] E. SCHRÖDINGER. *Gesammelte Abhandlungen* (Österreichische Akademie der Wissenschaften, Wien, 1984)
- [Sch99] E. SCHRODINGER. *About Heisenberg uncertainty relation*. Bulgarian Journal of Physics **26** (1999), 5: pp. 193. [arXiv:quant-ph/9903100](#)
- [Sch08] F. SCHWABL. *Quantenmechanik für Fortgeschrittene (QM II)* (Springer, Berlin/Heidelberg, 2008). [doi:10.1007/978-3-540-85076-2](#)
- [SMS06] T. SJOSTRAND, S. MRENNÄ and P. Z. SKANDS. *PYTHIA 6.4 Physics and Manual*. Journal of High Energy Physics **2006** (2006), 05: pp. 26. [arXiv:hep-ph/0603175](#), [doi:10.1088/1126-6708/2006/05/026](#). Software available at <http://home.thep.lu.se/~torbjorn/Pythia.html>
- [Sto30] M. H. STONE. *Linear Transformations in Hilbert Space: III. Operational Methods and Group Theory*. Proceedings of the National Academy of Sciences **16** (1930), 2: pp. 172
- [TS02] T. E. TILMA and G. SUDARSHAN. *Generalized Euler angle parametrization for SU(N)*. Journal of Physics A: Mathematical and General **35** (2002), 48: pp. 10467. [arXiv:math-ph/0205016](#), [doi:10.1088/0305-4470/35/48/316](#)
- [Wei96] S. WEINBERG. *The quantum theory of fields. Vol. 2: Modern applications* (Cambridge University Press, New York, 1996)
- [Wei00] S. WEINZIERL. *Introduction to Monte Carlo methods* (2000). [arXiv:hep-ph/0006269](#)
- [Wey28] H. WEYL. *Gruppentheorie und Quantenmechanik* (Hirzel, Leipzig, 1928)
- [ZFG90] W.-M. ZHANG, D. H. FENG and R. GILMORE. *Coherent states: Theory and some Applications*. Reviews of modern physics **62** (1990), 4: pp. 867. [doi:10.1103/RevModPhys.62.867](#)

Declaration

Hereby I declare the single handed composition of this thesis. Furthermore, I confirm that no other sources have been used than those specified in the thesis itself. This thesis has not been submitted as part of another examination process neither in identical nor in similar form.

Würzburg, September 06, 2016

Florian Amann